Genetic Inducible Fate Mapping (GIFM) and the Conditional Deletion of *Neurog1* in the Developing Mouse Cerebellum

by

Edwin A. Obana

Dissertation submitted to the Faculty of the
Neuroscience Graduate Program
Uniformed Services University of the Health Sciences
In partial fulfillment of the requirements for the degree of
Doctor of Philosophy 2018

UNIFORMED SERVICES UNIVERSITY, SCHOOL OF MEDICINE GRADUATE PROGRAMS
Graduate Education Office (A 1045), 4301 Jones Bridge Road, Bethesda, MD 20814

APPROVAL OF THE DOCTORAL DISSERTATION IN THE NEUROSCIENCE GRADUATE PROGRAM

Title of Dissertation: "Genetic Inducible Fate Mapping (GIFM) and the Conditional Deletion of *Neurog1* in the Developing Mouse Cerebellum"

Name of Candidate: Edwin A. Obana
Doctor of Philosophy
January 11, 2018

DISSERTATION AND ABSTRACT APPROVED:

DATE:

[redacted] 2/2/18
Regina Armstrong, PhD
DEPARTMENT OF ANATOMY, PHYSIOLOGY & GENETICS
Committee Chairperson

[redacted] 2/2/18
Martin Doughty, PhD
DEPARTMENT OF ANATOMY, PHYSIOLOGY & GENETICS
Dissertation Advisor

[redacted] 2/2/18
Sharon Juliano, PhD
DEPARTMENT OF ANATOMY, PHYSIOLOGY & GENETICS
Committee Member

[redacted] 2/2/18
Zygmunt Galdzicki, PhD
DEPARTMENT OF ANATOMY, PHYSIOLOGY & GENETICS
Committee Member

[redacted] 2/2/18
Galina Petukhova, PhD
DEPARTMENT OF BIOCHEMISTRY & MOLECULAR BIOLOGY
Committee Member

ACKNOWLEDGMENTS

I would like to thank my mentor, Dr. Martin Doughty – thank you for being patient and understanding, yet challenging. You kept me optimistic whenever we had issues and obstacles to overcome with this project. I have learned and grown very much from your mentorship and being apart of your lab.

Thank you to my Thesis Committee members: Dr. Regina Armstrong, Dr. Sharon Juliano, Dr. Zygmunt Galdzicki and Dr. Galina Petukhova for their guidance and support on my thesis.

Thank you to several people at USUHS: The staff and technicians at the Center for Laboratory Animal Medicine (LAM) for helping maintain our mouse colony. Dr. McDaniel in the Biomedical Instrumentation Center (BIC) for the constant assistance on the microscopes. Lisa Myers at the Histopathology Core for processing tissue. Tina and the Graduate Education Office (GEO) for their administrative support. The Program in Neuroscience and the Department of Anatomy, Physiology and Genetics (APG) – it has been a pleasure working alongside with all of you.

Thank you to Doughty Lab members, past – Travis Lundell, Kevin Yi, Kryslaine Radomski, Ana Efthymiou and present –Qiong Zhou, Michael Nieves, Orion Furmanski. I am grateful for all the help you have provided for this project but also creating a fun atmosphere to work. The lunches and snack breaks in the hallway were the perfect balance to collecting data.

My Neuroscience classmates: Robert Long, Teresa Ferrara-Bowens, Ramona von Leden and Maria Sanchez. We had the best study sessions and graduate school was a lot better because of all of you. Thank you for helping me get through this process.

To my many friends: thank you for making my time in graduate school and D.C. very memorable. Thank you to Spencer, Ivan & Maria, and Brandon for being like family away from home and keeping me strong.

I would like to thank my family – my siblings Christine, Jenn & Mike, and Darius. You all have always been very supportive, understanding and keep it real with me. I look up to each of you as role models as I finish graduate school and begin my career. Thank you for always looking out and being there for me. Thank you to my parents for working extremely hard for their children and teaching us the value of education and family. Mom and Dad, you've always been supportive of my research career and believed I could do anything, for which I am grateful. Lastly, thank you to my Mom, for her weekly phone calls from San Diego to make sure I was eating well, taking care of myself and staying focused in grad school. I love you and miss you very much.

DEDICATION

For Mom. I am now your “Ph.D. researcher son.”

COPYRIGHT STATEMENT

The author hereby certifies that the use of any copyrighted material in the dissertation manuscript entitled: Genetic Inducible Fate Mapping (GIFM) and the Conditional Deletion of *Neurog1* in the Developing Mouse Cerebellum is appropriately acknowledged and, beyond brief excerpts, is with the permission of the copyright owner.

Edwin A. Obana

May 18, 2018

DISCLAIMER

The views presented here are those of the author and are not to be construed as official or reflecting the views of the Uniformed Services University of the Health Sciences, the Department of Defense or the U.S. Government.

ABSTRACT

Genetic Inducible Fate Mapping (GIFM) and the Conditional Deletion of *Neurog1* in the Developing Mouse Cerebellum:

Edwin A. Obana, Ph.D., 2018

Thesis directed by: Martin L. Doughty, Ph.D., Associate Professor, Department of Anatomy, Physiology and Genetics

During neural development, proliferation and maturation of progenitor cells is regulated so neuronal cell types are generated in a controlled spatio-temporal sequence. The transcriptional programs driving diverse GABAergic neuron populations from their common progenitor pools in the developing cerebellum remain unclear. *Neurog1* is a pro-neural basic helix-loop-helix (bHLH) transcription factor expressed in progenitor cells in the ventricular zone (VZ) of embryos and subsequently in the presumptive white matter (pWM) tracts of developing postnatal mice. We used genetic inducible fate mapping (GIFM) with a transgenic *Neurog1-CreER* allele to characterize contributions of *Neurog1* lineages to the cerebellum of mice. *Neurog1*-expressing progenitors are fate-mapped to become Purkinje cells (PCs) and all inhibitory interneuron cell types of the cerebellar cortex but not glia. PCs are labeled between embryonic days (E)10.5 to E12.5 and GABAergic interneurons are labeled between E11.5 to postnatal day (P)7 with their final resting position following an inside-to-outside pattern in the cerebellar cortex. Long-term

BrdU retention of GIFM lineages reveals PCs express *Neurog1* around the time they become post-mitotic, in contrast to *Neurog1* expression in mitotic and post-mitotic interneurons. *Neurog1-CreER* GIFM reveals a correlation between the timing of *Neurog1* expression and the spatial organization of GABAergic neurons in the cerebellar cortex. As conventional $Neurog1^{Neo}$ knockout mice are neonatal lethal, we generated $Neurog1^{loxP}$ mutant mice to examine the effects of conditional *Neurog1* deletion on postnatal development in the cerebellum. Targeted *Neurog1* loss-of-function does not result in significant differences in cerebellar morphology or number of GABAergic neurons in the cerebellar cortex of P21 mice. We quantified rates of cell proliferation and cell cycle progression or re-entry in embryonic $Neurog1^{Neo}$ and postnatal $Neurog1^{loxP}$ knockouts. Data revealed no significant effect of *Neurog1* loss-of-function on E12.5 VZ progenitors or on P5 and P6 progenitors in the pWM at P7. However, 4-5 day pulse-labeling of P5 and P6 progenitors revealed reductions in inhibitory interneuron dispersal from the pWM to the cerebellar cortex in P10 conditional $Neurog1^{loxP/loxP}$ knockout mice. Thus our conditional *Neurog1* knockout approach reveals a requirement for the gene in inhibitory interneuron cell dispersal from pWM tracts. Taken together our data reveals *Neurog1* is expressed in cerebellar progenitors that generate GABAergic neuronal cell types in a spatio-temporal inside-out sequence and required for inhibitory interneuron maturation during postnatal cerebellar development.

TABLE OF CONTENTS

LIST OF TABLES xiii

LIST OF FIGURES xiv

CHAPTER 1: Introduction 1

Anatomy of the Cerebellum 2
The Cerebellum as a Model System to Study Developmental Neurogenesis 5
Cerebellum Development 6
Isthmic Organizer 6
Cerebellar Primordium 7
Glutamatergic Neurogenesis 9
GABAergic Neurogenesis 10
Gliogenesis 11
Proneural Basic Helix-Loop-Helix (bHLH) Transcription Factors 12
Proneural bHLH factor *Neurog1* 13
Clinical Relevance of Studying Genes in Mouse Models of Cerebellar Development 14
Summary 16

CHAPTER 2: *Neurog1* genetic inducible fate mapping (GIFM) reveals the existence of complex spatiotemporal cyto-architectures in the developing cerebellum 20

Abstract 20
Introduction 20
Material and Methods 23
Neurog1-CreER^{T2} and Cre reporter mouse lines 23
Genetic inducible fate-mapping (GIFM) 23
Immunohistochemistry (IHC) 24
In situ hybridization (ISH) 25
Cell fate quantification 26
BromodeoxyUridine (BrdU) delivery 27
Quantification of Ki67+ and BrdU+ cells 27
Results 28
Short-term *Neurog1-CreER*; *R26$^{td\text{-}Tomato}$* labeling is consistent with Neurog1 ISH in sites of GABAergic neurogenesis 29
E10.5 to E12.5 *Neurog1-CreER* GIFM labels Purkinje cells with distinct medial-lateral settling patterns in the adult cerebellum 32
Overlapping *Neurog1* and *Ascl1* expression in Purkinje cell progenitors 39
Neurog1-CreER GIFM transitions from Purkinje to Golgi cell interneuron fates beginning ≈ E11.75 42
Temporal *Neurog1-CreER* GIFM marks exclusively interneurons from E14.5 to P7 45
Co-expression of *Neurog1* and *Ascl1* in interneuron progenitors 47

Neurog1 is expressed in Purkinje cells around the time they become post-mitotic but in mitotic and post-mitotic interneurons 49
GABAergic interneuron progenitors in the presumptive white matter tracts enter the cell cycle around the time they express *Neurog1* 53
Neurog1-CreER GIFM labels DCN interneurons during late embryogenesis 54
Discussion 56
Neurog1-CreER GIFM labels exclusively neurons in the cerebellum 56
E12.5 GIFM labeled Purkinje cells settle in distinct parasagittal stripes in the vermis and paravermis 58
The timing of *Neurog1* expression in cerebellar progenitors differs between early and later phases of GABAergic neurogenesis 59
Conclusion 60

CHAPTER 3: Conditional deletion of *Neurog1* in the cerebellum of postnatal mice delays inhibitory interneuron maturation 62

Abstract 62
Significance Statement 63
Introduction 63
Material and Methods 67
Mouse Lines 67
Cell cycle analysis in Neurog1$^{Neo/Neo}$ knockout mice 69
Thymidine Analog Delivery 69
Immunohistochemistry (IHC) 70
In Situ Hybridization (ISH) 71
Cresyl Violet Staining 72
Stereo Investigator (MBF Bioscience) 72
Cavalieri Method 74
Cell Quantification (IHC) 74
Statistical analysis 74
Results 75
Neurog1 loss-of-function effects on cell proliferation in the VZ during the period of peak Purkinje cell production 75
Neurog1 deletion in the cerebellar primordium of E12.5 conditional *Neurog1$^{loxP/loxP}$* knockout mice 77
Stereological quantification of cerebellar GABAergic neuronal cell types at P21 in conditional *Neurog1$^{loxP/loxP}$* knockout mice 81
Neurog1 loss-of-function effects on cell proliferation of Pax2+ inhibitory interneurons in the presumptive white matter tracts at P7 83
Neurog1 loss-of-function effects on Pax2+ inhibitory interneuron migration from the presumptive white matter tracts 85
Discussion 89
Neurog1 loss-of-function impairs inhibitory interneuron cell dispersal to granule and molecular layers 89
Purkinje cell progenitors express *Neurog1-CreER* around the time they become post-mitotic but *Neurog1* is not required for cell cycle progression or exit from the cell cycle in E12.5 VZ progenitors 91

Conditional *Neurog1* deletion does not result in reductions of GABAergic neurons in P21 conditional knockout mice 92
Conditional *Neurog1*$^{loxP/loxP}$ knockout mice are viable and can be used to study the long-term effects of *Neurog1* loss-of-function in mice 93

CHAPTER 4: Discussion 96

Neurog1-CreER GIFM exclusively labels GABAergic neurons in the cerebellum 98
E12.5 GIFM-labeled PCs that settle in distinct parasagittal stripes 100
Analysis of *Neurog1* function during early and later phases of GABAergic neurogenesis 103
Neurog1 loss-of-function in VZ progenitors 104
Neurog1 loss-of-function effects Pax2+ interneuron dispersal from pWM 106
Conditional *Neurog1*$^{loxP/loxP}$ knockout mice are viable and can be used to study the long-term effects of *Neurog1* loss-of-function in mice 108
Future Directions 108
Conclusion 110

REFERENCES 113

LIST OF TABLES

Table 1. Antibodies.....71

LIST OF FIGURES

Figure 1. A simplified schematic of the structure and cellular organization of the adult mouse cerebellum 3
Figure 2. Cerebellum cytoarchitecture and afferents 4
Figure 3. Temporal neurogenesis in the mouse cerebellum 6
Figure 4. Mouse cerebellar primordium 8
Figure 5. *Neurog1-CreER*;*R26*$^{td\text{-}Tomato}$ reporter gene expression patterns in the cerebellum are largely consistent with sites of Neurog1 expression revealed by in situ hybridization (ISH). 31
Figure 6. GIFM using the *Neurog1-CreER* transgene fates cerebellar Purkinje cells from E10.5 to E12.5 in mice. All mice were analyzed at P42. 33
Supplementary Figure 14. Patterns of GIFM Purkinje cells following TMX on E12.5 do not coincide with expression patterns of Zebrin II or Hsp25. 37
Supplementary Figure 15. GIFM is specific to Purkinje cell lineages in *Neurog1-CreER*;*R26*$^{td\text{-}Tomato/+}$ mice but RFP reporter expression occurs independent of TMX delivery in some basket, stellate and Golgi cells. 39
Figure 7. Overlapping *Neurog1* and *Ascl1* expression patterns in the ventricular zone of the cerebellar anlage at E12.5. 41
Figure 8. *Neurog1-CreER*;*R26*$^{td\text{-}Tomato}$ GIFM transitions from Purkinje to Golgi cell fate with TMX injection at E13.5 43
Figure 9. E14-.5 to P7 *Neurog1-CreER* GIFM labels interneurons in an inside-to-outside settling pattern in the adult cerebellar cortex. 47
Figure 10. Similarities in the spatiotemporal pattern of Neurog1 with Ascl11 (see (74)) are supported by ISH data showing overlapping expression of the two bHLH transcription factor genes. 49
Figure 11. *Neurog1* is expressed in Purkinje cells around the time they become post-mitotic and in mitotic and post-mitotic interneurons. 51
Figure 12. Mitotic GABAergic interneuron progenitors express *Neurog1*. 54
Figure 13. Late embryogenesis *Neurog1-CreER* GIFM labels interneurons in the deep cerebellar nuclei (DCN). 56
Fig. 16. *Neurog1* loss-of-function does not affect cell cycle dynamics in E12.5 to E13 VZ progenitors 76
Fig. 17. *Neurog1* targeting for conditional deletion in mice 77
Fig. 18. *Neurog1* deletion in the E12.5 cerebellar primordium. 79
Fig. 19. Stereological quantification of cerebellar GABAergic neuronal cell types. 82
Fig. 20. Cell proliferation of Pax2^{+} interneurons in the presumptive white matter tracts at P7 84
Fig. 21. Pax2^{+} interneuron migration from presumptive white matter tracts 87
Figure 22. Summary Diagram: *Neurog1-CreER* GIFM in the developing mouse cerebellum 96
Figure 23. Summary Diagram: Conditional *Neurog1* deletion in postnatal mouse cerebellum 97

CHAPTER 1: Introduction

The cerebellum is located in the anterior portion of the hindbrain and is primarily known for its function in motor coordination. Other functions of the cerebellum contribute to the planning and coordinating of movements, maintaining posture and balance, controlling eye movements, as well as processing sensory information and higher cognitive functions (11; 21). Cerebellum organization and circuitry has been studied ever since Santiago Ramón y Cajal described the morphology and connections of nerve cells in the avian cerebellum in 1888 (73). In humans, the cerebellum begins to develop around the ninth gestational week and continues beyond birth. Cerebellar developmental mechanisms are conserved between humans and rodents, making studies in mice highly valuable in determining the pathologies of CNS developmental diseases and disorders. In more recent years, advances in techniques and technology contribute to our understanding of the mechanisms regulating development of the stereotyped circuitry of the cerebellum. The establishment of cerebellar circuitry and structure provide a powerful model for studying developmental neurogenesis and how functional brain networks are formed.

The complex circuitry of the brain arises from an extended developmental process modulated by genetic and environmental factors. Neurodevelopmental disorders such as autism, attention deficit hyperactivity disorder, cerebral palsy, and other developmental delays are estimated to account for about 15% of the population (6; 77; 78), highlighting the importance of studying brain development. Neuropsychiatric disorders, such as autism or schizophrenia, have been linked to imbalances of excitatory versus inhibitory neurotransmission (9). More recently, the cerebellum has been associated with processing

higher cognitive functions and cerebellar dysfunction has been linked to autism (24). Thus, identifying molecular programs that regulate cerebellar development and GABAergic neurogenesis has the potential to inform our understanding of autism. Cerebellar dysfunction is the primary cause of cerebellar ataxias, a heterogeneous group of disorders that are characterized by abnormal gait, motor incoordination and imbalance, and oculomotor defects (36). Although many of these ataxias are late-onset diseases, it seems likely developmental processes play a role in disease predisposition again highlighting the importance of a more complete understanding of the development of this CNS structure.

ANATOMY OF THE CEREBELLUM

Although comprised of millions of neurons, the uniform cytoarchitecture of the cerebellum contains a limited number of neuronal cell types, characterized by distinct morphological features, topographical location and expression of cell-type specific markers. These characteristics make the cerebellum an ideal system to study developmental neurogenesis and the formation of diverse neurons. The regularly foliated surface of the rodent cerebellum comprises of 10 lobules (I-X) consisting of a tri-laminar cortex, white matter tracts and deep cerebellar nuclei (DCN) (Figure 1). The cerebellar cortex is organized into three distinct laminar layers: the internal granule cell layer, the Purkinje cell layer, and the outermost molecular layer (81) (Figure 2). The adult cerebellum is comprised of two cerebellar hemispheres and the vermis located in between the two hemispheres (Figure 1).

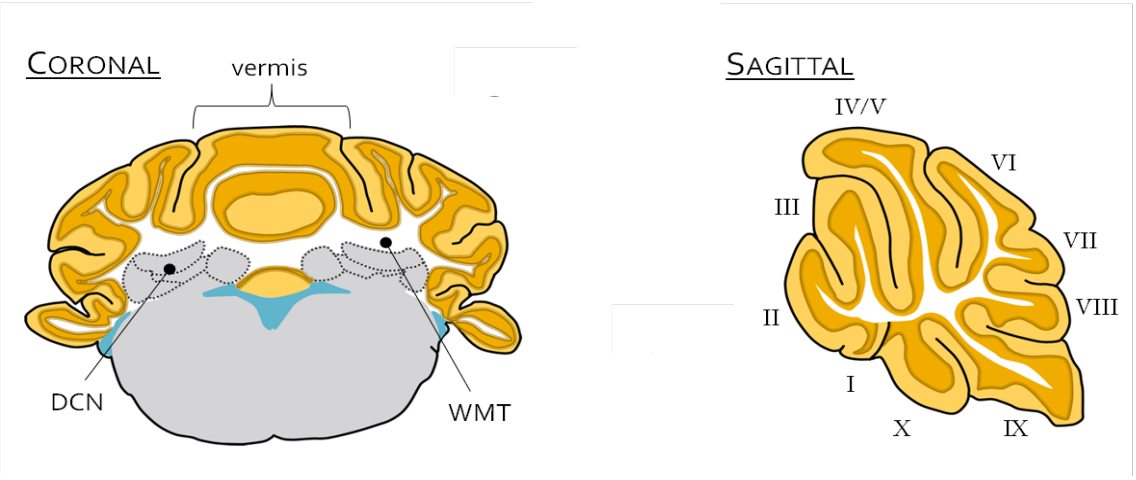

Figure 1. A simplified schematic of the structure and cellular organization of the adult mouse cerebellum
(Left) The coronal image demonstrates the three cortical layers divided into two hemispheres on either side of the vermis. Deep to the cortex are the white matter tracts (WMT) and 4 pairs of deep cerebellar nuclei (DCN). (Right) The sagittal image shows the 10 lobules of the cerebellar vermis (image and text adapted by permission of Dr. Karl Schilling).

The tri-laminar cerebellar cortex contains two groups of neurons: excitatory glutamatergic neurons and inhibitory gamma-aminobutyric acid (GABA)ergic neurons, each produced from separate progenitor pools. These distinct types of neurons form interconnected circuits to perform complex neural functions (26). Granule cells and unipolar brush cells (UBCs) are glutamatergic neurons of the cerebellar cortex that are located in the internal granule cell layer. GABAergic neurons of the cerebellar cortex include Lugaro and Golgi cells in the granule cell layer, Purkinje cells (PCs) and candelabrum cells in the Purkinje cell layer, and basket and stellate cells in the molecular layer (10) (Figure 2). Purkinje cells are the sole output cells of the cerebellar cortex and project to DCN in the white matter.

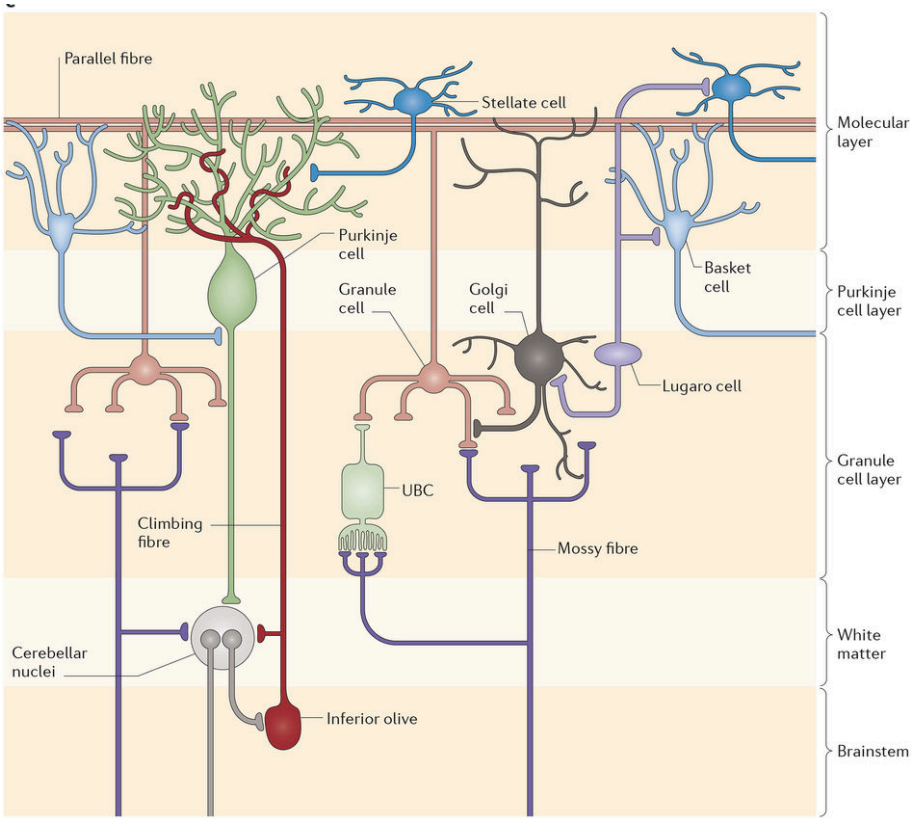

Figure 2. Cerebellum cytoarchitecture and afferents

A simplified schematic of basic cerebellum cytoarchitecture and afferents including Purkinje cells (the sole output cells of the cerebellar cortex), granule cells, Golgi cells, Lugaro cells, unipolar brush cells (UBCs), stellate and basket cells (candelabrum cells not shown in diagram). The two main afferents that project in to the cerebellum are the climbing fibres that synapse directly on Purkinje cells, and the mossy fibres that synapse on granule cells. The axons of the granule cells ascend to the molecular layer where they bifurcate to form parallel fibres. Figure adapted from Cerminara et al., 2015.

The two main afferent inputs of the cerebellum are excitatory and include the climbing fibers (CFs) and mossy fibers (MFs) (Figure 2). The CFs originate exclusively from the inferior olivary nuclei (ION) in the medulla oblongata of the brainstem and project directly on to PC dendrites in the molecular layer. The MFs originate from precerebellar nuclei including pontine gray matter nuclei, reticulotegmental nuclei, external cuneate nuclei, and lateral reticulate nuclei, and synapse on granule cell dendrites that are in contact with Golgi cells, to form the cerebellar glomeruli (81). PCs

are the primary output of the cerebellar cortex and project to DCN. Excitatory granule cells synapse with PCs. While CFs excite PCs directly, MFs excite PCs indirectly via granule cells. DCN include the fastigial nucleus that projects to the spinal cord, interpositus nucleus that projects to the red nucleus, and dentate nucleus that projects to the thalamus (85). DCN efferent fibers project to the cerebral cortex via the thalamus and the brainstem to control motor coordination and balance (10).

THE CEREBELLUM AS A MODEL SYSTEM TO STUDY DEVELOPMENTAL NEUROGENESIS

The mouse cerebellum is an experimentally tractable system when studying the structure, function and development of the central nervous system. The protracted development of the cerebellum spans embryonic and postnatal time periods making this region of the brain accessible to study neurogenesis. The limited number of neuronal cell types and uniform cytoarchitecture (Figure 2) of the cerebellar cortex provide a model system where any defects from induced alterations can be measured. Cerebellar motor behavior in mice can be tested by footprint analysis to assess for gait abnormalities, a balance beam test to assess for ataxia, tremor and balance, or an accelerating rotorod test to evaluate motor coordination and balance (13). Furthermore, cerebellar development has well delineated morphogenetic milestones, cell birth dates (Figure 3), as well as spatially and genetically distinct progenitor pools in which all cerebellar neuronal cell types are generated. All these factors make the mouse cerebellum an excellent model to study molecular programs in neuronal specification and differentiation.

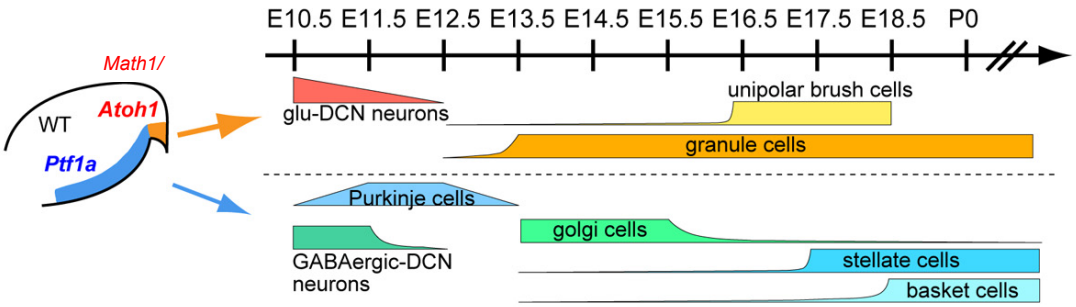

Figure 3. Temporal neurogenesis in the mouse cerebellum
Temporal schematic of neurogenesis from the mouse cerebellar primordium. Note the production of cells in an inside-out positional sequence where early born neurons are those that settle in the inner granule cell layer and later born neurons are those that settle in the outer molecular layer. Figure adapted from Yamada et al., 2014.

CEREBELLUM DEVELOPMENT

Isthmic Organizer

The cerebellum originates from the dorsal portion of the rostral hindbrain during mid-embryogenesis. During neurodevelopment the neural tube is highly regionalized with precise spatial and temporal gene expression. The regionalized genetic boundaries along the anteroposterior or dorsoventral axes of the neural tube provide structural polarity for cerebellar development. The anterior portion of the neural tube generates three brain vesicles: the forebrain (prosencephalon), midbrain (mesencephalon) and hindbrain (rhombencephalon). The caudal neural tube generates the spinal cord. The rhombencephalon segments are called rhombomeres (r) and from rostral to caudal known as r0-r7. The boundary surrounding the mesencephalon and rhombencephalon is known as the isthmic constriction (r0) (52). The isthmic constriction of the neural tube contains the isthmic organizer (IsO) where transcription factors Otx2 and Gbx2 are expressed in

rostral and caudal domains, respectively. This gene interaction, or reciprocal repression of Otx2 and Gbx2, creates the mid-hindbrain boundary. The IsO is defined by the expression of secreted molecule fibroblast growth factor 8 (Fgf8) at the mid-hindbrain junction around E8.5 in mice (15). Loss-of-function of Gbx2 or alterations of Fgf8 leads to massive defects in the mid-hindbrain boundary due to gene patterning deregulation (82). The morphogenetic activity of the IsO along with Fgf8 signaling regulates specification and structural development necessary for cerebellar neuroepithelial territories. Cerebellar histogenesis begins at E9 following territorial specification and closure of the neural tube. Cerebellar progenitors are generated by the neuroepithelium of the alar plate of r1 located rostrally to the isthmus. The most dorsal region of r1 gives rise to the roof plate, while ventral and intermediate regions of the neuroepithelium become the ventricular zone and the rhombic lip (52).

Cerebellar Primordium

The development of the cerebellar territory is followed by the formation of two spatially distinct germinal zones: the rhombic lip (RL) located between the fourth ventricle and the roof plate, and the ventricular zone (VZ) (Figure 4). Each germinal zone exclusively gives rise to either glutamatergic or GABAergic cerebellar neurons, respectively. Cerebellar neuronal subtypes depend on when and where they are generated from neural precursors. Pro-neural basic helix-loop-helix (bHLH) transcription factors generate different cerebellar neuronal subtypes through well-defined spatiotemporal programs. Genetic fate mapping and viral lineage tracing experiments have helped determine the origins of glutamatergic and GABAergic neurons of the cerebellar cortex and also delineate their spatiotemporal sequence in which they are generated during

development. Genes encoding bHLH transcription factors are essential in neuronal development, activating regulatory pathways controlling neuronal specification and differentiation programs.

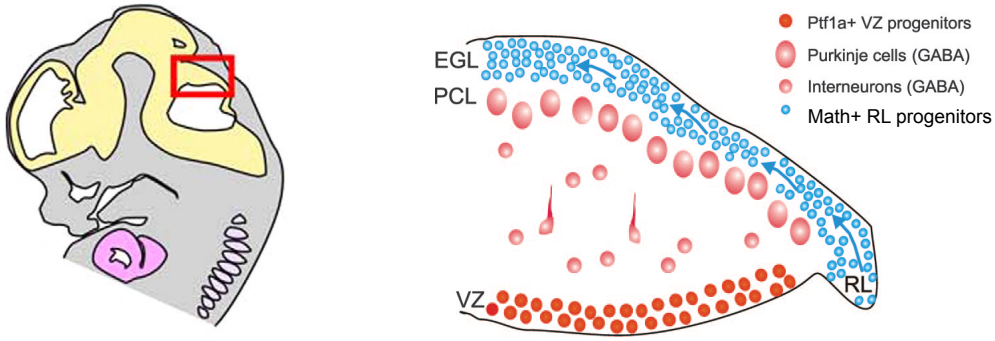

Figure 4. Mouse cerebellar primordium
(Left) Schematic diagram of a sagittal view of the developing ~E12.5 mouse embryo with the cerebellar primordium outlined in the red box. Figure adapted from Seto et al., 2013. (Right) Schematic diagram of a sagittal view of the cerebellar primordium. Ptf1a-expressing VZ progenitors generate GABAergic cells in the cerebellum, including PCs and interneurons (red). Math1-expressing RL progenitors produce granular cell precursors located in the EGL (blue). EGL, external granule cell layer; PCL, Purkinje cell layer. Figure adapted from Pascual et al., 2007.

Math1 (mouse atonal homolog 1) encodes a bHLH transcription factor that is expressed in RL progenitors and is required for the generation of all glutamatergic neurons in the cerebellum (4; 10). *Ptf1a* (pancreas transcription factor 1a) is another gene encoding a bHLH transcription factor expressed in the VZ and required to drive neural precursors to differentiate into GABAergic neurons in the cerebellum (30) (Figure 4). Loss of the *Ptf1a* gene in mutant mice, *cerebelless*, where *Ptf1a* expression is lost in the cerebellum but maintained in the pancreas, results in a deficiency of GABAergic neuron formation from the cerebellar VZ (30). *Ptf1a* acts, in part, by suppressing the glutamatergic granule cell phenotype from VZ progenitor cells suggesting its requirement

for the specification and normal production of PCs and interneurons (65). Furthermore, ectopic *Ptf1a* expression in the RL or ectopic *Math1* expression in the VZ overthrows the identity of precursor-derived neurons in these two germinal zones with GABAergic neuronal fates ectopically maintained in the RL or glutamatergic neuronal fates ectopically maintained in the VZ (88). Combined these studies demonstrate *Math11* and *Ptf1*a are essential and sufficient for neuronal specification from the cerebellar RL and VZ neuroepitheliums respectively (88).

Glutamatergic Neurogenesis

Glutamatergic granule cells are the predominant neuronal population in the cerebellum and the most abundant neuronal type in the adult brain. Proliferating granule cell progenitors originating in the RL migrate across the surface of the cerebellar anlage to form the external granule layer (EGL) (Figure 4). The proliferation of granule cell progenitors in the external granule layer is regulated by Sonic hedgehog (Shh) that is secreted from Purkinje cells (83). Proliferation of granule cell precursors continues in the EGL until postnatal day (P)15. Granule cell bodies migrate inward from the EGL along Bergmann glia fibers to the internal granule layer (IGL) (86) starting at birth until P20 when cerebellar histogenesis of the brain is complete (49).

Developing granule cell progenitors exit the cell cycle and extend axons (parallel fibers) that synapse with Purkinje cell dendrites in the molecular layer, and finally migrate inward past Purkinje cell bodies to their final destination, the internal granule layer. Mice lacking *Math1* fail to form granule cells and are born with a cerebellum lacking an external granule layer (4). Glutamatergic neurons in the cerebellar nuclei are specified in the RL at early stages (E10.5-12.5) and granule cells are specified in the RL

after E12.5 onward (49; 80; 81). Unipolar brush cells are glutamatergic interneurons that develop during late embryonic periods (E15.5) and migrate out of the upper rhombic lip into cerebellar white matter prior to entering the internal granule layer by P10 (18).

GABAergic Neurogenesis

All GABAergic interneurons are produced embryonically up to the second postnatal week through an inside-out positional sequence where early born cells become interneurons in the DCN followed by the granule cell layer and later born cells become interneurons in the outer molecular layer. Deep cerebellar nuclei interneurons are first to be born at E10.5-E11.5, followed by granule layer interneurons, and then molecular layer interneurons (44). Purkinje cells are born relatively early at E10.5-E13.5 in mice. Early born Purkinje cells form a layer several layers thick called the Purkinje cell plate by E14.5. The transient plate expands through the presumptive cerebellar cortex until late embryonic periods before forming a Purkinje cell monolayer during early postnatal periods. Purkinje cell maturation includes the formation of the Purkinje cell monolayer and dendritogenesis (32). The elaborate dendritic tree extends toward the pial surface and branches in the molecular cell layer (81). Golgi cells are born at about E13.5- P0. Later developing GABAergic interneurons, including basket and stellate cells, are born during late embryonic periods from the presumptive white matter up to P5 (43).

All GABAergic cerebellar interneurons, including Golgi, basket, stellate cells and interneurons in DCN express *Pax2* (51) and can be referred to as *Pax2*+ interneurons. *Pax2*-expressing cells are found in the cerebellar VZ at E13 and migrate throughout the prospective white matter during postnatal periods and eventually settle in DCN and cerebellar cortical layers. *Pax2*+ cells in the white matter tracts continue to proliferate up

to P7 (51). The production of 75% of all inhibitory interneurons occurs prior to P7 with the peak increase around P5 (84). Basket and stellate cells have been shown to proliferate until at least P7 and migrate into the outer molecular layer during the second postnatal week (43). Therefore, these interneuron progenitors originate from the *Ptf1a*-expressing VZ and continue their developmental process in the prospective white matter in postnatal mice prior to settling in their destined cortical layer.

GABAergic neuron progenitors in the *Ptf1a* domain can be divided into two distinct populations: Purkinje cell progenitors (PCPs) that express *Olig2,* a bHLH transcription factor, in the dorsal region, and *Pax2+* interneurons that express *Gsx1,* a homeobox transcription factor, in the ventral region. Throughout development PCPs transition to become *Pax2+* interneurons spreading from ventral to dorsal in the VZ. This temporal identity transition of GABAergic progenitors from PCPs to *Pax2+* interneurons is negatively regulated by *Olig2* and positively by *Gsx1* (68). Although this study shows two distinct subpopulations of progenitors in the *Ptf1a*-expressing domain, the key determinants regulating the temporal identity transition remains elusive since loss of *Olig2* or *Gsx1* gene still produces PCPs and *Pax2+* interneurons.

Gliogenesis

In the adult mammalian cerebellum there are four astroglial subtypes: fibrous astrocytes in the white matter, multipolar (velate) astrocytes with multiple tiny processes in the GL, slender (protoplasmic) astrocytes in the GL, and radial Bergmann glia cells spanning from cell bodies in the Purkinje cell layer through the ML up to the pial surface (41). At E14, the first astrogliogenic wave gives rise to radial glial progenitors from the VZ that displace their cell bodies towards the presumptive WM tracts, and transform into

progenitors of Bergmann glia (87). Later stages of embryonic development leads to a second wave of astroglial-like progenitors that proliferate in the cerebellar presumptive WM to form astroctyes in the prospective GL and white matter (87). Unlike cerebellar neurons, the precise timing and amplification of astroglial progenitors in the cerebellum remain unknown. However, Bergmann glia morphogenesis does require highly regulated interaction with surrounding cerebellar microenvironment including PCs, migrating and proliferating granule cells, as well as the basement membrane (pial surface) (8).

Proneural Basic Helix-Loop-Helix (bHLH) Transcription Factors

Transcriptional programs that regulate the development of cerebellar neuronal subtypes remain elusive. Previous studies reveal coexpression of bHLH factors in VZ progenitors that overlap with *Ptf1a* expression (91). The mechanisms by which diverse GABAergic neuron populations arise from their common *Ptf1a*-expressing progenitor pool are still unclear. Therefore, it is important to identify transcriptional programs that specify GABAergic Purkinje cell and interneuron cell types from *Ptf1a*-expressing progenitors.

Neuronal specification in the cerebellum requires genes encoding proneural bHLH transcription factors. *Neurogenin1* (*Neurog1*), *Neurogenin2* (*Neurog2*), and *achaete-scute homolog-1* (*Ascl1*, previously *Mash1*) are proneural bHLH transcription factor genes co-expressed in different subdomains of the *Ptf1a*-expressing VZ and give rise to GABAergic progenitors fated to become Purkinje cells and all inhibitory interneurons of the cerebellar cortex (35; 91). Expression of these bHLH factors does not overlap with *Math1*-expressing progenitors in the RL suggesting their selective contribution to GABAergic cell type specificity in the cerebellum (91). Also, ectopic

expression of *Ptf1a* in the RL produced GABAergic PCs and interneurons implying *Ptf1a* is sufficient to change fate of neurons in the RL from glutamatergic to GABAergic (88). Yet, the mechanism by which each GABAergic cell type is specified from *Ptf1a*-expressing progenitors still remain unclear.

Recent genetic tracing, birth dating and gene knockout studies have determined the origins of distinct subtypes of cerebellar neurons. Cre-flox genetic fate-mapping demonstrated *Ascl1*-expressing progenitor cells give rise to PCs, GABAergic inhibitory interneurons, DCN interneurons, and oligodendrocyte cell lineages depending on the embryonic stage of expression (34). The PTF1-J trimeric transcription factor complex, which includes the bHLH *Ptf1a* factor, has been demonstrated to regulate *Neurog2* expression (29) and *Neurog2*-expressing progenitors contribute PCs and DCN GABAergic inhibitory interneurons but almost no cortical inhibitory interneuron cell types (19). Conditional deletion of *Ascl1* in the cerebellum of mice results in a reduction of cerebellar interneurons (74). Similarly, the conditional deletion of *Neurog2* delays cell cycle progression, affects the maturation of PC dendritic arbors and leads to a reduction in cerebellar volume (19). The data does reveal distinct requirements for bHLH genes in the development of GABAergic PCs and interneurons from *Ptf1a*-expressing progenitors.

Proneural bHLH factor *Neurog1*

In the CNS, most *Neurog1*-expressing progenitors generate glutamatergic neurons contributing to the olfactory bulb, hippocampus, cerebral cortex, and thalamus (35). However, in the cerebellum, *Neurog1* is expressed in cell lineages contributing to GABAergic PCs and inhibitory interneuron cell types of the cerebellar cortex (35). *Neurog1* is expressed in progenitors during embryonic and postnatal time periods in

regions including the VZ, caudal cerebellar primordium, and subsequently the white matter tracts, areas of GABAergic neurogenesis (45). These studies suggest specific functions in the development of GABAergic neuronal lineages in the cerebellum. Based on these expression studies, I hypothesize the *Neurog1* gene is required for the normal development of GABAergic neurons in the mouse cerebellar cortex. Understanding the function of each proneural bHLH transcription factor expressed in the cerebellum should provide insights on the development and regulation of neuronal subtype specificity that form functional circuits in the adult cerebellum.

Clinical Relevance of Studying Genes in Mouse Models of Cerebellar Development

Cerebellar developmental mechanisms are conserved between humans and mice, making studies in mice excellent models for studying the pathologies of developmental diseases and disorders. In particular, human cerebellar development begins around the ninth gestational week and continues after birth. This protracted developmental timeframe makes the human cerebellum vulnerable to environmental insults. There are several cerebellar malformations in humans with most causing cognitive, motor and sensory integration deficits (41). While genetic components that lead to these malformations remain unclear, inflammation, fetal hemorrhage and premature birth are also contributing factors (41). Dandy Walker Malformation (DWM) is the most common human cerebellar malformation and patients display a variety of symptoms ranging from cognitive impairment to autism, with some patients displaying no defects (5). DWM is characterized by enlarged posterior fossa, cerebellar vermis hypoplasia and an enlarged fourth ventricle (5). Research in rodent models indicate deletions in *FOXC1* causes disruptions in posterior fossa signaling from mesenchyme-secreted signaling molecules

to the embryonic cerebellum, in turn causing dramatic reductions in cerebellar anlage neuronal progenitor proliferation and abnormal migration from the RL (1). Cerebellar agenesis is another malformation that is extremely rare. It is defined by the complete or partial absence of the cerebellum (77). Patients display several neurological defects related to movement and speech (77). Interestingly, homozygous mutation of the *PTF1A* gene has been associated with cerebellar agenesis in humans (67). Similarly, loss of the *Ptf1a* gene in mutant mice results in a deficiency of GABAergic neuron formation from the cerebellar VZ, consequently this leads to the loss of RL-derived progenitors resulting in cerebellar agenesis in neonates (30).

Cerebellar ataxias comprise of a heterogeneous group of neurological disorders including gait abnormalities, defects in motor coordination and balance, dysarthria and oculomotor defects (36). The pathogenesis of cerebellar ataxias have been linked to PC developmental abnormalities. Studies in the *staggerer* mouse, which has an autosomal recessive mutation in the *Rora* gene encoding RORα (a transcription factor with abundant expression in PCs), exhibit cerebellar atrophy and ataxia. The *staggerer* mouse serves as a model for studying spinocerebellar ataxia as these mice display impairments in PC dendritogenesis, spine development, and synaptogenesis (56).

Medulloblastomas (MBs) are developmental neuroectodermal tumors of the posterior cranial fossa highly linked to abnormal cerebellar development (79). MBs are the most common solid tumors in pediatric patients and a major cause of mortality. There are four main molecular subgroups of MB: WNT, SHH, Group 3, and Group 4. The WNT and SHH subgroups have been associated with constitutive activation of the WNT/β-catenin and SHH signaling, respectively, and also show good to intermediate

prognoses in patients (79). The main cell of origin for SHH MBs are granule cell precursors, and WNT MBs arise from precursor cells outside the cerebellum, in embryonic dorsal brainstem (41; 89). Group 3 and 4 MBs are not characterized as well and have poor and intermediate prognoses, respectively (76). While Group 4 MBs have expression profiles resembling glutamatergic neurons, Group 3 MBs express genes resembling photoreceptors and GABAergic neurons (76). Group 3 MBs exhibit overexpression of the MYC oncogene, are highly associated with metastasis, and have the poorest prognosis among other MB groups (76; 79). These combined characteristics of Group 3 MBs, particularly the tumors expressing markers of GABAergic neurons and poor prognosis, highlight the importance of determining the underlying pathogenesis of this subgroup. Additionally, studying the normal development of GABAergic progenitors may lead to insights of the tumorigenic potential of these progenitors and perhaps their contribution to Group 3 MBs. In addition to environmental insults that lead to cerebellar malformations in humans, genes have been identified as contributing factors to cerebellar agenesis, ataxias and medulloblastoma. Therefore, animal models are extremely useful to help us understand pathological mechanisms of these cerebellum-related disorders for the development of improved diagnostic tools and potential treatments.

SUMMARY

A fundamental question in neural developmental is to determine how neuronal subtypes are generated in a well-defined temporal and spatial manner to form functional circuits. The purpose of this dissertation is to determine the contribution of *Neurog1*-expressing progenitors to adult cerebellar circuit formation. Tracking a subset of progenitors arising from the cerebellar neuroepithelium that develop to mature neurons in

the adult cerebellum has been made possible through transgenic cre-flox mouse models. Genetic inducible fate mapping (GIFM) allows us to trace cell lineages from progenitor cells to post-mitotic differentiated cells in the adult brain (19; 74). This strategy allows for cell lineage analysis to determine when and in what cell type(s) a gene is active during development and how these cells contribute to the adult structure.

A complete fate map of *Neurog1* cell lineages in the cerebellum has not been completed. Developing a detailed spatiotemporal fate map and determining the loss-of-function effects of *Neurog1* will identify the contributions of *Neurog1*-expressing cell lineages to the adult cerebellar circuit and the requirement for *Neurog1* activity in normal cerebellar development. Determining the function of *Neurog1* in the organization and function of the adult cerebellum requires a long-term study of cerebellar development and associated behaviors. Conventional *Neurog1*$^{Neo/Neo}$ *null* mutant mice are neonatal lethal from a probable suckling defect due to the absence of certain cranial sensory ganglia (47), preventing the study of loss-of-function effects on postnatal cerebellar development, the period during which a majority of inhibitory interneurons of the cerebellar cortex are generated (43). In order to overcome the problem of neonatal lethality in conventional *Neurog1* null mutants, I will develop a conditional *Neurog1*^{loxP} mutant mouse model to selectively delete the gene in the cerebellum to enable the study of *Neurog1* loss-of-function effects in postnatal mice.

In this study, I will use genetic inducible fate mapping with a transgenic *Neurog1-CreER*^{T2} allele to characterize contributions of *Neurog1* lineages to cerebellar cell types in mice. We generated a *floxed* mutant mouse line to conditionally eliminate *Neurog1* in the developing cerebellum using either knock-in *En2-CreER*^{T2} (60) or *Ptf1a-Cre* (33) mutants

to target the cerebellum. *Engrailed2* (*En2*) gene is expressed in all cerebellar cell types in the presumptive cerebellar territory (60). *Ptf1a* is expressed in the VZ and required to drive neural precursors to differentiate into GABAergic neurons in the cerebellum (30). Both *En2-CreER*^{T2} and *Ptf1a-Cre* mutant mouse lines have been successfully used to genetically mark cells of the cerebellar primordium (70) and to target gene deletion in the cerebellum (74). This dissertation will contribute to our understanding of proneural bHLH transcription factor programs that specify the diverse set of GABAergic neurons populating the cerebellum.

CHAPTER 2: *Neurog1* genetic inducible fate mapping (GIFM) reveals the existence of complex spatiotemporal cyto-architectures in the developing cerebellum

ABSTRACT

Neurog1 is a pro-neural basic helix-loop-helix (bHLH) transcription factor expressed in progenitor cells located in the ventricular zone and subsequently the presumptive white matter tracts of the developing mouse cerebellum. We used genetic inducible fate mapping (GIFM) with a transgenic *Neurog1-CreER* allele to characterize the contributions of *Neurog1* lineages to cerebellar circuit formation in mice. GIFM reveals *Neurog1*-expressing progenitors are fate-mapped to become Purkinje cells and all GABAergic interneuron cell types of the cerebellar cortex but not glia. The spatiotemporal sequence of GIFM is unique to each neuronal cell type. GIFM on embryonic days (E) 10.5 to E12.5 labels Purkinje cells with different medial-lateral settling patterns depending on the day of tamoxifen delivery. GIFM on E11.5 to P7 labels interneurons and the timing of tamoxifen administration correlates with the final inside-to-outside resting position of GABAergic interneurons in the cerebellar cortex. Proliferative status and long-term BrdU retention of GIFM lineages reveals Purkinje cells express *Neurog1* around the time they become post-mitotic. In contrast, GIFM labels mitotic and post-mitotic interneurons. *Neurog1-CreER* GIFM reveals a correlation between the timing of *Neurog1* expression and the spatial organization of GABAergic neurons in the cerebellar cortex with possible implications for cerebellar circuit assembly.

INTRODUCTION

The cerebellum is an ideal model system to study regulatory pathways in neurogenesis and neuronal pattern formation. Although comprised of millions of neurons, the cerebellum consists of few principal neuronal cell types arranged within a uniform cortical cyto-architecture and three pairs of deep cerebellar nuclei (DCN) embedded in the white matter (31; 63). Cerebellar neurogenesis is protracted, spanning embryonic and postnatal development, and is characterized by spatially and temporally restricted patterns of neuronal production (10). Cerebellar neurons are generated from two distinct germinative zones: a ventricular zone (VZ) lying dorsal to the fourth ventricle; and from the upper rhombic lip (uRL), a specialized region lying between the fourth ventricle and the roof plate. These two germinative zones express distinct basic helix-loop-helix (bHLH) transcription factor genes - *Ptf1a* (Pancreas transcription factor 1a), *Ascl1* (Achaete-scute homolog 1) and Neurogenins *Neurog1* and *Neurog2* in the VZ, and *Atoh1* (Atonal homolog 1) in the uRL - that have each been used in the genetic fate mapping of progenitors.

Genetic inducible fate mapping (GIFM) with a transgenic *Atoh1-CreER* allele reveals uRL progenitors are fate mapped to become glutamatergic DCN projection neurons and subsequently glutamatergic granule cell interneurons in the cerebellum (49). Cumulative fate-mapping using a $Ptf1a^{Cre}$ (pancreas transcription factor 1a) knock-in allele labels GABAergic Purkinje cells, DCN inhibitory interneurons and Golgi, basket and stellate cell inhibitory interneurons of the cerebellar cortex (30; 65). More recently GIFM of *Ascl1*, a bHLH gene expressed throughout the *Ptf1a* expression territory in the VZ (91), has been used to define the spatiotemporal production of neurons from the VZ (34; 74). Knock-in $Ascl1^{CreER}$ mice reveal Purkinje cells are labeled during embryonic day

(E) 10.5 to E12.5 and have distinct settling patterns in the adult cerebellum depending on the day they express *Ascl1* (74). GABAergic DCN neurons are the first interneurons to be labeled at E10.5-E11.5 with inhibitory interneurons of the cerebellar cortex subsequently fate-mapped to granule, Purkinje cell and then molecular layers of the cerebellar cortex (74).

Fate-mapping of Neurogenin-expressing progenitors reveals differing contributions from *Neurog1*- and *Neurog2*-expressing lineages to the cerebellum. GIFM using a *Neurog2*^{CreER} knock-in allele labels Purkinje cells and DCN GABAergic neurons but little contribution to GABAergic interneurons in the cortex (19). In contrast, we have shown progenitors expressing *Neurog1* contribute to Purkinje cells and multiple GABAergic interneuron cell types in the cerebellar cortex using transgenic *Neurog1-EGFP* and *Neurog1-Cre* alleles to short-term and cumulatively map cell fates respectively (45). A CNS-wide GIFM study using transgenic *Neurog1-CreER* mice extends this observation revealing Purkinje cells are fate-mapped E10.5 to E12.5 and are followed by GABAergic interneurons in the granule cell layer at E14.5 and E17.5 (35). Thus preliminary *Neurog1* GIFM data suggests similarities between *Neurog1* and *Ascl1* spatiotemporal fate-maps in the cerebellum and the possibility that the two bHLH genes act coordinately to establish cerebellar circuitry.

In this study we used *Neurog1-CreER* GIFM to generate a detailed spatiotemporal fate-map of *Neurog1* lineages in the cerebellum. We show *Neurog1*-expressing progenitors are fate-mapped to become GABAergic neuronal cell types of the cerebellum with the spatiotemporal sequence of fate-mapping unique to each cell type. We confirm Purkinje cells are the first cerebellar neurons to be labeled at E10.5 to E12.5 and are

followed by inhibitory interneurons of the granule cell, Purkinje cell and molecular layers. BrdU birth dating and markers of cell proliferation reveal *Neurog1* is expressed in Purkinje cells around the time they become post-mitotic but in mitotic and post-mitotic GABAergic interneurons suggesting distinct Neurog1 functions in Purkinje cell and interneuron cell lineages.

MATERIAL AND METHODS

Neurog1-CreER^{T2} and Cre reporter mouse lines

Neurog1-CreER^{T2} recombinase and *Cre* reporter mouse lines used in this study have been described previously. See (35; 37) for details of the BAC transgenic mouse line *Neurog1-CreER^{T2}*. See (50) for details of the knock-in *Rosa26$^{loxP\text{-}STOP\text{-}td\text{-}Tomato}$* (here referred to as *R26$^{loxP\text{-}STOP\text{-}td\text{-}Tomato}$*) reporter mouse line. See (58) for details of the transgenic reporter mouse line *Z/EG* (pCAGGS-Bgeo/EGFP). Mice were obtained from The Jackson Laboratory, Bar Harbor, ME. All procedures were approved by the Uniformed Services University of the Health Sciences Institution for Animal Care and Use Committee (IACUC). Mice were housed in the Uniformed Services University's Center for Laboratory Animal Medicine on a standard 12 hour light-dark cycle, with feed and water available *ad libitum*. Mice were genotyped using The Jackson Laboratory Genotyping PCR Protocols or, for *Z/EG* only, by β-galactosidase staining in X-Gal reagent (Mirus Bio LLC). Mice were timed-mated overnight and the presence of a vaginal plug the following morning used to denote embryonic day 0.5 (E0.5). Using this counting method mice give birth at E19.5. The day of birth was designated as postnatal day 0 (P0).

Genetic inducible fate-mapping (GIFM)

Two overnight breeding strategies were employed for GIFM: (1) *Neurog1-CreER^{T2}* were mated with heterozygous (*R26$^{loxP\text{-}STOP\text{-}td\text{-}Tomato/+}$*) or homozygous (*R26$^{loxP\text{-}STOP\text{-}td\text{-}Tomato/\ td\text{-}Tomato}$*) reporters; (2) *Neurog1-CreER^{T2}* were mated with transgenic Z/EG reporters. Homozygous *R26$^{loxP\text{-}STOP\text{-}td\text{-}Tomato/\ td\text{-}Tomato}$* mice are viable and fertile (The Jackson Laboratory). Timed-pregnant females or postnatal pups were administered tamoxifen dissolved in sunflower oil by intra-peritoneal injection. Mice were injected with 50mg/Kg tamoxifen at ≈ 9am and given a second injection of 50mg/Kg tamoxifen 6 hours later. Controls were given intra-peritoneal injections of sunflower oil only at equivalent times. Tamoxifen disrupted parturition and lactation in the mice resulting in poor progeny survival rates. To improve survival, mice were removed by terminal caesarian from E19.5 pregnant dams and fostered to lactating Swiss Webster females (Taconic).

Immunohistochemistry (IHC)

Mice were fixed for IHC as described previously (45). Adult tissue was processed for free-floating IHC as described previously (66). Embryonic tissue was collected on slides and processed for IHC as described previously (45). All immunofluorescent labeling, except for Pax2, was performed using Alexa Fluor ® 488, 555 or 647 dye-labeled secondary antibodies (Life Technologies) and the tissue counterstained with DAPI and mounted under Mowiol. Pax2 immunolabeling was revealed using a biotinylated anti-rabbit secondary antibody with Dy-Light 488 streptavidin (Vector Laboratories). Immunofluorescent images were captured on a Zeiss 710 laser scanning confocal microscope (LSCM), a Zeiss Pascal LSCM and a Leica AF6000 fluorescence microscope with motorized x, y and z planes. For bright-field microscopy, sections were immunolabeled with biotinylated secondary antibodies followed by Vectastain ABC

reagent and immunolabeling revealed with diaminobenzidine tetrahydrochloride (DAB) (Vector Laboratories). Bright-field images were captured on a Zeiss A1 microscope or Hammamatsu Nanozoomer 2.0-RS digital slide scanner.

Details of the primary antibodies used for IHC are as follows: (1) 1: 500 dilution of rat monoclonal anti-BrdU (Accurate Chemical & Scientific Corp.); (2) 1: 2,000 dilution of mouse monoclonal anti-Calbindin D_{28K} (anti-Calb1, Swant); (3) 1: 1,000 dilution of chicken polyclonal anti-green fluorescent protein (anti-GFP, Abcam); (4) 1: 1,000 dilution of mouse monoclonal anti-Glial Fibrillary Acidic Protein (anti-GFAP, Abcam); (5) 1: 2,000 dilution of rabbit polyclonal anti-Hsp25 (Enzo Life Sciences); (6) 1: 200 dilution of rabbit monoclonal anti-Ki67 (Thermo Scientific); (7) 1: 1,500 dilution of mouse monoclonal anti-metabotropic glutamate receptor 2 (anti-Grm2, AbCam) (8) 1: 500 dilution of rabbit polyclonal anti-Neurogranin (Abcam); (9) 1: 500 dilution of mouse monoclonal anti-NeuN (clone A60, Millipore); (10) 1:500 dilution of rabbit polyclonal anti-Olig2 (Millipore) (11) 1: 2,500 dilution of mouse monoclonal anti-parvalbumin (anti-Pvlb, Swant); (12) 1: 200 dilution of rabbit polyclonal anti-Pax2 (Zymed); (13) 1:400 dilution of rabbit polyclonal anti-phospho-histone H3 (phH3, Millipore); (14) 1: 100 dilution of rabbit polyclonal anti-PLCβ4 (Santa Cruz Biotechnology); (15) 1: 1,000 dilution of chicken polyclonal anti-Red Fluorescent Protein (anti-RFP, Rockland); (16) 1: 500 dilution of mouse monoclonal anti-S100β (Sigma) (17) 1: 250 dilution of rabbit polyclonal anti-ZebrinII/Aldolase C (gift of R. Sillitoe).

In situ hybridization (ISH)

Timed-pregnant Swiss Webster mice (Taconic) were fixed for ISH as described previously for IHC. The tissue was cryo-protected in sucrose and frozen sections cut on a

cryostat and post-fixed in fresh fixative. ISH was performed using RNAscope® probes for DAB single-plex and fluorescent multi-plex hybridizations according to the instructions from the manufacturer Advanced Cell Diagnostics (ACD). Neurog1 and Ascl1 probes were hybridized single-plex with DAB (3,3'-Diaminobenzidine) labeling on adjacent tissue sections for comparison or in duplex using ACD's green/red fluorescent probe labeling system.

Cell fate quantification

Cell fate counts were recorded from tiled 20X fluorescent images of cerebellar sections processed for anti-EGFP or anti-RFP reporter IHC. We used morphological criteria validated by dual IHC using anti-EGFP/anti-RFP antisera with cell-type specific antibodies to score cell fate. Purkinje cells were identified by their large, pear-shaped soma positioned between the granule cell and molecular layers of the cerebellar cortex and by their highly branched dendritic arbors (confirmed by anti-Calb1 IHC). Golgi cells were identified by their large, irregularly shaped soma within the granule cell layer (confirmed by anti-Nrg and anti-Grm2 IHC). Candelabrum and Lugaro cells were identified by the position of their relatively small soma within the Purkinje cell layer and supporting morphology. Candelabrum cells had 1-2 sparsely-branched dendrites and a characteristic beaded axonal arborization in the molecular layer (40). Lugaro cells had a fusiform cell body and horizontal bipolar dendrites (39). Candelabrum and Lugaro cells were counted together in this study as Purkinje cell layer (PCL) interneurons. Basket and stellate cells were identified by the position of their small, multipolar soma within the molecular layer (confirmed by anti-Pvlb IHC). The molecular layer was divided along the middle laminar axis into inner and outer sublayers and the number of basket and stellate

cell types counted by their location within the inner and outer halves respectively. Cell counts were recorded from 3-4 coronal sections spanning the full rostro-caudal extent of the cerebellum. When presented as the mean ± standard error of the mean (SEM), cell counts were obtained from at least 3 animals unless stated otherwise.

BromodeoxyUridine (BrdU) delivery

Timed-pregnant females or postnatal pups were administered BrdU dissolved in saline by intra-peritoneal injection. Mice were injected with 50mg/Kg BrdU at ≈ 9am and given a second injection of 50mg/Kg BrdU 6 hours later. RFP reporter expressing cells retaining BrdU were identified by punctate nuclear staining with anti-BrdU IHC.

Quantification of Ki67+ and BrdU+ cells

For Ki-67 cell counts, timed-pregnant females or neonates were processed for dual anti-Ki67/anti-RFP IHC 24 hours after the first tamoxifen injection. The percentage of total RFP reporter expressing cells in the cerebellum co-expressing Ki67 was quantified from 40X confocal Z stacks taken from serially-spaced sections of the cerebellum.

For short-term BrdU pulse labeling, timed-pregnant females or neonates were processed for dual anti-BrdU/anti-RFP IHC 24 hours after the first BrdU injection. The percentage of RFP+ cells in the cerebellum co-immunoreactive for BrdU was quantified from 40X confocal Z stacks as described for Ki67. For long-term BrdU pulse labeling, mice were processed for dual anti-BrdU/anti-RFP IHC on P42. The percentage of RFP+ cerebellar cell types co-immunoreactive for BrdU was quantified from tiled 20X fluorescent images of cerebellar sections.

RESULTS

We used *Neurog1-CreER^{T2}* mice in this study to develop a detailed spatiotemporal fate-map of *Neurog1*-expressing lineages in the cerebellum. *Neurog1-CreER^{T2}* mice (throughout referred to as *Neurog1-CreER)* carry copies of a modified BAC in which the single *Neurog1* coding exon was replaced with *CreER^{T2}*. Cre mRNA in situ hybridization (ISH) patterns re-capitulate Neurog1 mRNA ISH in *Neurog1-CreER* embryos demonstrating restricted expression of Cre to Neurog1 expression sites (35; 37). Two reporter lines were used to identify *Neurog1-CreER*-expressing cell lineages: *Rosa26$^{loxP\text{-}STOP\text{-}td\text{-}Tomato}$* (here referred to as *R26$^{td\text{-}Tomato}$*) labeled cells with red fluorescent protein (RFP), and *Z/EG* reporters labeled cells with enhanced green fluorescent protein (EGFP).

We analyzed mice heterozygous and homozygous for the *R26$^{td\text{-}Tomato}$* allele in this study and *Neurog1-CreER ; R26$^{td\text{-}Tomato/+}$* and *Neurog1-CreER ;R26$^{td\text{-}Tomato/td\text{-}Tomato}$* mice are collectively referred to as *Neurog1-CreER*; *R26$^{td\text{-}Tomato}$*. Although we did not observe a difference in the intensity or distribution of RFP epilfluorescence in the brain between *Neurog1-CreER; R26$^{td\text{-}Tomato/+}$* and *Neurog1-CreER; R26$^{td\text{-}Tomato/td\text{-}Tomato}$* mice, RFP fluorescence was enhanced by immunohistochemistry (IHC) to normalize reporter signal between mice heterozygous or homozygous for *R26$^{td\text{-}Tomato}$*. Mice carrying both the *Neurog1-CreER* and Z/EG transgene are referred to as *Neurog1-CreER*; *Z/EG* and the EGFP reporter signal was also enhanced by IHC.

Cre recombinase was activated in *Neurog1-CreER*; *R26$^{td\text{-}Tomato}$* and *Neurog1-CreER*; *Z/EG mice* by the delivery of tamoxifen (TMX) in sunflower oil. Mice were injected with tamoxifen the morning of a given embryonic day and given a second tamoxifen injection 6 hours later. Recombination at *loxP* sites is reported to occur within

6 hours of TMX delivery and continues for up to 36 hours (69). Thus E10.5 TMX delivery in *Neurog1-CreER* mice is predicted to label cells expressing *Neurog1* ≈ E10.75-E12.25. Mice injected with sunflower oil only were used to control for leaky Cre recombinase activity not controlled by TMX administration.

Short-term *Neurog1-CreER*; *R26*$^{td\text{-}Tomato}$ labeling is consistent with Neurog1 ISH in sites of GABAergic neurogenesis

We verified *Neurog1-CreER* marks cells of *Neurog1*-expressing lineages in the developing cerebellum by comparing short-term *Neurog1-CreER*; *R26*$^{td\text{-}Tomato}$ labeling patterns and ISH data for Neurog1. *Neurog1-CreER*; *R26*$^{td\text{-}Tomato}$ were given TMX on E11.5, E12.5 or E18.5 and fixed 24 hours later. ISH was performed on sections from E12.5, E13.5 and P0 Swiss Webster mice for comparison. The data reveal corresponding patterns of ISH and RFP reporter gene expression in the cerebellum and surrounding hindbrain structures in early cerebellar development (Fig. 5). ISH signal is present at the ventricular zone (VZ) but absent from the rhombic lip (RL) and midline of the developing cerebellar anlage of E12.5 and E13.5 mice (Fig. 5a, c). In E12.5 *Neurog1-CreER*; *R26*$^{td\text{-}Tomato}$ mice, RFP is localized to layers of cells adjacent and parallel to the VZ (but not to the RL or midline regions) in more dorsal aspects of the cerebellar anlage, consistent with the rapid dorsal migration of RFP marked cells from the Neurog1-expressing regions of the VZ (Fig. 5b). In E13.5 *Neurog1-CreER*; *R26*$^{td\text{-}Tomato}$ mice RFP labeling is present throughout the VZ (but not in the RL or midline) suggesting a slower VZ exit of E12.5 compared to E11.5 GIFM progenitors (Fig. 5d). ISH signal at P0 is markedly reduced in the cerebellum compared to E12.5 and E13.5. At this age, ISH labeled cells are clustered in lateral and dorsal aspects of the cerebellum parallel but deep to the external granule cell layer (EGL) (Fig. 5e). This pattern is consistent with Neurog1

expression in cells in deeper layers of the developing cerebellar cortex (Fig. 5e). RFP expressing cells are similarly distributed in the developing cerebellar cortex in P0 *Neurog1-CreER*; $R26^{td\text{-}Tomato}$ mice (Fig. 5f). However, dense RFP expression is also detected in the RL with E18.5 GIFM suggesting ectopic *Neurog1-CreER* expression in the RL during later embryogenesis (Fig. 5f arrow and inset). Combined, these data indicate *Neurog1-CreER* mice can be used to fate-map *Neurog1*-expressing lineages from the cerebellar VZ but that later fate-mapping could result in ectopic labeling of RL-derived cell lineages.

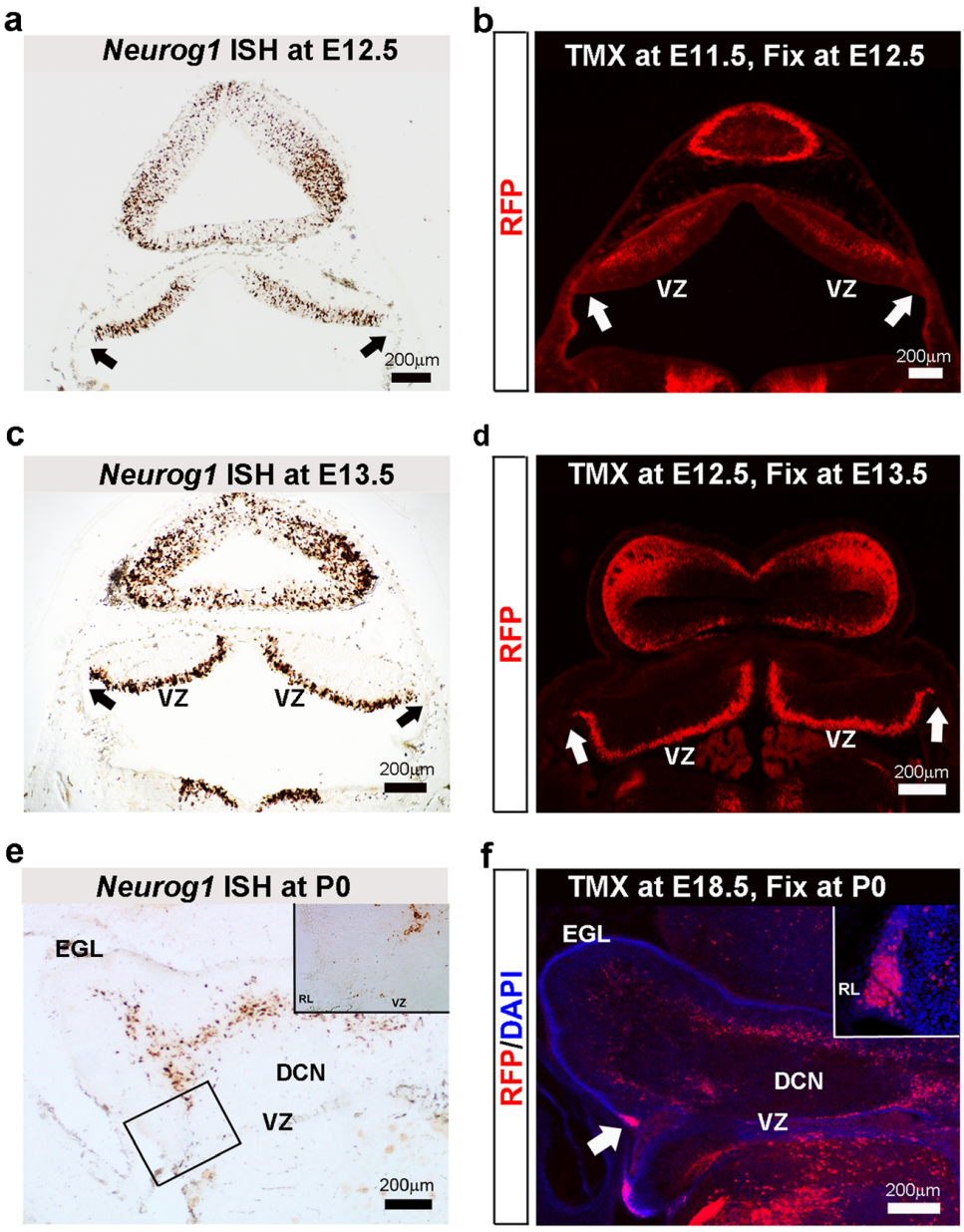

Figure 5. *Neurog1-CreER*;*R26*$^{td\text{-}Tomato}$ reporter gene expression patterns in the cerebellum are largely consistent with sites of Neurog1 expression revealed by in situ hybridization (ISH).
(a, c and e) Neurog1 ISH at E12.5, E13.5 and P0 respectively. Black arrows show absence of hybridization in the rhombic lip. Boxed area of rhombic lip and lateral ventricular zone in panel e is shown at higher magnification in the inset. (b, d and f) *Neurog1-CreER*;*R26*$^{td\text{-}Tomato}$ mice given tamoxifen E11.5, E12.5 and E18.5 respectively and fixed for analysis 24 hours later. White arrows point to the rhombic lip. Inset in panel f shows the reporter gene expression in the rhombic lip with E18.5 GIFM at higher magnification. Key: DCN, deep cerebellar nuclei; EGL, external granule cell layer; RL, rhombic lip; VZ, ventricular zone.

E10.5 to E12.5 *Neurog1-CreER* GIFM labels Purkinje cells with distinct medial-lateral settling patterns in the adult cerebellum

Cerebellar Purkinje cells have been fate-mapped at E10.5, E11.5 and E12.5 using *Neurog1-CreER* GIFM with a *Rosa26* β-glatactosidase ($R26^{Lacz/+}$) reporter (35). This CNS-wide study revealed E11.5 fate-mapping was the highest contributor to Purkinje cell fate and that E12.5 Purkinje cells settled preferentially in rostral cerebellar lobes. However, no other spatiotemporal characteristics of Purkinje cell fate were reported. In contrast, E10.5-E12.5 $Ascl1^{CreER}$ spatiotemporal Purkinje cell fate patterns form distinct anterior-posterior (A-P) stripes that shift in medio-lateral (M-L) axis depending on the day of TMX delivery (74). We examined whether alternative Cre reporters would reveal *Neurog1*-expressing progenitors that give rise to a similarly striped distribution of Purkinje cells.

GIFM using transgenic *Z/EG* reporters results in sporadic Purkinje cell labeling in adult *Neurog1-CreER; Z/EG* mice with TMX injection at E11.5 or E12.5 (Fig. 6a, b). The frequency of EGFP appears comparable to published *Neurog1-CreER*;$R26^{Lacz/+}$ data (35) and differences in the distribution of labeled Purkinje cells were noticeable between *Neurog1-CreER*; *Z/EG* mice injected with TMX on E11.5 or E12.5. With TMX at E11.5, EGFP Purkinje cells were scattered across the full M-L axis of the cerebellum, whereas TMX at E12.5 marked fewer Purkinje cells restricted to the vermis and paravermis (Fig. 6b).

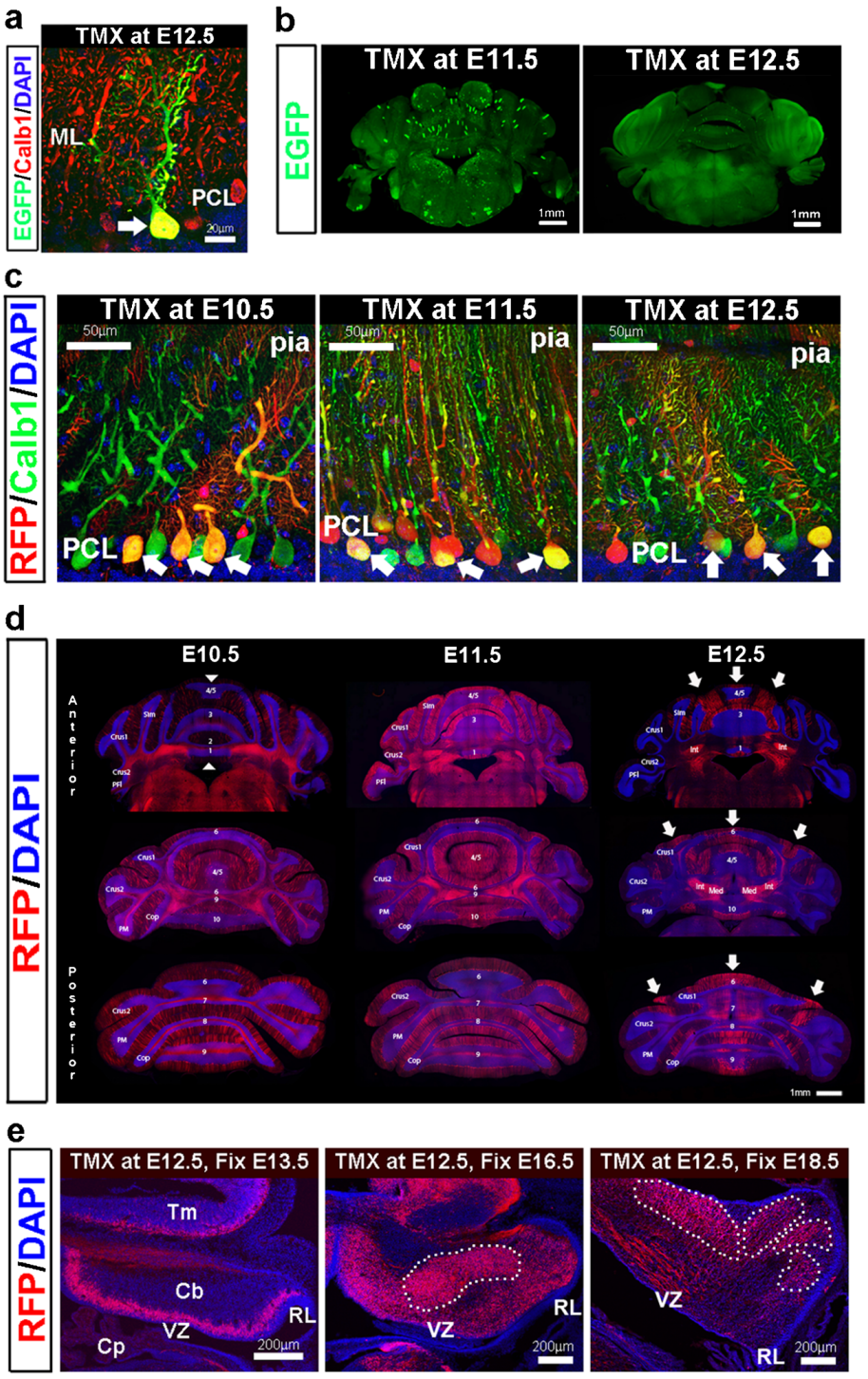

Figure 6. GIFM using the *Neurog1-CreER* transgene fates cerebellar Purkinje cells from E10.5 to E12.5 in mice. All mice were analyzed at P42.
(a) Dual anti-Calb1/anti-EGFP IHC confirms Purkinje cell fate (arrow) in *Neurog1-CreER*;*Z/EG* mice. (b) The distribution of EGFP marked Purkinje cells differs when TMX is given at E11.5 compared to E12.5. (c) Dual anti-Calb1/anti- RFP IHC identifies GIFM Purkinje cells (arrows) in *Neurog1-*

CreER;*R26*$^{td\text{-}Tomato}$ mice given TMX at E10.5, E11.5 or E12.5. Note the increased density of marked Purkinje cells using the *R26*$^{td\text{-}Tomato}$ compared to the *Z/EG* reporter. (d) Patterns of GIFM Purkinje cells following TMX on E10.5, E11.5 or E12.5. Arrow heads denote the narrow midline stripe of RFP- Purkinje cells with TMX at E10.5. E12.5 GIFM Purkinje cells settle in distinct bi-laterally symmetrical parasagittal stripes in the vermis and paravermis of adult *Neurog1-CreER*;*R26*$^{td\text{-}Tomato}$ mice (arrows). (e) E12.5 GIFM Purkinje cells are labeled across the full M-L axis of the E13.5 cerebellum and only aggregate into clusters during later embryogenesis. White dotted lines outline large RFP+ cell clusters. Key: ML, molecular layer; PCL, Purkinje cell layer; pia, pial surface; Med, medial DCN; Int, interposed DCN; Cop, copula of the pyramis; PM, paramedian lobule; PFl, paraflocculus; Sim, simple lobule (lobules annotated 1-10, etc. using (20)); Cb, cerebellum; Cp, choroid plexus; RL, rhombic lip; Tm, tectum; VZ, ventricular zone.

The frequency of Purkinje cell labeling was significantly increased when we used *Neurog1-CreER* GIFM with the knock-in *R26*$^{td\text{-}Tomato}$ reporter to mark cells with RFP. Numerous dual anti-RFP/anti-Calb1 Purkinje cells were present in *Neurog1-CreER*;*R26*$^{td\text{-}Tomato}$ mice given TMX at E10.5, E11.5 or E12.5 (Fig. 6c). TMX at E10.5 resulted in RFP imunolabeled Purkinje cells present across the majority of the M-L and A-P axis with only a narrow parasagittal strip of RFP negative cells present at the midline of the anterior lobes (Fig. 5d, arrow heads). The density of RFP Purkinje cell labeling increased with TMX at E11.5 in which marked Purkinje cells were present throughout the M-L and A-P axis of the adult cerebellum. A-P stripes of RFP negative cells were not present with E11.5 GIFM, although the density of RFP labeled Purkinje cells was reduced in lateral hemispheric regions compared to the vermal/paravermal regions (Fig. 6d).

E12.5 GIFM produced a dramatic change in the distribution of fate-mapped Purkinje cells. Purkinje cells marked at this time point settled in a bi-laterally symmetrical pattern of three parasagittal stripes along the M-L axis in the adult vermis and paravermis (Fig. 6d, arrows). A medial stripe of RFP labeled Purkinje cells spanned

the full A-P axis at the midline and was flanked by two relatively narrow, bi-laterally symmetrical RFP negative A-P stripes within the vermis. These RFP negative stripes were flanked laterally by an A-P stripe of RFP labeled cells at the border of the vermis and paravermis, segregating the RFP labeled population in the anterior vermis into 3 parasagittal RFP+ stripes. The midline RFP+ Purkinje cell population expands along the M-L axis such that the vermis contains a single medial A-P RFP stripe flanked by RFP negative Purkinje cells in the posterior cerebellum. Here the lateral A-P stripe of RFP labeled Purkinje cells is pushed out to the borders of the paravermis with the pontocerebellum where a parasagittal stripe of RFP labeled Purkinje cells runs along crus 1 and medial portions of crus 2, the pyramis and copula. A comparison of E10.5, E11.5 and E12.5 *Neurog1-CreER* GIFM maps (Fig. 6d) supports the view *Neurog1* is expressed in all Purkinje cell progenitors in the developing cerebellum. Of note, the E12.5 GIFM map overlaps the pattern of Purkinje cells marked at earlier time points implying these late fate-mapped Purkinje cells derive from a subset of progenitors in which earlier *Neurog1* expression is maintained past E13. The pattern of RFP+ axons in the deep cerebellar nuclei (DCN) of adult *Neurog1-CreER*;*R26*$^{td\text{-}Tomato}$ indicates E12.5 GIFM Purkinje cells form dense projections to the medial and interposed nuclei (Fig. 6d, see Med and Int annotations).

We next asked if E12.5 *Neurog1-CreER* fate-mapped Purkinje cells result from VZ progenitors organized in M-L stripes of RFP+ progenitors in the VZ. We gave *Neurog1-CreER*;*R26*$^{td\text{-}Tomato}$ mice TMX at E12.5 and fixed the embryos 24 hours post-TMX at E13.5, 4 days post-TMX at E16.5 or 6 days post-TMX at E18.5 (Fig. 6e). We found RFP marked cells were uniformly distributed along the M-L axis of the cerebellar

anlage at E13.5 arguing against any regionalization of *Neurog1*-expressing progenitors. Three days later RFP labeled cells had begun to cluster in the medial, dorsal cerebellum of E16.5 mice. When mice were analyzed at E18.5, the clustering of RFP marked cells was more distinct with 3-4 clusters of cells traceable in the dorsal cerebellum (Fig. 6e). The dispersal pattern of RFP marked cells following TMX demonstrates E12.5 GIFM Purkinje cells are generated uniformly from *Neurog1*-expressing progenitors in the VZ but aggregate into clusters along the M-L axis during late embryonic development. We also compared the adult distribution of E12.5 GIFM Purkinje cells with known Purkinje cell subtype markers Zebrin II (Aldolase C), Hsp25 and PLCβ4 using dual IHC but this did not reveal any noticeable correlation in RFP+ Purkinje cell distribution with the three markers (Supplementary Fig. 14).

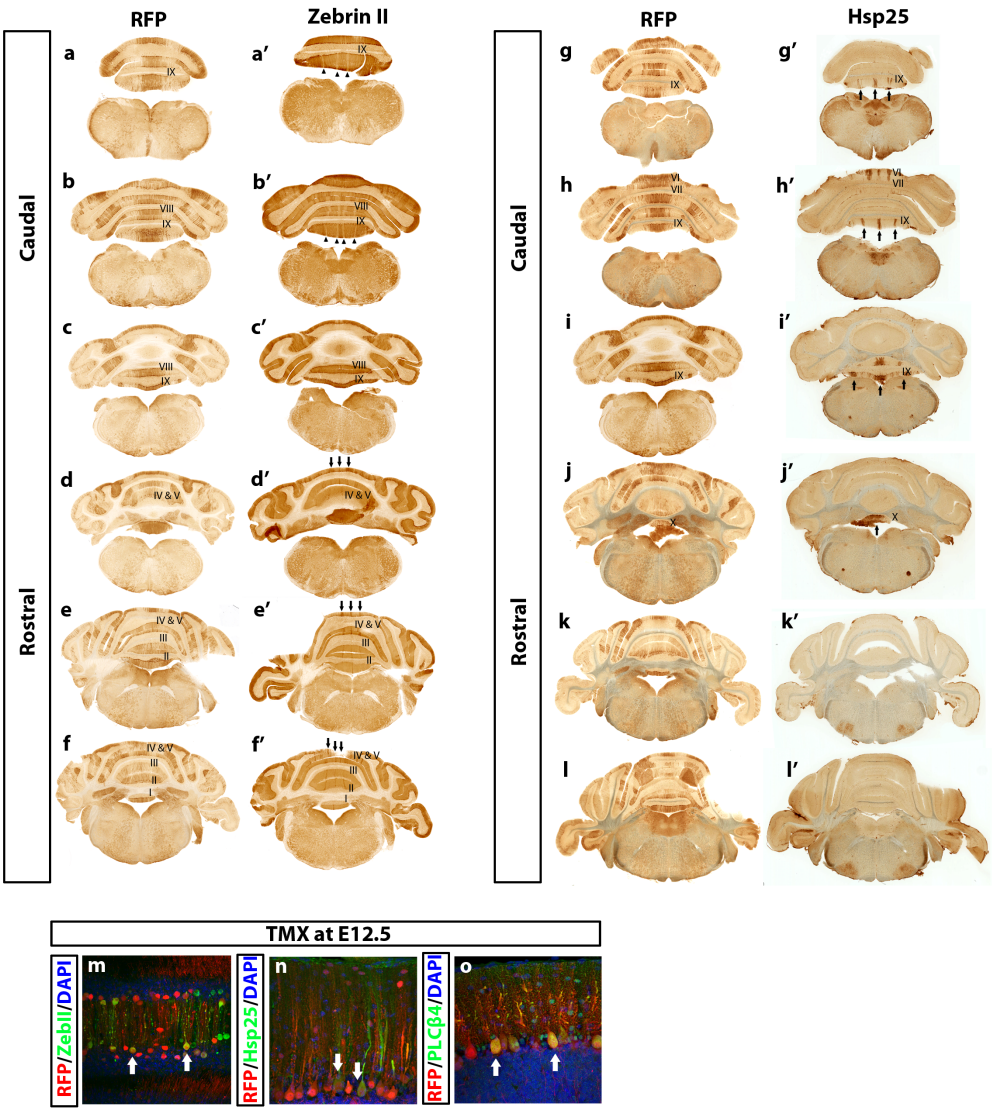

Supplementary Figure 14. Patterns of GIFM Purkinje cells following TMX on E12.5 do not coincide with expression patterns of Zebrin II or Hsp25.
Coronal sections through the rostro-caudal axis of the cerebellum were immunostained using ABC enhancement. All mice were analyzed at P42. Note there are some detachments from whole cerebellar sections during the IHC process such as the paraflocculus (e', f), simple lobule and Crus 1 (e', l, l'), or middle cerebellar peduncle region (e). Missing fragments do not interfere with our expression pattern analysis, which is focused on the vermis. E12.5 GIFM Purkinje cells settle in three parasagittal stripes along the medio-lateral axis of the adult vermis and paravermis (a-l). Consecutive slices were analyzed for Zebrin II and Hsp25 expression patterns. Multiple Zebrin II negative stripes (arrow heads) appear in lobules VIII and IX (a'-b') and three distinct Zebrin II positive stripes (arrows) appear in lobules I-V (d'-f'). Three Hsp25 positive stripes (arrows) appear in lobules VI, VII, IX and X (g'-j') and Hsp25 is not expressed in rostral sections (k'-l'). Dual IHC reveals RFP labeled Purkinje

cells expressing Zebrin II (m) or Hsp25 (n) indicated with arrows. (o) Although PLCβ4 expression patterns do not compliment GIFM Purkinje cells, dual anti-RFP/anti-PLCβ4 Purkinje cells are present in lobule VIII.

In addition to Purkinje cells, we observed RFP marked cells in the molecular layer (ML) (see Fig. 6c), and less frequently, in the granule cell layer (GL) in *Neurog1-CreER*;*R26*$^{td\text{-}Tomato}$ mice given TMX at E10.5-E12.5. Such early fate-mapping of basket and stellate cells was particularly unexpected and yet dual IHC with anti-Parvalbumin (anti-Pvlb) antibodies, a marker of basket and stellate cells in the cerebellum, confirms the identity of these cells (Supplementary Fig. 15). Similarly, dual IHC with Golgi cell marker anti-Neurogranin (anti-Nrg) antibodies confirm Golgi cell fates in E10.5-E12.5 GIFM mice (Supplementary Fig. 15). However, RFP expressing cells were also present in the ML and GL of adult *Neurog1-CreER*;*R26*$^{td\text{-}Tomato}$ mice injected with sunflower oil on E10.5-E12.5 (Supplementary Fig. 15). In contrast, no RFP-labeled cells with Purkinje cell morphology or anti-Calb1 immunoreactivity were detected in these controls (Supplementary Fig. 15). Combined these control data indicate GIFM is specific to Purkinje cell lineages in *Neurog1-CreER*;*R26*$^{td\text{-}Tomato/+}$ mice but RFP reporter expression occurs independent of TMX delivery in some basket, stellate and Golgi cells. Lastly, although E10.5 to E12.5 TMX delivery spans the period of deep cerebellar nuclei (DCN) neurogenesis (10), we did not fate-map cells in the DCN. This is in contrast to GIFM for the gene family member *Neurog2* using a knock-in *Neurog2*$^{CreER/+}$allele in which TMX on E11.25 to E12.25 fates GABAergic projection neurons in the DCN (19). Ascl1 GIFM at E10.5-E12.5 also labels DCN interneurons (74) in contrast to our findings.

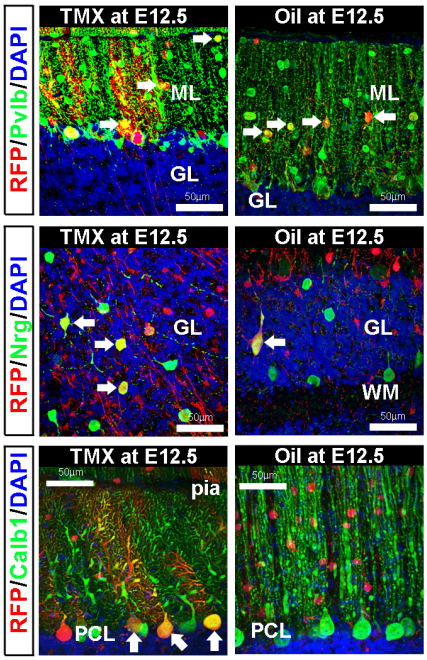

Supplementary Figure 15. GIFM is specific to Purkinje cell lineages in *Neurog1-CreER*;*R26*$^{td\text{-}Tomato/+}$ mice but RFP reporter expression occurs independent of TMX delivery in some basket, stellate and Golgi cells. *Neurog1-CreER*;*R26*$^{td\text{-}Tomato/+}$ mice administered with TMX or sunflower oil only on E12.5 were analyzed at P42. Dual IHC for RFP with the basket and stellate cell marker Pvlb or the Golgi cell marker Nrg co-labels RFP interneurons in mice injected with TMX or sunflower oil (arrows). Leaky RFP labeling in sunflower oil controls is more numerous in basket and stellate cell interneurons compared to Golgi cells. In contrast, RFP is not detected in Calb1+ Purkinje cells in the absence of TMX administration.

Overlapping *Neurog1* and *Ascl1* expression in Purkinje cell progenitors

Our E10.5-E12.5 GIFM data is similar to age matched *Ascl1*^{CreER} spatiotemporal Purkinje cell fate-map patterns produced by Sudarov and colleagues (74), suggesting co-expression of Neurog1 and Ascl1 in Purkinje cell progenitors in the VZ. Indeed an earlier ISH study has revealed overlapping expression patterns of multiple proneural bHLH transcription factors in the cerebellar VZ (91). We examined this possibility further by performing a detailed series of ISHs for both Neurog1 and Ascl1 in E12.5 mice. Neurog1 and Ascl1 probes were hybridized single-plex on adjacent tissue sections for comparison

or in duplex using fluorescent ISH. The data revealed overlapping patterns of Neurog1 and Ascl1 ISH in the E12.5 cerebellar VZ (Fig. 7). The medial and lateral boundaries of Neurog1 and Ascl1 ISH matched with both hybridization signals absent from both the rhombic lip and midline and there was no observable difference in the rostro-caudal distribution of Neurog1 and Ascl1 hybridization signal (Fig. 7a – h'). Dual fluorescent ISH confirms overlapping Neurog1 and Ascl1 expression in progenitor cells and suggests progenitors transition from Ascl1 to Neurog1 expression as they migrate dorsally from the VZ – the Neurog1 ISH territory overlaps but is shifted slightly dorsal to the Ascl1 ISH territory that predominates at the VZ (Fig. 7i-k').

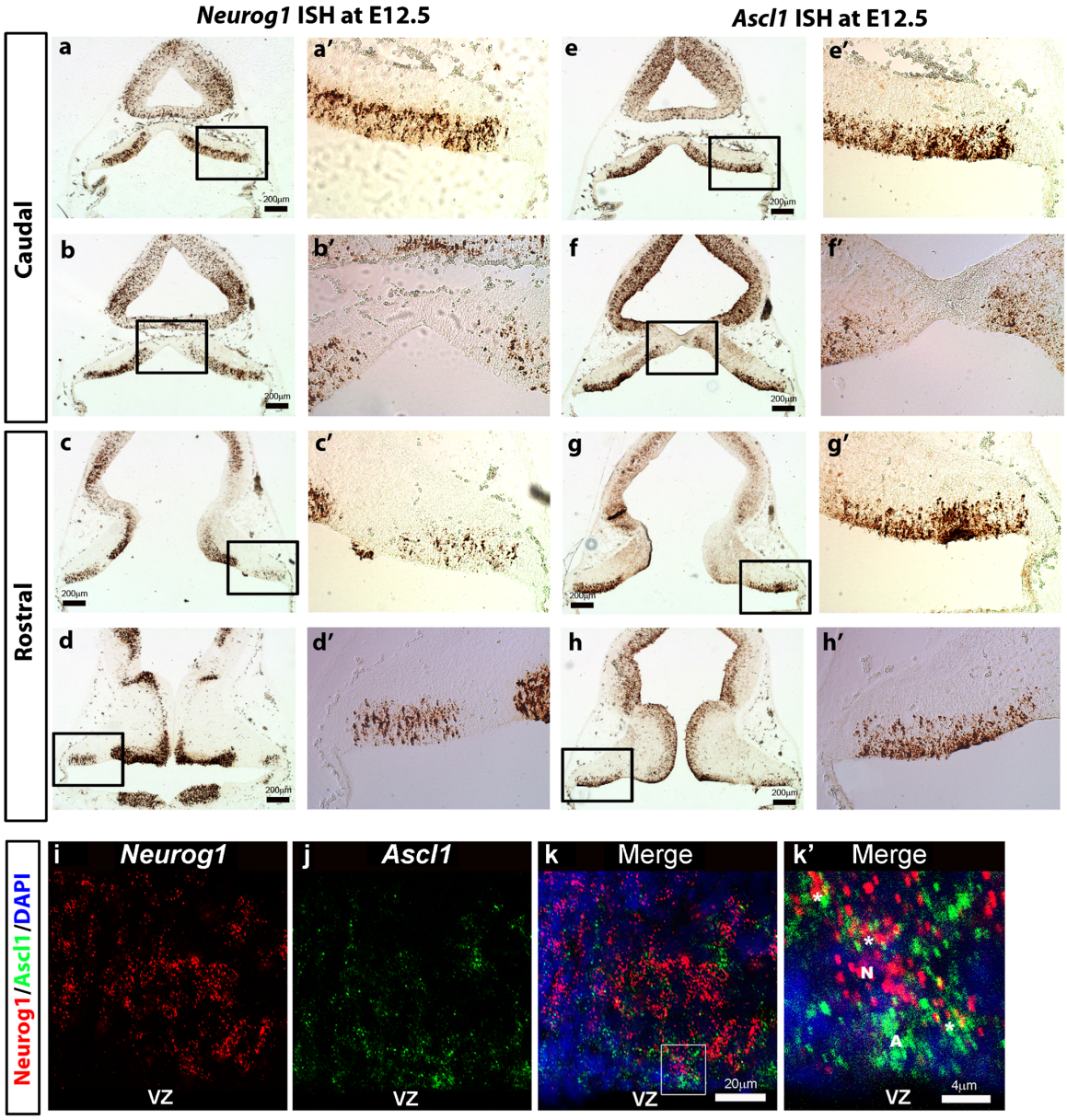

Figure 7. Overlapping *Neurog1* and *Ascl1* expression patterns in the ventricular zone of the cerebellar anlage at E12.5.

(a-h') Adjacent coronal sections were analyzed by single-plex ISH. Neurog1 (a-d) is expressed in progenitor populations that overlap with regions of Ascl1 (e-h) expression. Higher magnification images (a'-h') of the boxed regions in a-h show expression of Neurog1 and Ascl1 extending along the lateral (a' and e', c' and g') and medial (b' and f') axis of the VZ but absent from the rhombic lip and midline. (i-k') 2-plex-fluorescence ISH confirms overlapping expression of Neurog1 and Ascl1 in progenitors. Note the Ascl1 expression territory is slightly ventral to but overlaps the Neurog1 expression territory. The boxed area in image panel k is shown at higher magnification in k'. Key: A; Ascl1 ISH in a VZ progenitor; N, Neurog1 ISH in a VZ progenitor; asterisk, dual Ascl1/Neurog1 ISH in VZ progenitors.

Neurog1-CreER GIFM transitions from Purkinje to Golgi cell interneuron fates beginning ≈ E11.75

Cell birth dating and GIFM studies report inhibitory interneuron production commences E13 in mice following the production of Purkinje cells (44; 74). In agreement with these studies we see a shift away from Purkinje cell to other cell fates when we give *Neurog1-CreER*;*R26*$^{td\text{-}Tomato}$ mice TMX at E13.5. Only occasional, isolated RFP labeled Purkinje cells were detected in adult mice with TMX delivery at E13.5, most of which were present at the midline and all located in the vermis and paravermis. Indeed E13.5 GIFM Purkinje cells constituted < 0.5% of all Purkinje cells fate-mapped with TMX given at E10.5 to E13.5 in *Neurog1-CreER*;*R26*$^{td\text{-}Tomato}$ mice. In contrast RFP labeling in the adult granule cell layer (GL) increased significantly with TMX at E13.5 (Fig. 8a). RFP labeled cells in the GL contained soma larger than the surrounding granule cells and sparsely branched dendrites ascending to the ML, morphology consistent with a Golgi cell fate. This was confirmed with co-labeling with anti-Nrg (Fig. 8b, arrow). RFP marked basket and stellate cells in the ML were also present in adult *Neurog1-CreER*;*R26*$^{td\text{-}Tomato}$ mice given TMX at E12.5 (see Fig. 6a).

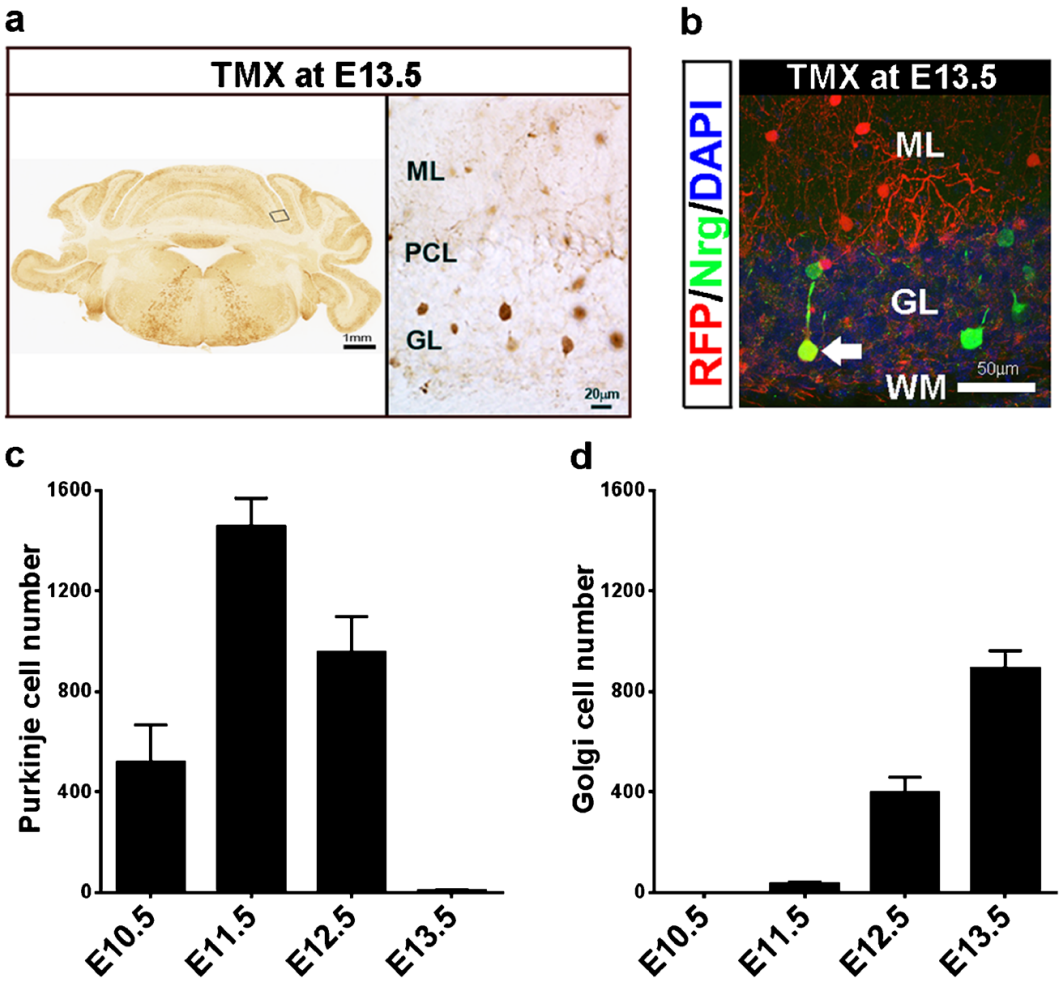

Figure 8. *Neurog1-CreER*;*R26*$^{td\text{-}Tomato}$ GIFM transitions from Purkinje to Golgi cell fate with TMX injection at E13.5.

All mice were analyzed at P42. (a) Anti-RFP IHC using ABC enhancement reveals extensive interneuron but negligible Purkinje cell fate-mapping with TMX at E13.5. The left panel shows a low magnification view of the whole cerebellum with the area shown in higher magnification to the right outlined. (b) Dual anti-Nrg/anti-RFP IHC confirms Golgi cells (arrow) are labeled with TMX at E13.5. (c) Quantification of RFP marked cells with Purkinje cell morphology. Purkinje cell GIFM peaks with TMX at E11.5 in *Neurog1-CreER*;*R26*$^{td\text{-}Tomato}$ and declines rapidly to less than 1% of total labeled Purkinje cells with TMX at E13.5. (d) Quantification of RFP marked cells with Golgi cell morphology. Golgi cells are first labeled with TMX at E11.5 and Golgi cell GIFM progressively increases from E11.5 to E13.5 as Purkinje cell fate declines. Histogram plots are mean plus standard error of the mean (SEM) error bar above ($n \geq 3$ except E13.5 $n = 2$). Key: ML, molecular layer; PCL, Purkinje cell layer; GL, Granule cell layer; WM, white matter tracts.

In view of the leaky RFP expression in Golgi, basket and stellate cells, we compared the number of cells with Golgi, basket and stellate cell morphology in *Neurog1-CreER*;*R26*$^{td\text{-}Tomato}$ mice given TMX or sunflower oil to determine the contribution of leaky RFP expression to interneuron cell fate. Mice were given sunflower oil only on E10.5, E11.5, E12.5 or E13.5 and the numbers of RFP+ neurons quantified and compared to TMX injected mice at P42. The data reveal TMX-independent RFP expression accounted for all of the Golgi cells present in *Neurog1-CreER*;*R26*$^{td\text{-}Tomato}$ mice given TMX at E10.5 (7.5 ± 1.6 oil versus 7.2 ± 3.4 TMX, n = 3), 43.1 ± 8.8% of Golgi cells present when TMX was administered at E11.5 (16.7 ± 2.2 oil versus 50.0 ± 17.7 TMX, n = 3), 9.3 ± 2.2% of Golgi cells with TMX at E12.5 (14.7 ± 2.5 oil versus 161.8 ± 3.4 TMX, n = 3) and 6.0 ± 0.3% of Golgi cells present with TMX at E13.5 (12 ± 4.0 oil versus 263 ± 66.2 TMX, n = 3 oil, n = 2 TMX). In contrast, basket and stellate cells were present in equal frequency in TMX or sunflower oil controls at each of the administration dates indicating TMX-independent expression accounted for all *Neurog1-CreER* GIFM basket and stellate cells with E10.5-E13.5 GIFM. We conclude Golgi cells, but not basket or stellate cells, are fate-mapped during early cerebellar development in *Neurog1-CreER*;*R26*$^{td\text{-}Tomato}$ mice and that Golgi cell fate commences with TMX at E11.5 and becomes the majority cell fate with TMX at E13.5

We compared the number of Purkinje cells and Golgi in *Neurog1-CreER*;*R26*$^{td\text{-}Tomato}$ mice given TMX at E10.5-E13.5 to measure the transition in *Neurog1-CreER* cell fate. Cell counts were corrected for the mean % leaky RFP expression in control mice injected with oil only at that age, for example E13.5 GIFM Golgi cell numbers were reduced 6% to generate a number representing TMX-induced RFP expression in this cell

lineage. The numbers reveal Purkinje cell GIFM increases from E10.5 to a peak with TMX at E11.5. RFP marked Purkinje cell numbers then decline by 35% with E12.5 GIFM and Purkinje cell numbers decline further to < 0.5% total when TMX is administered at E13.5 (Fig. 8c). Thus, peak *Neurog1* expression in Purkinje cell progenitors coincides with the mid-period of Purkinje cell neurogenesis at E11.75-E13.25 (10). In contrast, Golgi cell GIFM numbers progressively increase with TMX administration from E11.5 to E13.5 (Fig. 8d). When expressed as a percentage of the two RFP cell fates in the cerebellar cortex, Golgi cells represent 2% of the total when TMX is delivered at E11.5, 29% with TMX at E12.5 and 99% with TMX at E13.5. These cell counts demonstrate progenitors expressing *Neurog1* transition from Purkinje to Golgi cell fates from ≈ E11.75-E15.25 with the largest transition occurring from ≈ E13.75-E15.25.

Temporal *Neurog1-CreER* GIFM marks exclusively interneurons from E14.5 to P7

Short-term *Neurog1* fate-mapping using a *Neurog1-EGFP* BAC transgene labels multiple GABAergic interneuron cell types in the GL, Purkinje cell layer (PCL) and ML of the cerebellar cortex (45). GABAergic interneurons are born in an inside-to-outside temporal pattern in the cerebellum with interneurons in the GL developing prior to those in the outer ML (43; 44). Temporal $Ascl1^{CreER}$ GIFM produces a comparable inside-to-outside pattern of GABAergic interneurons in the adult cerebellum (74). We speculated *Neurog1-CreER* GIFM would similarly fate GABAergic interneurons in later embryogenesis and early postnatal development. We used *Neurog1-CreER*;*Z/EG* and *Neurog1-CreER*;$R26^{td\text{-}Tomato}$ mice to map interneuron fate in adult mice. As was the case for Purkinje cell labeling, *Neurog1-CreER*;*Z/EG* labels interneurons with less frequency than *Neurog1-CreER*;$R26^{td\text{-}Tomato}$ mice. However, unlike *Neurog1-CreER*;$R26^{td\text{-}Tomato}$ mice,

reporter labeled interneurons were not detected in significant numbers in *Neurog1-CreER*;*Z/EG* mice not given TMX (≤ 3 EGFP cells per cerebellar section were detected in the PCL or ML). We administered TMX to *Neurog1-CreER*;*Z/EG* mice at E14.5, E16.5, E18.5, P0 or P7 and determined GIFM cell types in the cerebellum of a single adult mouse for each GIFM. Cell fate was determined by topography, key morphological characteristics and, when available, cell-type specific antibodies (see Methods).

When TMX was given at E14.5 to *Neurog1-CreER*;*Z/EG* mice, only Golgi cell fates were identified in the cerebellar cortex, confirming the transition to Golgi cell fate was complete at this stage (Fig. 9a). Golgi cells still constituted the most common labeled cell type when TMX was administered at E16.5 but EGFP marked cells of either candelabrum and Lugaro morphology were also present in the Purkinje cell layer (PCL) (Fig. 9b). Candelabrum and Lugaro interneurons were the majority fate-mapped cell type with TMX at E18.5 (not shown). TMX at P0 primarily labeled cells in the inner ML with basket cell characteristics (Fig. 9c). In contrast, cells in the outer ML with stellate cell characteristics were the majority cell type labeled with TMX at P7 (Fig. 9e). Interestingly, GIFM from E11.5 to P7 did not label cells in the white matter tracts of the adult cerebellum and no reporter gene expressing cells exhibited astrocyte-like morphology in either *Neurog1-EGFP* or *Neurog1-CreER*;*R26*$^{td\text{-}Tomato}$ mice. IHC with antibodies to the oligodendrocyte marker Olig2 as well as the glial cell markers glial fibrilliary acidic protein (GFAP) and anti-S100β confirmed no oligodendrocytes or glia were fate-mapped in *Neurog1-CreER*;*R26*$^{td\text{-}Tomato}$ mice with TMX delivery at E13.5 or E18.5 (not shown). Combined these data demonstrate *Neurog1-CreER* mice fate map interneurons but not glial cell types of the cerebellar cortex and suggest that the timing of

Neurog1 expression in GABAergic interneurons correlates with their final resting position in the cerebellar cortex.

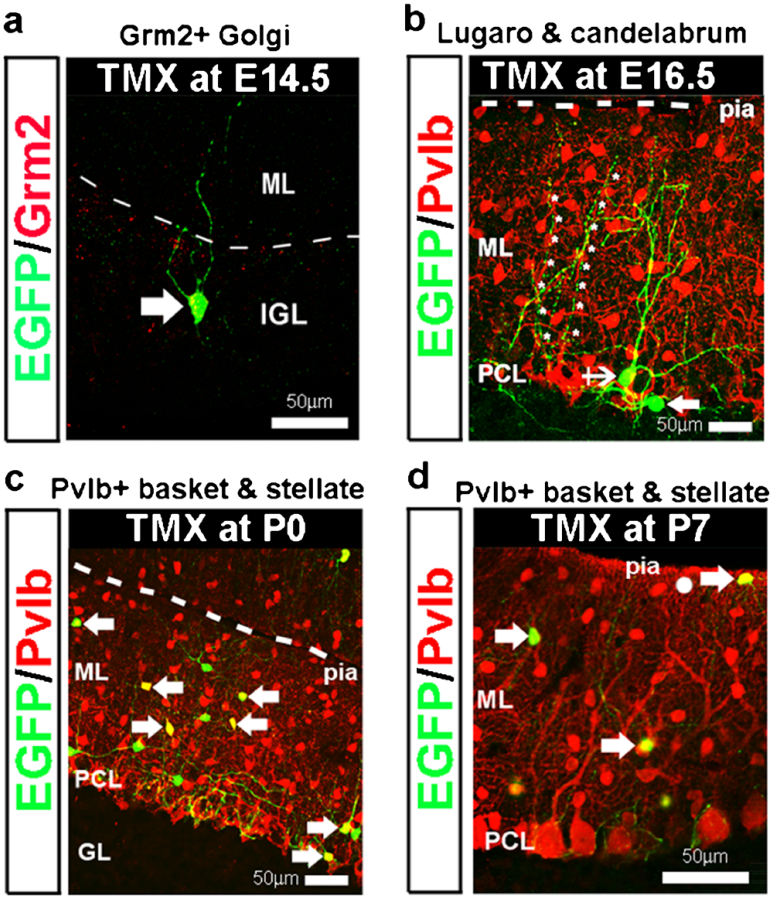

Figure 9. E14-.5 to P7 *Neurog1-CreER* GIFM labels interneurons in an inside-to-outside settling pattern in the adult cerebellar cortex.
All mice were analyzed at P42. (a) Dual IHC reveals EGFP labeled cells with TMX at E14.5 express the Golgi cell subset marker Grm2 (arrow). White hashed line indicates the Purkinje cell layer. (b) TMX at E16.5 labels EGFP+ cells with Lugaro cell (arrow) and candelabrum cell (crossed arrow) morphology. Note the characteristic beaded axonal arborization (asterisks) of the candelabrum cell. Both cells are not immunolabeled with antibodies to Pvlb, a marker for basket and stellate cell interneurons. (c and d) Dual Pvlb+/EGFP+ basket and stellate cells (arrows) with TMX at P0 or P7. Key: GL, granule cell layer; ML, molecular layer; PCL, Purkinje cell layer.

Co-expression of *Neurog1* and *Ascl1* in interneuron progenitors

The spatiotemporal sequence of *Neurog1-CreER* GIFM in interneurons show similarities to the detailed spatiotemporal *Ascl1*^{CreER} fate map produced by Sudharov and

colleagues and supports the finding by these authors (74) that PCL Lugaro and candelabrum interneurons follow the same spatiotemporal maturation pattern as other GABAergic interneurons. These similarities suggest co-expression of *Neurog1* and *Ascl1* in GABAergic interneuron progenitors. We examined this possibility by ISH in E13.5 and P0 mice. Neurog1 and Ascl1 probes were hybridized single-plex on adjacent tissue sections for comparison or in duplex using fluorescent ISH. Single-plex ISH revealed overlapping patterns of Neurog1 and Ascl1 ISH in the E13.5 cerebellar VZ (Fig. 10a-b') and the presumptive white matter tracts of the cerebellum of P0 mice (Fig. 10c-d'). Co-expression of Neurog1 and Ascl1 in progenitor cells was confirmed by dual fluorescent ISH labeling of E13.5 (Fig. 10e-g'') and P0 (Fig. 10h-j') cerebellum. Interestingly, P0 ISH patterns indicate more widespread Ascl1 expression in interneuron progenitors – Neurog1 ISH is primarily localized to the presumptive white matter tracts whereas Ascl1 ISH extends throughout the nascent cortex to the external germinal layer, consistent with more prolonged Ascl1 expression in developing GABAergic interneuron cell lineages.

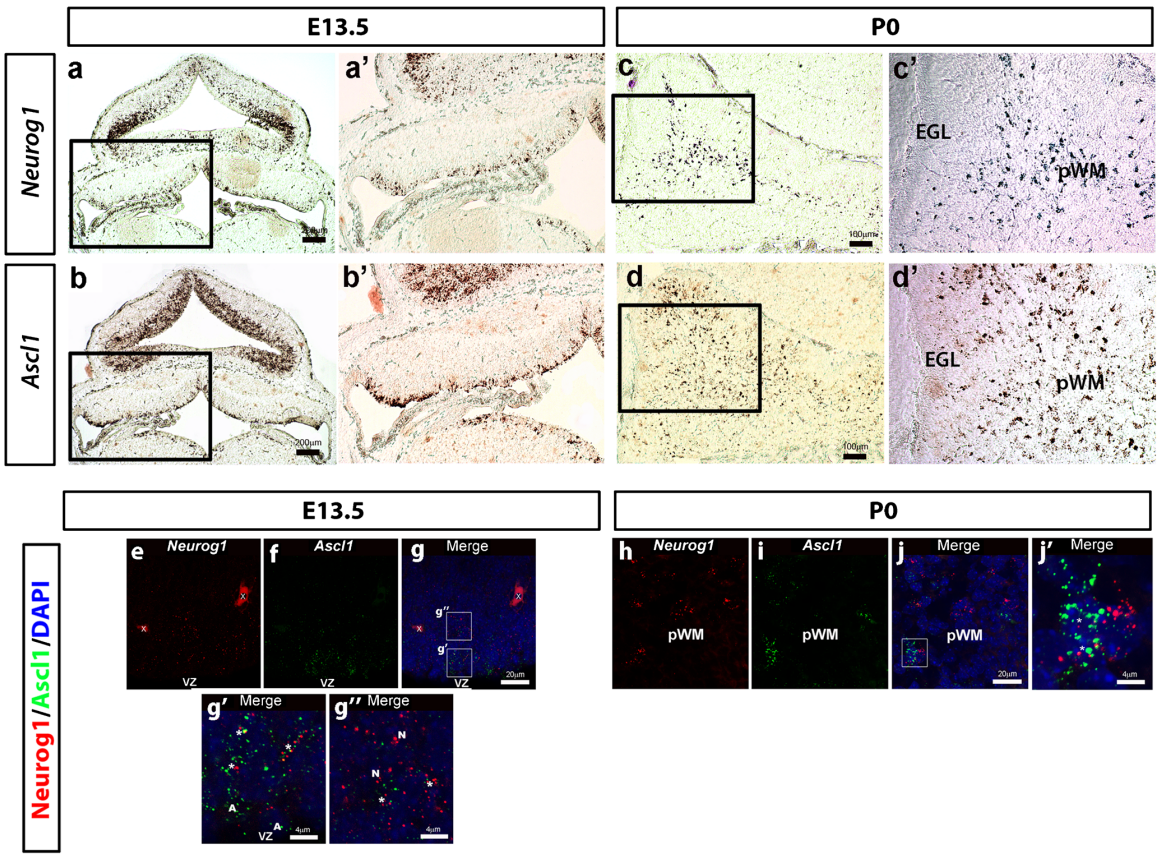

Figure 10. Similarities in the spatiotemporal pattern of Neurog1 with Ascl11 (see (74)) are supported by ISH data showing overlapping expression of the two bHLH transcription factor genes.
(a-d') Adjacent coronal sections were analyzed by single-plex ISH. Overlapping Neurog1 (a, c) and Ascl1 (b, d) expression in the VZ and developing cerebellar cortex of E13.5 and P0 mice. Higher magnification images (a', b', c' and d') of the boxed regions in a-d. (e-j') 2-plex-fluorescence ISH confirms co-expression of Neurog1 and Ascl1 in E13.5 and P0 progenitors. (g' and g'') Shows two boxed areas in image panel g at higher magnification to illustrate the transition from Ascl1 to dual Ascl1/Neurog1 to Neurog1 expression as VZ progenitors exit the VZ. X denote non-specific binding of the fluorescent red detection probe. (h-j') The boxed area in image panel j is shown at higher magnification in j'. Key: A; Ascl1 ISH in a VZ progenitor; EGL, external granule cell layer; pWM, presumptive white matter tracts; N, Neurog1 ISH in a VZ progenitor; asterisk, dual Ascl1/Neurog1 ISH in VZ progenitors.

Neurog1 is expressed in Purkinje cells around the time they become post-mitotic but in mitotic and post-mitotic interneurons

GIFM confirms *Neurog1* expressing progenitors initially give rise to Purkinje cells and then to an overlapping sequence of multiple interneuron cell types in the

cerebellum. We investigated the timing of *Neurog1-CreER* expression in progenitor cells, choosing the period of transition from Purkinje to Golgi cell fate (TMX E11.5-E13.5) and a later developmental period at which multiple interneuron cell types are labeled in the cerebellar cortex (TMX at E18.5). TMX was administered to pregnant dams and *Neurog1-CreER*;*R26*$^{td\text{-}Tomato}$ embryos were harvested 24 hours later for IHC with anti-Ki67 antibodies to determine the mitotic status of labeled cells (Ki67 is expressed during all phases of the cell cycle except the resting phase). A second set of pregnant dams were injected with sunflower oil only and *Neurog1-CreER*;*R26*$^{td\text{-}Tomato}$ embryos harvested 24 hours later to control for leaky RFP expression. Control mice harvested at E13.5 and E14.5 contained RFP reporter expression in peripheral ganglia, spinal cord, brain stem and midbrain but not the cerebellum. These same CNS sites exhibited RFP expression in controls analyzed at birth (P0) plus a few (3-5 per coronal cerebellar section) scattered RFP+ cells in the intermediate zone of the cerebellum. These controls reveal leaky RFP expression in the cerebellum commences during late embryogenesis and suggest the great majority of RFP+ interneurons present in oil only adult controls derive from postnatal reporter gene expression. Accordingly we concluded leaky expression of the RFP reporter would not undermine our analysis.

Dual anti-Ki67/anti-RFP IHC revealed minimal Ki67 expression in RFP marked cells in embryos given TMX at E11.5 and E12.5 with a thin zone of non-immunoreactivity separating Ki67+ cells at the VZ from RFP+ cells in the cerebellar primordium (Fig. 11a). Ki67+ and RFP+ cells abut when TMX is delivered a day later at E13.5 (Fig. 11a). In contrast, co-mingling of the two immunosignals is widespread when TMX is given at E18.5 in which dual Ki67+/RFP+ marked cells are found adjacent to the

VZ and in cells streaming toward the cerebellar cortex along the presumptive white matter tracts (pWM, Fig. 11a). Quantification of the number of RFP marked cells expressing Ki67 confirms a significant increase in the percentage of mitotic cells with GIFM at E18.5 ($p < 0.001$) compared to earlier GIFM dates - the percentage of RFP marked cells expressing Ki67 remains low at 2.9 to 6.8% when TMX was administered during E11.5 to E13.5 but increases substantially to 51% when TMX is administered at E18.5 (Fig. 11b). Dual IHC with anti-Pax2 antibodies, a marker for GABAergic interneuron progenitors in the cerebellum (51), confirms E18.5 labeled RFP+ cells express Pax2. Taken together these results demonstrate a significant increase in *Neurog1-CreER* expression in mitotic GABAergic interneuron progenitor cells during late embryonic development.

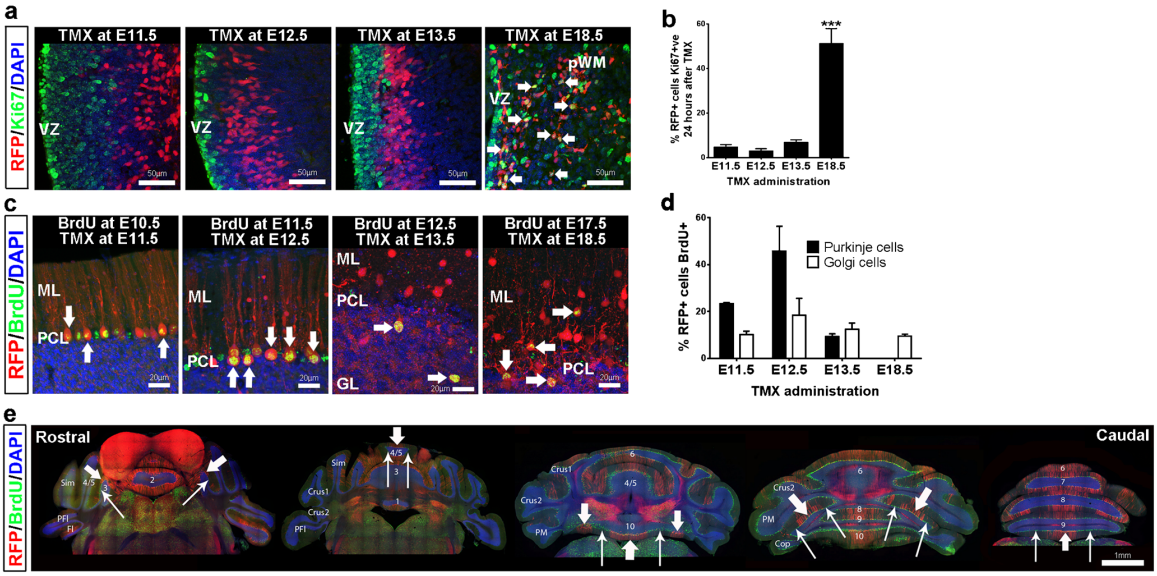

Figure 11. *Neurog1* is expressed in Purkinje cells around the time they become post-mitotic and in mitotic and post-mitotic interneurons.
(a, b) *Neurog1-CreER;R26*$^{td\text{-}Tomato}$ mice processed for dual anti-RFP/anti-Ki67 IHC 24 hours after TMX delivery. (a) Dual RFP+/Ki67+ cells are indicated by arrows. (b) Quantification confirms a significant increase in the percentage of RFP+ cells expressing Ki67 with GIFM at E18.5 (***$p < 0.001$, 1-way ANOVA with Tukey's multiple comparisons test, $n \geq 3$). (c, d, e) *Neurog1-CreER;R26*$^{td\text{-}Tomato}$ mice given BrdU 24 hours before TMX delivery and

processed for dual anti-RFP/anti-BrdU IHC at P42. (c) Dual RFP+/BrdU+ cells are indicated by arrows. (d) A quantitative comparison of the percentage of RFP+ cells immunoreactive for BrdU reveals higher BrdU retention in RFP marked Purkinje cells (n = 3 except E13.5 n = 2). (e) Patterns of BrdU and RFP immunolabeled Purkinje cells in adult mice do not reveal a relationship between the two markers when BrdU is injected 24 hours before a TMX delivery. Arrows indicate regions of BrdU+/RFP- Purkinje cells (slender arrows) adjacent to BrdU+/RFP+ Purkinje cells (thick arrows) within the same lobule.

We hypothesized the low percentage of dual RFP+/Ki67+ cells 24 hours post E11.5-E13.5 TMX were the result of *Neurog1-CreER* expression in progenitors around the time they exit cell division. To test this hypothesis we injected pregnant dams with BrdU the day before TMX and quantified the percentage of RFP marked cells immunolabeled with anti-BrdU antisera at P42. In this analysis, long-term BrdU retention resulting in anti-BrdU immunoreactivity at P42 would identify cells undergoing terminal cell division the day before genetic marking. We found BrdU was retained in 23 ± 0.5% of Purkinje cells marked with TMX at E11.5 and BrdU retention increased to 45 ±10.5% of Purkinje cells when TMX was administered at E12.5 (Fig. 11c arrows, d). Purkinje cell fating declines dramatically with TMX administration at E13.5 (< 0.5% of GIFM total) and 9.3 ±1.2% of these few late marked cells were BrdU+ (Fig. 11d). Thus high percentages of BrdU retention were observed in Purkinje cells during the period of greatest genetic marking (TMX at E11.5 or E12.5) consistent with many Purkinje cells undergoing terminal cell division in the day before GIFM. BrdU retention in interneurons fate-mapped to the cerebellar cortex was at a lower rate than in Purkinje cells but more constant with 10.6 ±1.2% to 18 ±7.3% of fate-mapped Golgi cells BrdU+ for each of the genetic marking days analyzed (Fig 11c, d). Combined Ki67 and BrdU cell counts support the view *Neurog1* is expressed in Purkinje cells around the time they become

post-mitotic whereas Neurog1 is expressed in mitotic and non-mitotic interneuron progenitors.

We next mapped BrdU retention and RFP marking in Purkinje cells to determine the spatial relationship between Purkinje cell birth and *Neurog1* expression. BrdU is retained in Purkinje cells located in the vermis and hemispheres of the adult cerebellum of mice injected at E10.5 or E11.5 using our injection protocol. A comparison of the adult patterns of BrdU and RFP immunolabeled Purkinje cells reveals BrdU+ and RFP+ Purkinje cell distributions do not match when BrdU is injected the day before TMX delivery on either E11.5 (not shown) or E12.5 (Fig. 11e). Dual RFP+/BrdU+ Purkinje cells (Fig. 11e, thick arrows) are located adjacent to RFP-/BrdU+ Purkinje cells (Fig. 11e, slender arrows) within the same lobules. These data reveal not all Purkinje cells born around the same time express *Neurog1* the following day.

GABAergic interneuron progenitors in the presumptive white matter tracts enter the cell cycle around the time they express *Neurog1*

Our analysis of Ki67 expression in GIFM cells suggests large numbers of E18.5 fate-mapped GABAergic interneuron progenitors proliferate around the time they express *Neurog1*. To test this hypothesis, mice were pulsed with BrdU the day following TMX administration and fixed 24 hours later for dual anti-RFP/anti-BrdU IHC. We chose two GIFM time points for BrdU delivery 24 hours post-TMX, E18.5 and E11.5 GIFM that fate interneurons and Purkinje cells respectively. As expected from the Ki67 data, cell counts reveal low numbers of 7.3 ± 1.5% (n = 2) of RFP+ cells at E13.5 immunopositive for BrdU following TMX delivery on E11.5 and BrdU on E12.5 (Fig. 12a). In contrast, 41.5 ± 5.6% (n = 3) of RFP+ cells in P1 neonates were immunolabeled with anti-BrdU antisera following TMX on E18.5 and BrdU on P0 (Fig. 12b). Triple IHC with Pax2

antisera confirms the majority of the RFP+/BrdU+ cells in the cerebellum of P1 neonates were GABAergic interneuron progenitors migrating to final destinations in the cerebellar cortex (Fig. 12c). These data support the view that *Neurog1* is expressed in cycling interneuron progenitor cells during later phases of neurogenesis in the pWM of the cerebellum. In contrast, long-term BrdU retention in adult Purkinje cells and low rates of either anti-BrdU or anti-Ki67 immunolabeling in RFP+ Purkinje cell progenitors are all consistent with the idea that *Neurog1* is expressed in VZ Purkinje cell progenitors around the time they become post-mitotic.

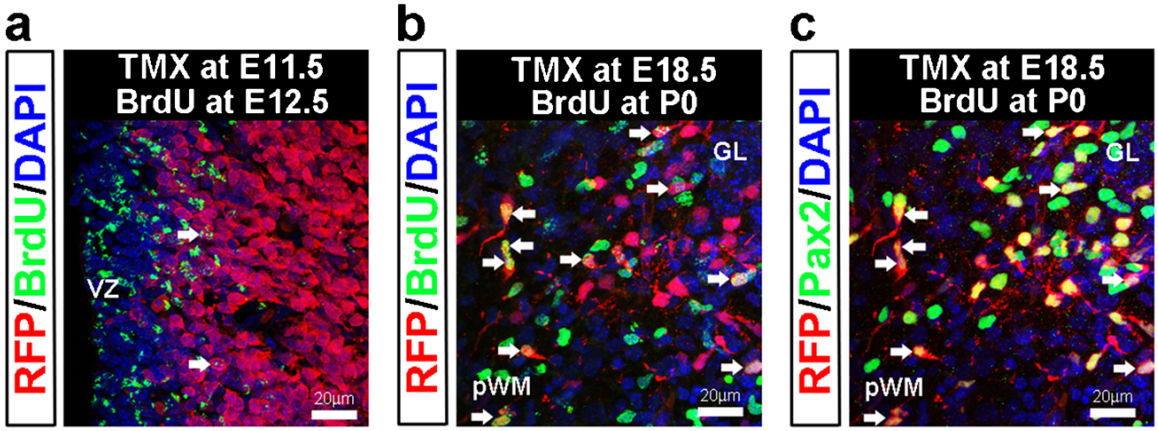

Figure 12. Mitotic GABAergic interneuron progenitors express *Neurog1*. *Neurog1-CreER*;*R26*$^{td\text{-}Tomato}$ mice were administered TMX at E11.5 or E18.5 and BrdU the following day. Mice were fixed the day after BrdU injection. (a) BrdU labels multiple progenitors in the E13.5 ventricular zone (VZ) but few RFP marked cells are immunoreactive for BrdU (arrows). (b) Multiple RFP+/BrdU+ interneuron progenitors (arrows) in the presumptive white matter tracts (pWM) of a P1 *Neurog1-CreER*;*R26*$^{td\text{-}Tomato}$ mouse. (c) Co-immunolabeling with Pax2 antibodies confirms the majority of the RFP+/BrdU+ cells in the cerebellum of P1 neonates are GABAergic interneuron progenitors. Panels b and c are taken from the same section processed for triple anti-RFP/anti-BrdU/anti-Pax2 IHC.

Neurog1-CreER GIFM labels DCN interneurons during late embryogenesis

Neurog1-CreER;*Z/EG* GIFM resulted in low level fate-mapping of cells with neuronal morphology in the DCN with TMX injected at E14.5 or older with the majority of cells fate marked with TMX E14.5 to E18.5. This finding was unexpected as DCN

fates were not observed in short-term and long-term fate mapping studies using *Neurog1-EGFP* and *Neurog1-CreER*; $R26^{Lacz/+}$ mice respectively (35; 45). DCN fates with *Neurog1-CreER* GIFM were confirmed in *Neurog1-CreER*;$R26^{td\text{-}Tomato/+}$ mice given TMX at E18.5 in which RFP marked cells were present in the medial, intermediate and lateral DCN (Fig. 13a). As was the case for other cerebellar cell fates, the frequency of reporter gene marking in the DCN was greater with the $R26^{td\text{-}Tomato}$ allele compared to the Z/EG transgene with TMX delivery at E18.5. DCN labeling was minimal in control *Neurog1-CreER*;$R26^{td\text{-}Tomato/+}$ mice injected with sunflower oil only and accounted for 5.7 ± 4.4% of RFP marked cells in the medial DCN, 3.1 ± 3.1% of RFP marked cells in the intermediate and 2.2 ± 1.1% in the lateral DCN (n = 3 for TMX and oil administered mice). The temporal sequence of RFP marking in the DCN (E14.5 GIFM onwards) is consistent with an interneuron cell fate. To identify DCN fates, we conducted dual IHC with antibodies to the DCN neuron marker NeuN, the projection neuron marker SMI32 and the interneuron subtype marker Calb2 (44). Dual IHC revealed RFP labeled cells express NeuN, a subset express Calb2 but none were immunolabeled with anti-SMI32 antibodies (Fig. 13b). When combined with the relatively small size of RFP+ cells compared to SMI32+ cells in the DCN, these data indicate *Neurog1* is expressed during late embryogenesis in VZ progenitors destined to become DCN interneurons. Interestingly, BrdU labeling 24 hours prior to TMX injection at E18.5 resulted in co-labeling of many BrdU+/RFP+ cells in the medial, intermediate and lateral DCN (Fig. 13c), consistent with cell birth around E17.5 and Neurog1 expression at E18.75-P0 in these DCN interneurons.

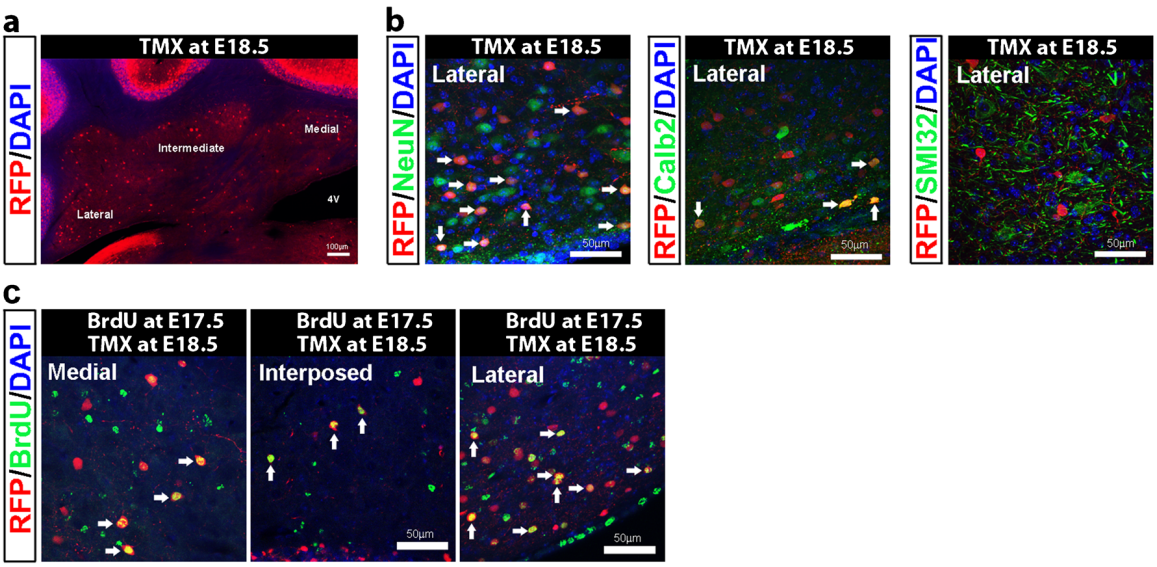

Figure 13. Late embryogenesis *Neurog1-CreER* GIFM labels interneurons in the deep cerebellar nuclei (DCN).
Mice were analyzed at P42. (a) Low magnification view of RFP fate-mapped cells in the DCN of adult *Neurog1-CreER*;*R26*$^{td\text{-}Tomato}$ mice with TMX administration at E18.5. (b) RFP+ DCN cells express NeuN (arrows) and a subset Calb2 (arrows) but do not express SMI32. (c) Co-immunolabeling of anti-BrdU/anti-RFP marked cells (arrows) in all three DCN following BrdU pulse labeling at E17.5 and GIFM at E18.5.

DISCUSSION

Neurog1-CreER GIFM labels exclusively neurons in the cerebellum

A principal finding of this study is that *Neurog1-CreER* GIFM labels all GABAergic neuronal cell types of the cerebellar cortex. Temporal *Neurog1-CreER* GIFM reveals GABAergic neurons are fate-mapped over a prolonged time-period spanning embryonic and postnatal stages of development. *Neurog1-CreER* labeling shifts from initially Purkinje cell to interneuron fate early in cerebellar development and GABAergic interneurons destined for the cerebellar cortex are fate-mapped in a temporal sequence that correlates with their final inside-to-outside resting position. Similar spatiotemporal features of GABAergic cell fate were observed with GIFM using knock-in *Ascl1*^{CreER} mice (74). However, *Ascl1*^{CreER} GIFM additionally marked Bergmann glia,

astrocyte or oligodendrocyte cell lineages with TMX delivery during embryonic development. Similarly, Bergmann glia are labeled with GIFM using knock-in *Neurog2*^{CreER} mice (19) and cumulative fating using a *Ptf1a*^{Cre} knock-in allele fates GFAP positive astrocytes in the cerebellum (30). Combined these studies provide compelling evidence radial glia cell types derive from VZ progenitors (for a review on VZ origins for glia see (8)). The absence of cerebellar glial cell fates in *Neurog1-CreER* mice therefore signifies *Neurog1* is distinct amongst the many pro-neural bHLH genes expressed at the VZ (91) in that progenitors expressing this gene exclusively give rise to neurons. As such *Neurog1-CreER* mice provide a useful tool to study neuronal cell types originating from the cerebellar VZ.

Lineage tracing reveals GABAergic interneurons and glia are generated from progenitors residing in the VZ that translocate to the presumptive white matter (pWM) during later embryonic development to generate the majority of interneurons (30; 34; 74; 90). Clonal analysis, GIFM, *null* and conditional mutants all support an ontogenetic relationship between astrocytes and neurons in the pWM (23; 30; 34; 54; 55; 74) and there is good evidence bHLH programs govern the lineage choice between interneuron and glial fate in pWM progenitors (8). For example, conditional *Ascl1* deletion in mice depletes the number of GABAergic interneurons in the cortex but increases the number of astrocytes (74). Our data implicate *Neurog1* as part of the transcription factor code specifying interneurons from pWM progenitors. Interestingly, cell grafting studies have shown the laminar placement and cell fate of GABAergic interneurons are related to intrinsic cell cycle dynamics and cell birth date but fate is only determined when cells become post-mitotic via local environmental cues within the pWM (42; 43). Previous

expression studies in our lab reveal Neurog1 is expressed in mitotic and non-mitotic progenitors as they migrate along the pWM. Neurog1 expression transiently increases as cells exit the pWM and enter the granule cell layer before being rapidly downregulated as cells disperse to their final location (45). It is therefore tempting to speculate cues within the local pWM environment signal through the regulation of *Neurog1* expression levels in progenitors to instruct interneuron cell fate.

E12.5 GIFM labeled Purkinje cells settle in distinct parasagittal stripes in the vermis and paravermis

E10.5, E11.5 or E12.5 GIFM each robustly labeled Purkinje cells in the adult cerebellum of *Neurog1-CreER*;*R26*$^{td\text{-}Tomato}$ mice with the highest number of Purkinje cells fate-mapped with TMX at E11.5. Purkinje cells were similarly labeled with E10.5 to E12.5 GIFM in *Ascl1*^{CreER} mice with maximal Purkinje cell fating with TMX delivery at E11.5 (74). A comparison of *Ascl1*^{CreER} and *Neurog1-CreER* Purkinje cell fate patterns indicates these two spatiotemporal maps converge with increasing age. E10.5 GIFM patterns differ substantially with Purkinje cells settled across the full M-L axis in *Neurog1-CreER*;*R26*$^{td\text{-}Tomato}$ mice but restricted to the lateral cerebellum in *Ascl1*^{CreER};*R26*$^{Lacz/+}$ mice. In contrast, GIFM patterns are remarkably alike with TMX at E12.5 producing similar parasagittal stripes in the adult vermis and paravermis of *Neurog1-CreER*;*R26*$^{td\text{-}Tomato}$ and *Ascl1*^{CreER};*R26*$^{Lacz/+}$ mice. Similarities in the E12.5 fate maps suggest *Neurog1*- and *Ascl1*-expressing Purkinje cell lineages converge to a distinct cohort destined for the vermis and paravermis. This observation is supported by ISH that reveal overlapping Neurog1 and Ascl1 mRNA territories in the E12.5 cerebellum (patterns that suggest progenitors transition from *Ascl1* to *Neurog1* expression). E12.5 GIFM patterns are also reminiscent of the parasagittal distribution of marked Purkinje

cells in the vermis and paravermis following the labeling of E12.5 VZ progenitors with replication-defective adenoviral vectors (27). Thus, CreER and viral vector labeling studies provide three independent lines of evidence that late-generated Purkinje cells are programmed for distinct parasagittal fates in the vermis and paravermis in the adult cerebellum.

Our GIFM data resulted in considerable overlap in *Neurog1-CreER*;*R26*$^{td\text{-}Tomato}$ Purkinje cell fate maps with TMX at E10.5, E11.5 or E12.5. This suggests individual Purkinje cells were labeled with TMX delivery on more than one date, consistent with sustained *Neurog1* expression during Purkinje cell specification. In particular, the relative distribution of RFP+ Purkinje cells with E11.5 and E12.5 GIFM indicates E12.5 marked cells are derived from a subset of Purkinje cells in which earlier *Neurog1* expression is maintained past E13. The molecular consequences of extended *Neurog1* expression in this Purkinje cell cohort are unknown but it seems plausible these cells require a distinct molecular identity linked to function.

The timing of *Neurog1* expression in cerebellar progenitors differs between early and later phases of GABAergic neurogenesis

Our data suggest the timing of *Neurog1* expression in cerebellar progenitors differs between early and later phases of GABAergic neurogenesis. E11.5 to E13.5 GIFM primarily marked non-mitotic cells in the VZ and long-term BrdU retention indicates Neurog1 is expressed in Purkinje cells around the time they become post-mitotic. In contrast, E18.5 GIFM fates interneuron progenitors in roughly equal ratios of mitotic and non-mitotic states in the presumptive white matter tracts (pWM). Differences in the timing of expression relative to mitotic status implies distinct *Neurog1* functions in VZ and pWM GABAergic progenitor cells, with probable neuronal differentiation functions

in VZ Purkinje cell progenitors and cell cycle regulatory functions in pWM progenitors. One possibility is that the progressive lengthening of the progenitor cell cycle that occurs during development contributes to the increase in Neurog1 expression in mitotic progenitors. Cell cycle lengthening regulates the transition from progenitor maintenance to differentiation in the CNS (57) and cell cycle regulators have been shown to modulate Neurog2 activity (2). Thus changes in cell cycle protein dynamics could trigger changes in Neurog1 expression timing in later generated progenitors.

Differing Purkinje and interneuron cell functions for Neurog1 are consistent with the multiple roles ascribed to Neurog1/2 activity in the literature. Neurogenins control neuronal commitment (75), progenitor cell cycle exit (7; 38; 53), neuroblast migration (25; 28) and neuronal differentiation (17; 48; 71). Furthermore, neuronal subtype specific functions for neurogenins have recently been described in the developing piriform cortex (17). Determining the precise differences in Neurog1 function in VZ and pWM progenitor cells will require the development of a conditional *Neurog1* mutant model to avoid the problem of neonatal lethality associated with the conventional knockout (46).

CONCLUSION

In this GIFM study we have shown *Neurog1* is expressed in progenitor cells fate-mapped to become Purkinje cells and GABAergic interneuron cell types of the cerebellum. We find that the timing of *Neurog1* expression is unique to each neuronal cell type and determines the final resting positions of neurons in the adult cerebellar cortex. Differences in the timing of *Neurog1* expression relative to cell cycle progression suggest distinct *Neurog1* functions in GABAergic progenitor cells in the VZ and pWM.

CHAPTER 3: Conditional deletion of *Neurog1* in the cerebellum of postnatal mice delays inhibitory interneuron maturation

ABSTRACT

The transcriptional programs that drive the generation of diverse GABAergic neuron populations from their common progenitor pools in the developing cerebellum remain unclear. *Neurog1* is a pro-neural basic helix-loop-helix (bHLH) transcription factor expressed in GABAergic progenitor cells in the ventricular zone (VZ) of embryos and subsequently in the presumptive white matter (pWM) tracts of developing postnatal mice. Genetic inducible fate-mapping labels Purkinje cells and all inhibitory interneuron cell types of the cerebellar cortex. As conventional $Neurog1^{Neo}$ knockout mice are neonatal lethal, we generated $Neurog1^{loxP}$ mutant mice to examine the effects of conditional *Neurog1* deletion on the postnatal development of the cerebellum. Targeted *Neurog1* loss-of-function in the developing cerebellum does not result in significant differences in cerebellar morphology or in the number of GABAergic neurons in the cerebellar cortex of mice at postnatal day 21 (P21). To determine the effects of *Neurog1* deletion on GABAergic progenitors, we quantified rates of cell proliferation and cell cycle progression or re-entry in embryonic $Neurog1^{Neo}$ and postnatal $Neurog1^{loxP}$ mutants. The data revealed no significant effect of *Neurog1* loss-of-function on embryonic day 12.5 (E12.5) VZ progenitors or on P5 and P6 progenitors in the pWM at P7. However, 4-5 day pulse-labeling of P5 and P6 progenitors revealed reductions in inhibitory interneuron dispersal from the pWM to the cerebellar cortex in P10 conditional $Neurog1^{loxP/loxP}$ knockout mice. Thus our conditional *Neurog1* knockout approach reveals a requirement for *Neurog1* activity in inhibitory interneuron cell dispersal from pWM tracts in the developing cerebellum of postnatal mice.

SIGNIFICANCE STATEMENT

Understanding transcription factor mechanisms that control the development of diverse neurons in the brain is a fundamental goal in neuroscience. In this study, we investigated the transcription factor *Neurog1* through a conditional gene loss-of-function approach in the cerebellum. *Neurog1* is expressed in progenitor cells located in regions of GABAergic neurogenesis in the developing cerebellum. Conditional *Neurog1* deletion allows longitudinal postnatal studies on the effects of *Neurog1* in the developing cerebellum since conventional *Neurog1* null mice are neonatal lethal. Using our conditional approach, we identify a requirement for *Neurog1* activity in the dispersal of newborn inhibitory interneurons from the presumptive white matter tracts of the cerebellum in postnatal mice.

INTRODUCTION

The cerebellum is an ideal model system to study developmental neurogenesis because of its highly stereotyped cytoarchitecture and protracted development spanning embryonic and postnatal periods. Cerebellar neurons are generated from two spatially distinct germinal zones in the embryonic cerebellum that give rise to divergent neurotransmitter cell types in the adult mouse – progenitors located in the ventricular zone (VZ) give rise to all GABAergic cerebellar neurons, while progenitors located in the rhombic lip (RL) give rise to all glutamatergic cerebellar neurons (10).

Genes encoding pro-neural basic helix-loop-helix (bHLH) transcription factors play distinct roles in the genesis of GABAergic and glutamatergic neuronal populations in the cerebellum. *Atoh1* (mouse atonal homolog 1) encodes a bHLH transcription factor that is expressed in RL progenitors and is required for the genesis of granule cells, the

predominant glutamatergic neuronal population of the cerebellum (4). In the VZ, the bHLH transcription factor *Ptf1a* (pancreas transcription factor 1a) is required for the specification of all GABAergic neurons of the cerebellum (30). *Ptf1a* acts, in part, by suppressing the alternate glutamatergic granule cell fate in VZ progenitor cells (65). Ectopic *Ptf1a* expression in the RL or ectopic *Atoh1* expression in the VZ subverts the identity of precursor-derived neurons in these two germinal niches with GABAergic neuronal fates ectopically maintained in the RL or glutamatergic neuronal fates ectopically maintained in the VZ. Combined these studies demonstrate *Atoh1* and *Ptf1*a are essential and sufficient for neuronal specification from the cerebellar RL and VZ neuroepitheliums respectively (88).

Previous studies reveal co-expression of a number of bHLH transcription factors within the *Ptf1a* expression territory of the VZ (91), suggesting mosaics of bHLH multiple transcription factor programs drive GABAergic cell-type specificity. More recently the bHLH transcription factor gene *Olig2* and the homeobox transcription factor gene *Gsx1* have been identified as key temporal regulators of VZ progenitor cell fate (68). Using gain- and loss-of-function mutations in mice, Seto et al. (2014) showed the switch from a PC to inhibitory interneuron cell fate from the VZ is negatively regulated by *Olig2* expression in the dorsal region and positively regulated by *Gsx1* expression in the ventral region. During development PC progenitors transition to become inhibitory interneuron progenitors spreading from ventral to dorsal (68). However the mechanism(s) by which each of the inhibitory interneuron cell-types of the cerebellum are derived from *Ptf1a*-expressing progenitors remains unknown.

Neurogenin1 (*Neurog1*), *Neurogenin2* (*Neurog2*), and *achaete-scute homolog-1* (*Ascl1*, *Mash1*) are pro-neural bHLH transcription factor genes co-expressed in different subdomains of the *Ptf1a*-expressing VZ (91). Expression of these bHLH transcription factors does not overlap with *Atoh1*-expressing progenitors in the RL and genetic inducible fate-mapping (GIFM) supports a role for all three genes in the generation of GABAergic cell-type specificity in the cerebellum. GIFM demonstrates *Ascl1*-expressing progenitor cells give rise to PCs, GABAergic inhibitory interneurons, deep cerebellar nuclei (DCN) interneurons, and oligodendrocyte cell lineages depending on the embryonic stage of expression (34). *Neurog2* GIFM labels PCs and DCN GABAergic inhibitory interneurons but almost no cortical inhibitory interneuron cell types (19). Our studies reveal *Neurog1* is expressed in progenitors in the VZ and presumptive white matter (pWM) tracts fated to become PCs and all inhibitory interneuron cell types of the cerebellar cortex but not glia (45; 59). The exclusive neuronal fate of *Neurog1* GIFM is unique among similar studies of pro-neural bHLH genes expressed in the VZ (19; 74). Furthermore, *Neurog1* cell lineages are largely glutamatergic in the central nervous system (CNS) implying distinct functions in the cerebellum (35). Interestingly, the timing of *Neurog1* expression in cerebellar progenitors differs between early and later phases of GABAergic neurogenesis. *Neurog1* is expressed in PCs around the time they become post-mitotic while it is expressed in post-mitotic and mitotic interneurons (59).

To determine the function(s) of *Neurog1* in cerebellar development, we adopted a gene deletion approach. Conditional deletion of *Ascl1* in the cerebellum of mice results in a reduction of cerebellar interneuron cell numbers (74). Similarly, the conditional

deletion of *Neurog2* delays cell cycle progression, affects the maturation of PC dendritic arbors and leads to a reduction in cerebellar volume (19).

To study the effects if *Neurog1* loss-of-function on PC progenitors in the embryonic cerebellum, we used conventional *Neurog1*$^{Neo/Neo}$ knockout mice developed by Ma and colleagues (47). However, the *Neurog1*$^{Neo/Neo}$ mutation is neonatal lethal in mice (47) preventing the study of loss-of-function effects on postnatal cerebellar development, the period during which a majority of inhibitory interneurons of the cerebellar cortex are generated. To overcome this limitation we generated a novel *floxed Neurog1* mutant mouse line (*Neurog1*^{loxP}) for conditional gene deletion. *Neurog1*^{loxP} mice were bred onto either knock-in *Engrailed2*$^{CreER/+}$ (60) or *Ptf1a*$^{Cre/+}$ (33) mutant backgrounds to target *Neurog1* deletion to the cerebellum; the *Engrailed2* (*En2*) gene is expressed in all cerebellar cell types in the presumptive cerebellar territory (60). This breeding strategy successfully deleted cerebellar *Neurog1* expression in viable mutant mice that survived to adulthood. Using stereological cell counting methods, we show *Neurog1* deletion did not significantly affect PC or GABAergic interneuron cell numbers in the brains of *Neurog1*$^{loxP/loxP}$ mice at P21. Similarly, *Neurog1* loss-of-function was not associated with significant differences in S-phase DNA synthesis or cell cycle re-entry rates in PC or inhibitory interneuron progenitors during *Neurog1*$^{Neo/Neo}$ embryogenesis or during early postnatal development in *Neurog1*$^{loxP/loxP}$ mice. However, *Neurog1* loss-of-function was associated with significant effects on the distribution of inhibitory interneurons born on P5 or P6 in the cerebellar cortex of *Neurog1*$^{loxP/loxP}$ mice. Overall these data suggest *Neurog1* functions in the dispersal of inhibitory interneurons from the pWM tracts of postnatal mice. We suspect *Neurog1* loss-of-function does not lead to long-term

disruptions in cerebellar cortex cytoarchitecture in *Neurog1*$^{loxP/loxP}$ mice due to possible compensatory activities of other bHLH transcription factor genes expressed in the cerebellum.

MATERIAL AND METHODS

Mouse Lines

The *Neurog1*$^{Neo/Neo}$ mouse line (47) was a gift from Jane Johnson at UT Southwestern Medical Center. The *En2*$^{CreER/+}$mouse line (70) was obtained from the Jackson Laboratory, Bar Harbor, ME. The *Ptf1a*$^{Cre/+}$ mouse line (33) was obtained from the Mutant Mouse Resource and Research Center at the University of North Carolina in Chapel Hill.

We have generated a floxed *Neurog1* mouse line where the single coding exon of the *Neurog1* gene is flanked by *loxP* sites (Fig. 17C). These mice were developed in collaboration with inGenious Targeting Laboratory, Ronkonkoma, NY. The targeting strategy for conditional inactivation of the *Neurog1* gene involved flanking the single coding exon of the *Neurog1* gene with a 5' *loxP* site and a 3' *loxP/FRTNeoFRT* cassette. The 5' *loxP* site was inserted ~1kb 5' to the beginning of the 5'UTR. The Neo cassette was placed ~280bps downstream of the end of the 3'UTR.

The Neo cassette was placed ~280bps downstream of the end of the 3'UTR. To avoid interruption of a predicted RNA Polymerase III associated regulatory region upstream of *Neurog1* coding sequences (Fig. 17A), the 5' *loxP* cassette was inserted upstream of this regulatory feature (Fig. 17B). The distance from the 5' *loxP* to the Neo cassette was approximately 3.5kb, i.e. within the size limits of efficient recombination by *Cre* recombinases. Progeny from crosses of the re-engineered *Neurog1*$^{loxP/+}$ mutants

survived to weaning in normal Mendelian ratios and were used to determine the effects of *Neurog1* loss-of-function on cerebellar development in mice.

All procedures were approved by the Uniformed Services University of the Health Sciences Institution for Animal Care and Use Committee (IACUC). Mice were housed in the Uniformed Services University's Center for Laboratory Animal Medicine on a standard 12 h light-dark cycle, with food and water available *ad libitum*. Jax mice were genotyped using the recommended genotyping PCR protocol. The following primers (5'-3') were used to genotype $Neurog1^{loxP/+}$ mice: NDEL1, CAC CCG ACT ATC GCC AAG AAC GA; NDEL2, GCT CCA AGA GTA GAC CCT TCT GAT TGC. Mice were timed-mated overnight, and the presence of a vaginal plug the following morning designated E0.5. Using this counting method, mice give birth at E19.5. The day of birth was designated as postnatal day P0.

Two overnight breeding strategies with $Neurog1^{loxP/+}$ mice were employed to conditionally delete *Neurog1* in cerebellar cell lineages: $Neurog1^{loxP/+}$ mice were crossed onto either (1) $En2^{CreER/+}$mice or (2) $Ptf1a^{Cre/+}$ mice backgrounds. Timed-pregnant $En2^{CreER/+}$; $Neurog1^{loxP/+}$ females were administered tamoxifen (TMX) dissolved in sunflower oil by intra-peritoneal injection at E9.5. Mice were injected with 50-75 mg/Kg TMX at ~10AM. TMX disrupted parturition and lactation in the mice resulting in poor progeny survival rates. To improve survival, embryos were removed by terminal caesarian from E19.5 pregnant dams and fostered to lactating Swiss Webster females (Taconic). $Ptf1a^{Cre/+}$; $Neurog1^{loxP/+}$ mice give birth to normal litter sizes and do not require fostering with no disruption.

En2$^{CreER/+}$*; Neurog1*$^{loxP/loxP}$ mice (hereafter referred to as cKO mice) were compared to control littermates with genotype *En2*$^{CreER/+}$*; Neurog1*$^{+/+}$. *Ptf1a*$^{Cre/+}$*; Neurog1*$^{loxP/loxP}$ mice (hereafter referred to as pKO mice) were compared to control littermates with genotype *Ptf1a*$^{+/+}$*; Neurog1*$^{loxP/loxP}$ or *Ptf1a*$^{+/+}$*; Neurog1*$^{+/+}$. Both sexes were equally used in our studies. P7 and P10 mice had their sex determined by measuring the anatomical distance between their anus and genitalia. Females have a shorter distance between their anus and genitalia and may also display nipples.

Cell cycle analysis in Neurog1*$^{Neo/Neo}$ *knockout mice

Heterozygous *Neurog1* knockout mice *Neurog1*$^{Neo/+}$ were overnight timed-mated. Pregnant females were administered three successive intraperitoneal injections of 50 mg/Kg BrdU on E12.5 each spaced 2 hours apart. Mice were sacrificed at two time-points after the last BrdU injection: (1) at +3 hours for dual anti-BrdU/anti-phH3 IHC; (2) at +6 hours for dual anti-BrdU/anti-Ki67 IHC. Embryos were genotyped as described previously (16) and serially sectioned in the coronal plane. Confocal Z stacks recorded at 40X magnification from every fourth section beginning with a randomly chosen starting section from 1 to 4. Three images, each adjacent to the other, were taken from the full rostral-caudal axis of the cerebellum. Two columns along the ventricular zone were randomly selected for counting by a blinded observer. For cell cycle progression analysis, the number of total BrdU+, BrdU+/phH3+, BrdU+/phH3-, phH3+/BrdU- and total phH3+ cells were recorded. For cell cycle exit analysis, the number of total BrdU+, BrdU+/Ki67+, BrdU+/Ki67-, Ki67+/BrdU- and total Ki67+ cells were recorded.

Thymidine Analog Delivery

Postnatal pups were administered 100 mg/Kg ethynyldeoxyuridine (EdU) and 100 mg/Kg bromodeoxyuridine (BrdU) by intraperitoneal injection on designated postnatal days at ~10AM. EdU was dissolved in sterile phosphate buffered saline (PBS) and BrdU was dissolved in sterile saline. EdU+ cells were identified through a copper-catalyzed click chemistry reaction and BrdU+ cells were identified by anti-BrdU IHC. Both thymidine analogs had punctate nuclear staining.

Immunohistochemistry (IHC)

Mice were placed under anesthesia in an induction chamber containing a mixture of O_2 and isoflurane (2-4%) delivered by a vaporizer. Anesthesia was maintained during intra-cardiac perfusion-fixation by a mixture of O_2 and 2% isoflurane using a nose cone. Mice were exsanguinated with ice-cold PBS and perfused with 4% paraformaldehyde (PFA) in PBS for all histological analysis. Brains were post-fixed in fresh fixative overnight at 4°C. For vibratome sectioning, postnatal brains were rinsed in PBS and cut into 40 μm thick sagittal sections and stored in PBS with azide at 4°C until use.

P7 and P10 cerebellum tissue processed for IHC underwent antigen retrieval in 10mM sodium citrate with 0.05% Tween 20 pH 6.0 for 30 min in a 60°C water bath and agitated every 10 min. Tissue was rinsed with ddH_2O before proceeding to a copper-catalyzed click chemistry reaction to detect EdU. Click chemistry reaction mixture included 1:500 dilution 10mM stock Azide Fluor 488, 1:20 dilution of 0.2M Tris pH 8.5, 1:100 dilution of 1M $CuSO_4$, and 1:5 dilution of 0.5M Ascorbate (added to mixture last). Tissues were incubated in click chemistry reaction for 30 min and washed in TBS and then PBS prior to blocking. All sections were blocked in 10% normal goat serum (NGS) in PBS for 1 hr at room temperature and incubated in primary antibodies (Table 1)

overnight at 4°C. All primary antibodies were diluted in PBS containing 1% NGS and 0.2% Triton X-100. The following day sections were washed in PBS and incubated with Alexa Fluor 555 dye-labeled secondary antibody (Life Technologies) at 1:2000 dilution in PBS for 1 hr at room temperature, counterstained with DAPI and mounted under mowiol. Pax2 immunolabeling was revealed using a biotinylated anti-rabbit secondary antibody with a Dy-Light 647 steptaviden (Vector Laboratories). Details of the primary antibodies used for IHC are as follows: (1) 1:500 dilution of rat monoclonal anti-BrdU (Accurate Chemical & Scientific Corporation); (2) 1:200 dilution of mouse monoclonal anti-Ki67 (Abcam); (3) 1:200 dilution of rabbit polyclonal anti-Pax2 (Zymed Laboratories); (4) 1: 1000 dilution of rat monoclonal anti-phH3 (Abcam). Immunofluorescent images were captured on a Zeiss 700 laser scanning confocal microscope (LSCM). Bright-field images were captured on a Zeiss color camera.

Table 1. Antibodies

Antibody	**Structure of Immunogen**	**Manufacturer, catalog number, RRID, host species**	**Concentration**
anti-BrdU	Bromodeoxyuridine	Accurate Chemical & Scientific Corporation, OBT0030, rat monoclonal	1:500 in PBST
anti-Ki67	A synthetic peptide derived from the human Ki-67 protein	Abcam, ab6526, AB_305543, mouse monoclonal	1:200 in PBST
anti-Pax2	A GST-Pax-2 fusion protein derived from the C-terminal domain (aa188-385) of the murine Pax-2 protein	Zymed Laboratories (now Thermo Fisher Scientific), 71-6000, AB_2533990, rabbit polyclonal	1:200 in PBST
anti-phH3	Synthetic peptide corresponding to Human Histone H3 aa 23-35 (phospho S28) conjugated to Keyhole Limpet Haemocyanin (KLH)	Abcam, ab10543, AB_2295065, rat monoclonal	1:1000 in PBST

In Situ Hybridization (ISH)

Embryos were decapitated and the head was fixed by immersion in fixative overnight at 4°C. For cryostat sectioning, embryonic tissue were rinsed in PBS and cryopreserved in 30% sucrose/PBS at 4°C and frozen in OCT compound. Sagittal sections (14-16 μm thick) were cut on the cryostat and stored at -20°C until use. Cryostat section slides were air-dried at room temperature for 2 hrs and post-fixed in 4% PFA for 5 min prior to use. ISH was performed using RNAscope probes for DAB singleplex hybridization according to the instructions from the manufacturer Advanced Cell Diagnostics (ACD), Newark, CA. The *Neurog1* probe was hybridized singleplex with DAB labeling on equivalent control and *Neurog1* knockout (KO) embryonic tissue sections for comparison.

Cresyl Violet Staining

Postnatal day 21 old mice were perfusion-fixed with 4% PFA as described for IHC and the brain removed, hemisected and embedded in a block of Paraplast Plus and cut on a Microm HM325 Microtome into 5 μm thick sagittal sections. Sections were de-waxed in xylene, dehydrated in 100% ethanol, and hydrated in distilled water prior to incubating in 45 mL Cresyl echt violet solution (0.5 g Cresyl echt violet, 80 mL distilled water, 20 mL 100% ethanol) and 15 drops of acetic acid for 8 min. Sections were rinsed in tap water to remove excess staining solution, dehydrated with 100% ethanol, cleared in xylene and allowed to dry in fume hood before being mounted with Permount solution.

Stereo Investigator (MBF Bioscience)

Estimated total population of GABAergic interneurons and Purkinje cell numbers were quantified using the Stereo Investigator system (MBF Bioscience, Williston, VT) on a Zeiss AxioImager M2 upright microscope. A random section was selected as the initial

Reference section with the consecutive section as the Lookup section; these two sections comprise of the first section pair. The next section pair was 80 μm away from the previous section pair moving in the direction from medial to lateral. Using this section pair selection method, 6-10 section pairs were quantified per animal. The entire sagittal section of the cerebellum was outlined in a closed contour using a 5x objective, and cells were counted with a 20x objective using the Physical Fractionator method with a 5 μm depth and no top guard zone. The counting frame size was 100 x 100 μm and the grid size was set so that there was an average of 10 sites on an averaged sized contour. Cells only on the Reference image, but not on the Lookup image, were counted. All stereological measures yielded a Gundersen coefficient error of <0.16.

The Cresyl violet method uses basic aniline dye to stain RNA blue. The Nissl substance (rough endoplasmic reticulum) appears dark blue from the staining of ribosomal RNA; DNA present in the nucleus stains a similar color. Therefore, all GABAergic interneurons and Purkinje cells of the cerebellar cortex that were quantified must have one or more dark DNA clusters surrounded by a mottled cytoplasm (see Fig. 19). Basket and stellate cells had a round or oval multipolar soma. The molecular layer was divided along the middle laminar axis into the inner and outer sublayers, and the number of basket and stellate cell types were counted by their location within the inner and outer halves, respectively. Purkinje cells were identified by their large, pear-shaped soma positioned between the granule cell and molecular layers of the cerebellar cortex with some staining of their highly branched dendritic arbors in the molecular layer. Golgi cells were quantified in the densely packed granule layer and had large, irregularly

shaped soma. Golgi cells had a larger circumference and lightly stained cytoplasm in comparison to the small, dark stained cytoplasm of granule cells.

Cavalieri Method

The Cavalieri Method was used to estimate cerebellar volume using MBF Bioscience software. The same closed contour that outlined the entire sagittal section of the cerebellum using a 5x objective for Stereology was used with the Cavalieri probe to estimate cerebellum volume. All Cavalieri estimator measures yielded a Gundersen coefficient error of <0.1.

Cell Quantification (IHC)

For Pax2/EdU, Pax2/BrdU, or Pax2/EdU/BrdU cell counts, P7 or P10 cerebellum tissue were processed for double anti-Pax2/anti-BrdU and EdU click chemistry reaction. Cell counts were recorded from 40x oil confocal Z stacks of 3-4 sagittal sections per animal that spanned the full medio-lateral extent of the cerebellar vermis. Images for P7 sections focused on the presumptive white matter tracts. Images for P10 sections were taken specifically in the molecular layer or granule layer. Sagittal sections of the cerebellar vermis reveal a stereotypical foliation pattern consisting of 10 lobules. The cerebellum can be further divided along the anterior-posterior axis into transverse domains: anterior (lobules I-V), central (lobules VI-VII), posterior (lobules VIII and anterior IX), and nodular (lobules posterior IX and X) (61). In our study, we refer to lobules I-V as anterior, VI-VII as central and VIII-X as posterior lobules.

Statistical analysis

All of the data are presented as mean ± SEM. Statistical analysis was conducted using the unpaired Student's *t*-test or two-way ANOVA using GraphPad Prism 7 software. ANOVA is a robust test that can tolerate violations to its normality assumption. A $P<0.05$ was used as the threshold for statistical significance.

RESULTS

Neurog1 loss-of-function effects on cell proliferation in the VZ during the period of peak Purkinje cell production

Our genetic inducible fate-mapping (GIFM) data demonstrates *Neurog1* is expressed in progenitors fated to become PCs from E10.5 to E13.5, with the peak period of PC labeling with GIFM at E11.5 (59). BrdU pulse-labeling with GIFM indicated *Neurog1* expression in PC progenitors occurred around the time they become post-mitotic, consistent with a functional role in cell cycle progression and/or cell cycle exit. To test this hypothesis we used conventional $Neurog1^{Neo/Neo}$ knockout mice (47) to measure the effects of *Neurog1* loss-of-function on VZ cell cycle parameters in E12.5 mice. We reasoned VZ cell activity at E12.5 would include the period of peak PC GIFM with TMX on E11.5 (TMX is predicted to label cells +6 to +36 hours after delivery). E12.5 mice were given three successive injections of BrdU each 2 hours apart and sacrificed for IHC at 3 or 6 hours after the last BrdU injection (Fig. 16A), end points equivalent to approximately E12.8 or E13.

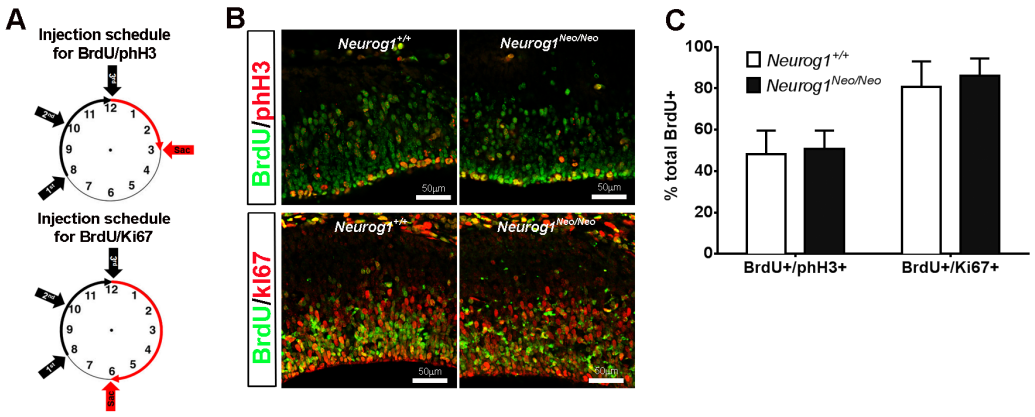

Fig. 16. *Neurog1* loss-of-function does not affect cell cycle dynamics in E12.5 to E13 VZ progenitors.
(**A**) A time frame of BrdU injections at black arrows relative to sacrifice (Sac, red arrow) for either dual anti-BrdU/anti-phH3 or dual anti-BrdU/anti-Ki67 IHC. (**B**) Representative images of the VZ processed for anti-BrdU/anti-phH3 or anti-BrdU/anti-Ki67 IHC. (**C**) A comparison of the percentage of BrdU+/phH3+ and BrdU+/Ki67+ cells relative to the total BrdU+ cells reveals no difference in S-phase to G2/M phase cell cycle progression or cell cycle exit.

Mice sacrificed at ≈ E12.8 were analyzed for cell cycle progression using the G2/M phase cell cycle marker phospho-Histone H3 (phH3) (Fig. 16B). Quantification of the numbers of total BrdU+, BrdU+/phH3+, phH3+/BrdU- and total phH3+ cells did not reveal differences between *Neurog1*$^{Neo/Neo}$ and *Neurog1*$^{+/+}$ embryos. When expressed as a percentage of the total BrdU+ cell population to normalize for variations in BrdU delivery, there was no significant difference in the percentage of cells BrdU+/phH3+ (i.e. BrdU+ cells that had progressed to G2/M-phase) between *Neurog1*$^{Neo/Neo}$ versus *Neurog1*$^{+/+}$ embryos (Fig. 16C). We next compared rates of cell cycle exit in ~ E13 mice using dual anti-BrdU/anti-Ki67 IHC (Fig. 16B). Again no differences in the numbers of total BrdU+, BrdU+/Ki67+, Ki67+/BrdU- and total Ki67+ cells were observed between *Neurog1*$^{Neo/Neo}$ and *Neurog1*$^{+/+}$ embryos. Similarly, the percentage of cells BrdU+/Ki67+

(i.e. BrdU+ cells remaining in mitosis) was not statistically different between *Neurog1*$^{Neo/Neo}$ versus *Neurog1*$^{+/+}$ embryos. Combined the results indicate *Neurog1* loss-of-function does not disrupt the rate of S-phase to G2/M-phase cell cycle progression or the rate of exit from the cell cycle in E12.5-E13 VZ progenitors in the cerebellum.

Neurog1 deletion in the cerebellar primordium of E12.5 conditional *Neurog1*$^{loxP/loxP}$ knockout mice

In this study we generated a *Neurog1*^{loxP} mutant mouse line to examine the effects of conditional *Neurog1* gene inactivation on the postnatal development of the cerebellum in mice. Conventional *Neurog1* knockout mice die shortly after birth (47) preventing any longitudinal study of the effects of *Neurog1* loss-of-function on cerebellar development. *Neurog1*^{loxP} mutant mouse were engineered to include *loxP* sites flanking the single *Neurog1* coding exon – see Materials and Methods section and Figure 17 for the targeting strategy of *loxP* insertions surrounding the single coding exon of the *Neurog1* gene.

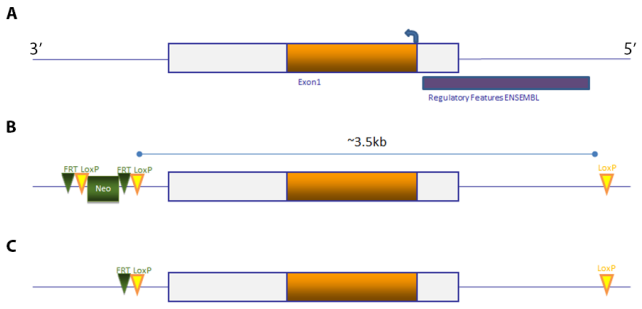

Fig. 17. *Neurog1* targeting for conditional deletion in mice.
(**A**) Wild-type allele showing single exon and Ensemble predicted RNA III polymerase regulatory region. (**B**) Targeting cassette for homologous recombination showing the positions of the *LoxP* insertions 5' and 3' of *Neurog1* coding sequences and the FRT-LoxP flanked Neomycin (Neo) selection cassette. Exon 1 and ~1.6kb of 5' genomic sequence is flanked by *loxP* sites. The *FRT-LoxP* flanked Neo cassette is downstream of the 3' UTR. (**C**) The *LoxP* flanked *Neurog1* allele after FLP-mediated deletion of the Neo cassette.

To confirm Cre-mediated recombination could be used to conditionally ablate *Neurog1* expression in the cerebellum, we first wanted to confirm our knockout mice had *Neurog1* expression deleted in the cerebellum only. We crossed $Neurog1^{loxP}$ mutants onto an $En2^{CreER}$ background. GIFM in $En2^{CreER/+}$ mice demonstrates TMX administration at E9.5 specifically labels midbrain-hindbrain progenitor cell populations that give rise to ~ 90 % of all cerebellar cell lineages in adult mice (70). A dose of 50 mg/Kg TMX was administered at E9.5 to pregnant $Neurog1^{loxP/loxP}$; $En2^{CreER/+}$ (cKO) dams and embryos were harvested at E12.5, sectioned and processed for ISH (Fig. 18A-18H') to assess for *Neurog1* mRNA expression in the cerebellar primordium. Control embryos (Fig. 18A-18D') show *Neurog1* hybridization in lateral and medial sagittal sections of the cerebellar primordium. Although the 50 mg/Kg TMX dose markedly reduced ISH signal in the cerebellar primordium, ISH signal indicates it did not completely ablate *Neurog1* mRNA expression in cKO mice (Fig. 18E-18H'). Accordingly an increased dose of 75 mg/Kg TMX was administered to pregnant cKO dams at E9.5 and embryos harvested at E12.5. ISH labeling confirms the higher dose of TMX was sufficient to ablate *Neurog1* mRNA expression in the entire cerebellar primordium of cKO mice (. 18I-18L') and this dose was used throughout this study to induce conditional *Neurog1* inactivation in cKO mice.

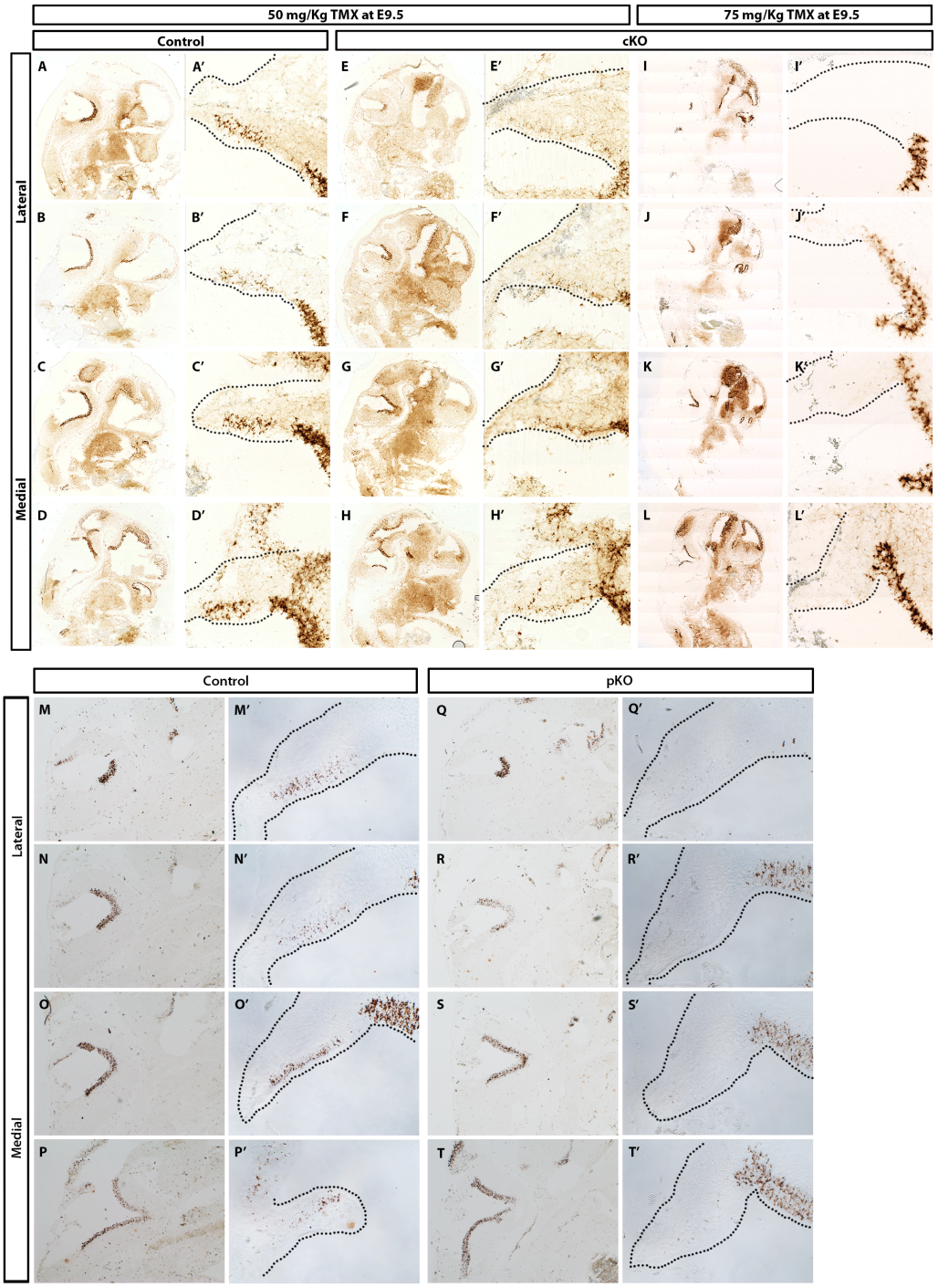

Fig. 18. *Neurog1* deletion in the E12.5 cerebellar primordium.
Low magnification (**A-T**) and high magnification (**A'-T'**) bright field images of *Neurog1* ISH on E12.5 sagittal sections spanning the mediolateral axis with the cerebellar primordium outlined in a dotted line (**A'-T'**). Note *Neurog1* expression in the pontine neuroepithelium. (**A-L'**) $En2^{CreER/+}$ mice drive *Neurog1* mRNA deletion in the E12.5 cerebellar primordium with TMX injection at E9.5 in cKO mice. (**A-D'**) *Neurog1* mRNA expression in the cerebellar primordium of control

mice. (**E-H'**) 50mg/Kg dose of TMX at E9.5 did not completely ablate *Neurog1* mRNA expression in the cerebellar primordium. (**I-L'**) 75mg/Kg dose of TMX at E9.5 is sufficient to delete *Neurog1* expression in the cerebellar primordium. (**M-T'**) $Ptf1a^{Cre/+}$ mice drives *Neurog1* mRNA deletion in the E12.5 cerebellar primordium. (**M-P'**) *Neurog1* mRNA expression in the cerebellar primordium of control mice. (**Q-T'**) *Neurog1* expression deleted in the cerebellar primordium of pKO mice.

Due to TMX toxicity and the difficulties of fostering neonates, the numbers of pups that survive to weaning from cKO mice are low. Therefore we used an additional, complementary breeding strategy to conditionally delete *Neurog1* in the cerebellum of postnatal mice. In this strategy $Neurog1^{loxP}$ mice were crossed onto a $Ptf1a^{Cre/+}$ background. Cre recombinase expression in $Ptf1a^{Cre/+}$ mice is localized to the cerebellar ventricular zone (VZ) in the brain and the line can be used to spatially target gene deletion to cerebellar VZ cell lineages without the need for TMX administration (33). To determine if this breeding strategy successfully inactivated *Neurog1* expression in the cerebellum, we replicated *Neurog1* ISH experiments in $Neurog1^{loxP/loxP}$; $Ptf1a^{Cre/+}$ (pKO) and littermate control embryos harvested at E12.5 (Fig. 18M-18T'). Control embryos show *Neurog1* expression patterns in lateral and medial sagittal sections of the cerebellar primordium, similar to control littermates of cKO mice (Fig. 18M-18P'). ISH on pKO mice reveal *Neurog1* expression is completely absent from the E12.5 cerebellar primordium (Fig. 18Q-18T'). We conclude both $En2^{CreER/+}$ (cKO) with a 75 mg/Kg TMX dose and $Ptf1a^{Cre/+}$ (pKO) recombinases are sufficient to ablate *Neurog1* cerebellar expression in $Neurog1^{loxP/loxP}$ mice. Using this breeding strategy we observed cKO and pKO mice survive to weaning in numbers comparable to background strain C57BL6/J mice and show no obvious evidence of ataxia or any behavioral phenotype.

Stereological quantification of cerebellar GABAergic neuronal cell types at P21 in conditional *Neurog1*$^{loxP/loxP}$ knockout mice

To determine the effects of conditional *Neurog1* loss-of-function on the survival of GABAergic cell types of the cerebellar cortex, we used the Cavalieri Estimator to estimate cerebellum volume and the Physical Fractionator Workflow (MBF Bioscience) to estimate the number of Purkinje cell, Golgi cell, basket and stellate cells in the cerebellum of P21 cKO or pKO mice and their control littermates. P21 is the earliest postnatal development time point where cell genesis and cell positioning is complete. Cells were counted from Cresyl violet stained sections (Fig. 19A, 19B, 19H, 19I) using morphological and topographical criteria (see Material and Methods) from hemi-cerebella. Observations of Cresyl violet stained sections revealed no gross differences between cKO or pKO cerebellum and their control littermates. The unpaired students *t*-test was used to compare differences between cKO or pKO mice with their control littermates.

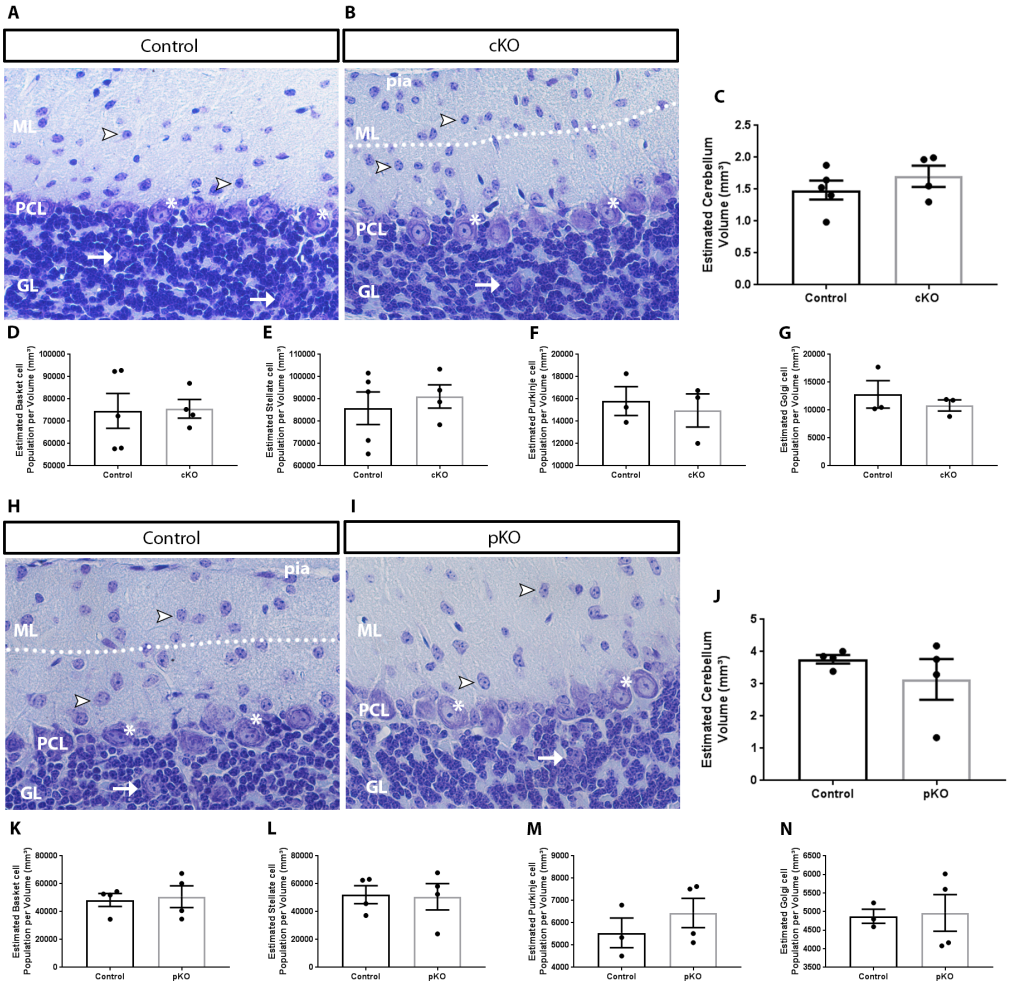

Fig. 19. Stereological quantification of cerebellar GABAergic neuronal cell types. Stereological quantification was completed on sagittal sections of the P21 cerebellum stained with Cresyl violet in ckO (**A-G**) and pKO (**H-N**) mice. (**A, B, H, I**) Representative cells that were quantified include Purkinje cells (*asterisk*), Golgi cells (*arrow*) and basket or stellate cells (*arrow heads*). (**B, H**) The ML is divided in half by a dotted line to distinguish basket cells in the half closest to the PCL, and stellate cells in the half closest to the pial surface. (**C, J**) The Cavalieri estimator used to measure cerebellar volume did not yield significant differences in *Neurog1* cKO or pKO mice. Stereological quantification of basket cells (**D, K**), stellate cells (**E, L**), Purkinje cells (**F, M**) and Golgi cells (**G, N**) did not yield significant differences in *Neurog1* cKO or pKO mice. (mean ± SEM; $n \geq 3$; unpaired *t* test; all C.E. values < 0.16). Key: *ML* Molecular layer, *PCL* Purkinje cell layer, *GL* granule layer, *pia* pial surface.

In cKO mice, there is no significant difference in (Fig. 19C) the estimated cerebellum volume (control = 5, cKO = 4; P = 0.3666). Cell quantification reveals no significant differences in (Fig. 19D) basket cell number (control = 5, cKO = 4; P = 0.925), (Fig. 19E) stellate cell number (control = 5, cKO = 4; P = 0.5954), (Fig. 19F) Purkinje cell number (n = 3; P = 0.6912), or (Fig. 19G) Golgi cell number (n = 3; P = 0.4978). Due to breeding difficulties and TMX toxicity in pregnant dams, we shifted our focus on analyzing pKO mice and their control littermates for the remainder of our studies.

Similar to cKO mice, in pKO mice there is no significant difference (n = 4; P = 0.3704) in the estimated cerebellum volume (Fig. 19J). Cell quantification reveals no significant differences (n = 4; P = 0.8009) in basket cell number (Fig. 19K), stellate cell number (n = 4; P = 0.8952) (Fig. 19L), Purkinje cell number (control = 3, pKO = 4; P = 0.3926) (Fig. 19M), or Golgi cell number (control = 3, pKO = 4; P = 0.8896) (Fig. 19N). Combined these stereological cell counts reveal *Neurog1* deletion in the cerebellum using either conditional $En2^{CreER}$ or constitutive *Ptf1a-Cre* drivers does not result in significant differences in cerebellar volume or GABAergic cell number in the cerebellar cortex of mice at P21.

Neurog1 loss-of-function effects on cell proliferation of Pax2+ inhibitory interneurons in the presumptive white matter tracts at P7

To determine the effects of cerebellar *Neurog1* loss-of-function on the proliferation of inhibitory interneuron progenitor cells, we injected mice with thymidine analogs. About 75% of all Pax2+ interneurons are generated prior to P7 with maximal increase around P5 (84). Therefore, we injected pKO mice with EdU at P5, BrdU at P6 and analyzed the cerebellum at P7 (Fig. 20A). Sagittal sections of the cerebellum

spanning the mediolateral axis were processed for double anti-Pax2/anti-BrdU IHC and EdU click chemistry reaction (Fig. 20B, 20C). Cells were quantified in the anterior (I-V), central (VI-VII) or posterior (VIII-X) lobules of the cerebellum and two-way ANOVA used to compare cell numbers in pKO (n = 5) and control littermates (n = 4) at age P7.

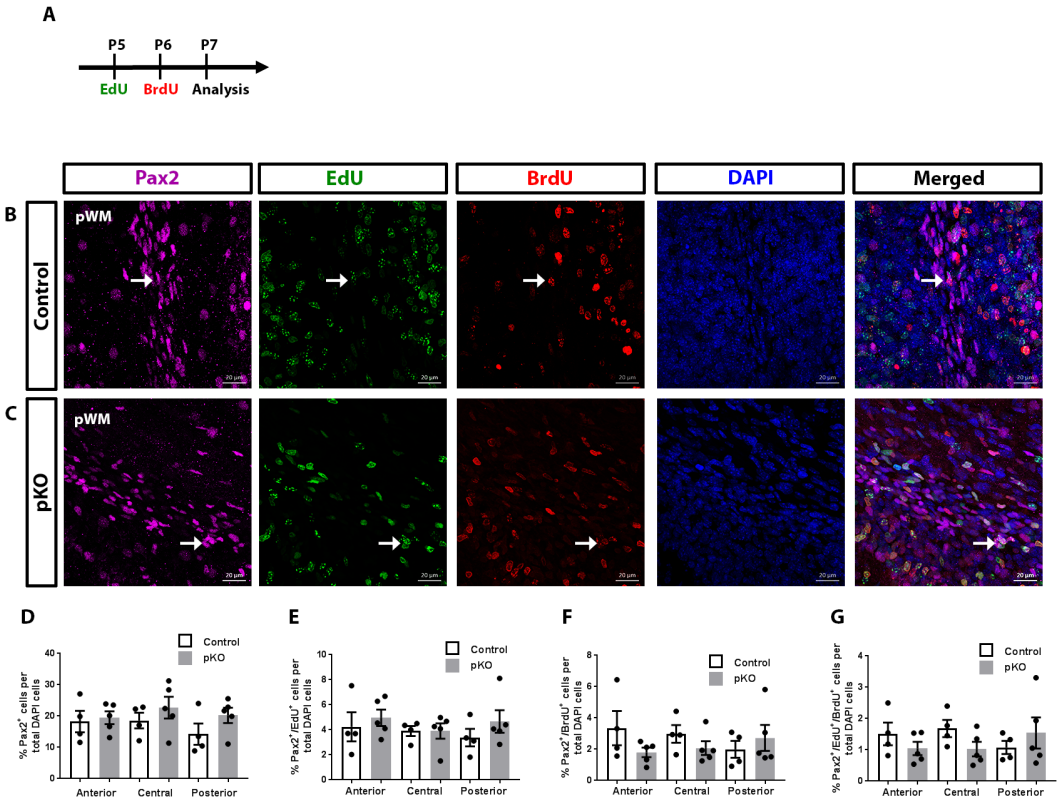

Fig. 20. Cell proliferation of Pax2^{+} interneurons in the presumptive white matter tracts at P7.

(**A**) Schematic timeline of thymidine analog injections prior to analysis at P7. (**B, C**) Control and pKO mice processed for double anti-Pax2/anti-BrdU IHC, EdU click chemistry reaction and counterstained with DAPI 48 h after EdU delivery, 24 h after BrdU delivery. Example of triple Pax2+/EdU+/BrdU+ cell indicated by arrow. (**D-G**) Cells were quantified from sagittal sections of the cerebellum from lobules I-V (anterior), VI-VII (central) or VIII-X (posterior). (**D**) Number of Pax2+ interneurons does not differ in *Neurog1* pKO mice. Cell proliferation was assessed by thymidine analog incorporation into Pax2+ interneurons at P5 (**E**) or P6 (**F**), or incorporated at P5 and P6 (**G**). There are no significant differences in cell proliferation of *Neurog1* pKO mice. (mean ± SEM; $n \geq 4$; two-way ANOVA, multiple comparisons). Key: *pWM* presumptive white matter tracts.

The distribution of EdU and BrdU labeled cells in the cerebellar cortex reveals substantially more labeling with EdU at P5 than BrdU at P6 (not quantified). Although, as mentioned, the proliferation of inhibitory interneurons peaks at P5 (84), we suspect these differences also relate to differences in EdU/BrdU delivery and detection sensitivity. Overall cell counts do not reveal significant differences in Pax2+/EdU+/BrdU+ interneuron cell numbers between control and pKO mice at P7. There is no significant effect of genotype on Pax2+ ($F(1, 21) = 2.505$; $P = 0.1284$) (Fig. 20D), Pax2+/EdU+ ($F(1, 21) = 1.139$; $P = 0.2980$) (Fig. 20E), Pax2+/BrdU+ ($F(1, 21) = 1.139$; $P = 0.2980$) (Fig. 20F) or Pax2+/EdU+/BrdU+ ($F(1, 21) = 0.6892$; $P = 0.4158$) (Fig. 20G) cell numbers between control and pKO mice. There are similarly no differences in cell number between lobules and no significant interactions between genotype and lobule (all P values > 0.05). We conclude these data indicate *Neurog1* loss-of-function did not significantly effect the number, proliferation or P5 to P6 cell cycle re-entry rates of Pax2+ inhibitory interneuron progenitors in the cerebellum.

Neurog1 loss-of-function effects on Pax2+ inhibitory interneuron migration from the presumptive white matter tracts

We next asked if *Neurog1* loss-of-function has any effects on the distribution of inhibitory interneuron progenitor cells migrating from the pWM tracts. Basket and stellate cells proliferate at least until P7 and migrate into the molecular layer during the second postnatal week (43). To compare inhibitory interneuron cell distribution, we injected pKO mice and their control littermates as before with EdU at P5, BrdU at P6. In this series of experiments we analyzed mice at the later time-point of P10 to encompass the dispersal of EdU/BrdU-labeled inhibitory interneurons from the pWM through the granule layer (GL) to molecular layer (ML) destinations (Fig. 21A). Sagittal sections of

the cerebellum spanning the mediolateral axis were processed for double anti-Pax2/anti-BrdU IHC and EdU click chemistry reaction (Fig. 21B, 21C, 21H, 21I). As before cells were quantified in the anterior (I-V), central (VI-VII) or posterior (VIII-X) lobules of the cerebellum. We quantified proliferating Pax2+ interneurons migrating in the GL (Fig. 21B-21G) and ML (Fig. 21H-21M) and used two-way ANOVA to compare the data from pKO (n = 4) and control (n = 3) mice.

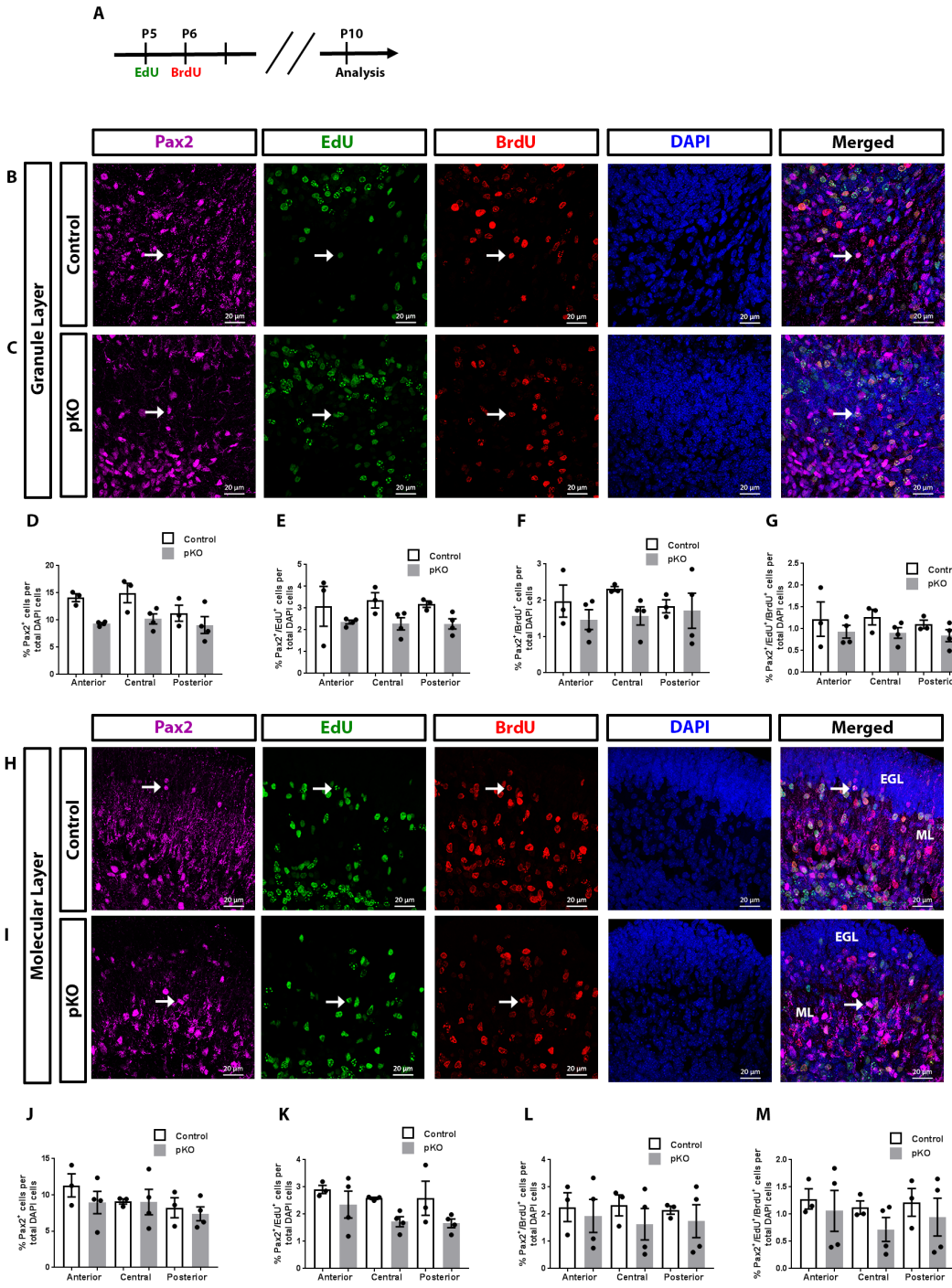

Fig. 21. Pax2^{+} interneuron migration from presumptive white matter tracts. (**A**) Schematic timeline of thymidine analog injections prior to analysis at P10. (**B, C, H, I**) Control and pKO mice processed for double anti-Pax2/anti-BrdU IHC, EdU click chemistry reaction and counterstained with DAPI at P10. Example of triple Pax2+/EdU+/BrdU+ cell indicated by arrow. Cells were quantified from sagittal sections of the cerebellum from lobules I-V (anterior), VI-VII (central) or

VIII-X (posterior) in either the GL (**B-G**) or ML (**H-M**). Cell migration was assessed by localizing and quantifying Pax2+ interneurons (**D, J**) and Pax2+ interneurons that incorporated thymidine analogs at P5 (**E, K**) or P6 (**F, L**), or incorporated both analogs at P5 and P6 (**G, M**). There are significantly less Pax2+ interneurons in the GL (**D**) of pKO mice compared to control mice [$F(1,15) = 15.69$; $n \geq 3$; $P = 0.0013$], but there was no difference in the number of Pax2+ interneurons seen in the ML (**J**). There are significantly less Pax2+/EdU+ cells in both the GL (**E**) [$F(1,15) = 8.276$; $n \geq 3$; $P = 0.0115$] and ML (**K**) [$F(1,15) = 7.593$; $n \geq 3$; $P = 0.0147$]. There are no significant differences between pKO and control mice in the number of Pax2+ interneurons that incorporated BrdU at P6 (**F, L**) or both EdU at P5 and BrdU at P6 (**G, M**) in the GL or ML. (mean ± SEM; $n \geq 3$; two-way ANOVA, multiple comparisons). Key: *EGL* external granule layer, *ML* Molecular layer, *PCL* Purkinje cell layer.

In the GL, there is a significant effect of genotype ($F(1, 15) = 15.69$; $P = 0.0013$) on the number of Pax2+ cells (Fig. 21D) but no significant effect of lobule ($F(2, 15) = 2.086$; $P = 0.1588$) or the interaction between genotype and lobule ($F(2, 15) = 0.7651$; $P = 0.4826$) on Pax2+ cell number. Similarly there is a significant effect of genotype ($F(1, 15) = 8.276$; $P = 0.0115$) on the numbers of double Pax2+/EdU+ cells from P5 in the GL (Fig. 21E) but no significant effect of lobule ($F(2, 15) = 0.1064$; $P = 0.8997$) or the interaction between genotype and lobule ($F(2, 15) = 0.1064$; $P = 0.8997$). For cell counts including BrdU-labeled cells, there is no significant effect of genotype on Pax2+/BrdU+ cells ($F(1, 15) = 2.805$; $P = 0.1147$) (Fig. 21F) or Pax2+/EdU+/BrdU+ cells ($F(1, 15) = 3.861$; $P = 0.0682$) (Fig. 21G) in the GL, although both p-values are approaching significance. We suspect the failure to detect differences in BrdU- compared to EdU-labeled cell distribution in the GL could be due to the substantially lower rates of BrdU incorporation in our mice. Two-way ANOVA also reveals no differences in Pax2+/BrdU+ or Pax2+/BrdU+/EdU+ cell number between lobules and no significant interactions between genotype and lobule (all P values > 0.05). Overall these cell counts reveal *Neurog1* loss-of-function results in a significantly lower number of Pax2+ and P5

labeled Pax2+/EdU+ cells in the GL at P10. The lack of a significant effect of lobule or the interaction between genotype and lobule indicates there was no topographical effect on the reduced number of Pax2+ inhibitory interneuron numbers in pKO mice.

In the ML, there is no significant effect of genotype on the number of Pax2+ cells ($F(1, 15) = 0.882$; $P = 0.3625$) (Fig. 21J) and no significant lobule effect ($F(2, 15) = 1.333$; $P = 0.2931$) or interaction between genotype and lobule ($F(2, 15) = 0.3345$; $P = 0.7209$). In contrast there is a significant effect of genotype ($F(1, 15) = 7.593$; $P = 0.0147$) on the number of double Pax2+/EdU+ cells in the ML but the effect of lobule ($F(2, 15) = 1.348$; $P = 0.2895$) or interaction between genotype and lobule ($F(2, 15) = 0.1592$; $P = 0.8542$) is not significant. The number of Pax2+/BrdU+ cells in the ML (Fig. 21L) reveals no significant effect of genotype ($F 1, 15) = 1.117$; $P = 0.3072$). Similarly there is no significant effect of genotype ($F(1, 15) = 1.535$; $P = 0.2344$) on numbers of Pax2+/EdU+/BrdU+ cells in the ML (Fig. 21M); and 2-way ANOVA also did not reveal significant lobule or lobule and genotype interaction effects for Pax2+/BrdU+ or Pax2+/EdU+/BrdU+ cell numbers (P values ≥ 0.3). Again we suspect low level BrdU labeling could account for the lack of statistical significance in BrdU- versus EdU-labeled cells between pKO and control mice. Overall we conclude differences in Pax2+ and Pax2+/EdU+ cell distribution in the GL and ML between pKO and control mice are consistent with a significant impairment of inhibitory interneuron cell dispersal from the pWM with *Neurog1* loss-of-function.

DISCUSSION

Neurog1 loss-of-function impairs inhibitory interneuron cell dispersal to granule and molecular layers

In this study we investigated the effects of *Neurog1* loss-of-function on pre- and postnatal cerebellar development in knockout mice. The effects of *Neurog1* deletion on embryonic cerebellar development were investigated using an existing $Neurog1^{Neo/Neo}$ *null* mutant mouse line (Ma, Chen, del Barco Barrantes, de la Pompa, & Anderson, 1998). As the $Neurog1^{Neo/Neo}$ mutation is neonatal lethal in mice, we generated a novel $Neurog1^{loxP}$ mutant mouse line for *Cre-flox* mediated conditional gene deletion in the cerebellum. Using these complementary knockout tools, we show *Neurog1* is dispensable for the normal proliferation of GABAergic progenitor cells in the cerebellar VZ and pWM tracts of embryonic and postnatal mice respectively. Consistent with this finding, stereology did not reveal differences in cerebellum size or in the numbers of GABAergic Purkinje cells or inhibitory interneurons in the cerebellar cortex of P21 mice. We conclude *Neurog1* is not required for GABAergic neurogenesis in embryonic or postnatal mice.

Prolonged pulse-labeling of Pax2+ GABAergic interneuron progenitors in the postnatal cerebellum did reveal reduced cell dispersal from the pWM tracts to the granule and molecular layers of the cerebellar cortex with *Neurog1* deletion. This suggests a post-mitotic requirement for *Neurog1* in the differentiation and migration of progenitors from the pWM. A functional requirement for pro-neural bHLH transcription factor genes (including *Neurog1*) in the migration of new neurons has been established in the developing neocortex. *Neurog2* has been shown to function in the migration of newly generated cortical neurons through the expression of a GTP binding protein, *Rnd2* (28). Moreover, cortical expression of *Rnd2* was severely reduced in *Neurog2* null-mutant embryos and completely eliminated in *Neurog1;Neurog2* double mutant embryos, suggesting *Neurog1* transcriptional activation is necessary for the expression of an

essential regulator of neuronal migration. Similarly, *Ascl1* has been shown to promote neuronal migration in the embryonic cortex through regulation of *Rnd3* (62), where disruption of either *Ascl1* or *Rnd3* expression causes a defect in cortical neuron migration. The fact that disruptions in Pax2+ inhibitory interneuron cell dispersal did not lead to differences in GABAergic cell numbers in mutants suggests the requirement for *Neurog1* is transitory and that delayed maturation does not impair interneuron cell survival and integration into adult cerebellar circuits.

Purkinje cell progenitors express *Neurog1-CreER* around the time they become post-mitotic but *Neurog1* is not required for cell cycle progression or exit from the cell cycle in E12.5 VZ progenitors

Our previous analysis of the proliferative status of PC progenitors and their long-term BrdU retention showed *Neurog1-CreER* was expressed in PCs immediately following or at terminal cell division (59). *Neurog2*^{CreER} is similarly expressed in PC progenitors exiting the cell cycle but conditional *Neurog2* loss-of-function delays G1 progression in E12.5 VZ progenitor cells rather than disrupt cell cycle exit (19). In our analysis, *Neurog1*$^{Neo/Neo}$ loss-of-function did not result in significant changes in the rate of progression from S-phase to G2/M-phase of the cell cycle nor did it disrupt the rate of cell cycle exit in E12.5 VZ progenitors. Possible explanations for our findings are that: like *Neurog2*, *Neurog1* functions during G1-phase of the cell cycle; that it functions redundantly with other bHLH genes such as *Neurog2* to control cell cycle dynamics; or that *Neurog1* functions post-mitotically to establish early cell polarity and migratory activity, as has been demonstrated for *Neurog2* in cortical pyramidal cells (25; 28). Neonatal lethality in *Neurog1*$^{Neo/Neo}$ mice prohibits the long-term analysis of loss-of-

function effects and a more comprehensive understanding of *Neurog1* function in PCs should be permissible using a conditional mutant currently under development.

Conditional *Neurog1* deletion does not result in reductions of GABAergic neurons in P21 conditional knockout mice

Stereological cell counts of GABAergic Purkinje cells, Golgi cells, basket and stellate cells did not reveal differences in cell number between conditional knockouts and littermate controls using either an inducible or constitutive Cre recombinase-mediated approach at P21. The lack of effect of *Neurog1* loss-of-function on cerebellar GABAergic cell survival or cerebellar size suggests a transient requirement for *Neurog1* in the maturation of GABAergic cerebellar neurons that is not required for long-term cell survival. This is in contrast to data from similar conditional deletion studies of VZ co-expressed bHLH transcription factors *Ascl1* and *Neurog2*. Sudarov et al. (2011) have shown conditional deletion of *Ascl1* resulted in a smaller cerebellum and reduced Golgi, basket and stellate cell (as well as in oligodendrocyte) numbers in adult mice. Interestingly these authors show reduced inhibitory interneuron cell numbers were associated with increased numbers of astrocytes in the cerebellar cortex of *Ascl1* mutants suggesting a mis-specification of pWM interneuron progenitors to glia. Conditional deletion of *Neurog2* in mice also resulted in a smaller cerebellar volume in addition to associated disruptions in VZ progenitor cell cycle progression, Purkinje cell survival and dendritogenesis (Florio et al. 2012). It is possible either *Ascl1* or *Neurog2* or both genes function in concert with *Neurog1* and that their function compensates for *Neurog1* deletion in GABAergic cell specification (although the minimal < 1% labeling of cortical inhibitory interneurons with *Neurog2* GIFM argues against a strong role for this gene in Golgi, basket or stellate cell specification).

Our lab has shown co-expression of *Neurog1* and *Ascl1* in individual progenitor cells in the VZ of the cerebellar anlage at E12.5 (59; 91). Since *Ascl1* has been shown to be required for the generation of late-born GABAergic cerebellar interneurons (74), *Ascl1* may be responsible for genetic compensation of *Neurog1* in our conditional knockout mouse and the reason we do not see reductions in GABAergic cell populations at P21. If this is the case, the generation of double knockouts floxed for both *Ascl1* and *Neurog1* would be expected to result in greater losses of inhibitory interneurons than occurs with *Ascl1* cerebellar deletion alone. These experiments are now possible with the development of our *Neurog1*^{loxP} line. Another possibility is that *Ptf1a* function compensates for *Neurog1* deletion to ensure normal GABAergic cell specification in our conditional mutants. *Neurog1*, *Neurog2* and *Ascl1* expression overlap with the *Ptf1a* expression domain in the VZ (91) and *Ptf1a* plus *Ascl1* double mutant mice have shown *Ptf1a* functions with *Ascl1* in generating interneurons in the ML (74). Mice lacking one copy of the *Ptf1a* gene in *Ascl1* conditional knockouts had a stronger phenotype of reduced stellate interneurons when compared to mice lacking only *Ascl1* in the cerebellum, suggesting overlap in the functions of *Ptf1a* and *Ascl1* in regulating generation of ML interneurons (74). Again the generation of *Ptf1a* plus *Neurog1* double cerebellar mutants would be necessary to test this hypothesis; currently these experiments would be challenging as Florio et al. used a CreER knock-in strategy and only 4 % of CD1-outbred *Neurog2*$^{CreER/CreER}$ survived past P15.

Conditional *Neurog1*$^{loxP/loxP}$ knockout mice are viable and can be used to study the long-term effects of *Neurog1* loss-of-function in mice

We generated a viable mutant in which *Neurog1* is fully inactivated in the developing cerebellum. Our mutant mice survive to weaning age and generate litter sizes

comparable to the background C57BL6/J strain of mice. We show *Neurog1*^{loxP} mutants can be used for targeted gene deletion studies in mice when bred to constitutive Cre or inducible CreER recombinase mice - ISH labeling of *Neurog1* mRNA was entirely absent from the cerebellar primordium at E12.5 cKO mutants while *Neurog1* ISH signal remained robust in the adjacent pontine neuroepithelium. Although we experienced some TMX toxicity effects and parturition issues when crossing *Neurog1*^{loxP} mice with inducible *En2*$^{CreER/+}$ mice, we were nevertheless able to generate viable postnatal cerebellar knockouts with this approach with a 75 mg/Kg TMX dose, highlighting the potential widespread use of *Neurog1*^{loxP} mice in CreER-mediated spatiotemporal gene deletion studies. We therefore predict *Neurog1*$^{loxP/loxP}$ mice can be used with available Cre or CreER mice to study the long-term effects of *Neurog1* deletion in multiple regions of CNS expression such as the hippocampus, cortex or thalamus (Kim et al., 2011). Thus our *floxed Neurog1* mutant mouse can serve as an important tool to assess *Neurog1* function in CNS cell circuit specification and associated behaviors in postnatal mice.

CHAPTER 4: Discussion

In this study we sought to determine the transcription factor programs that specify GABAergic neuron diversity in the cerebellum. Based on spatiotemporal expression data by our lab and others, we focused on the basic helix-loop-helix (bHLH) transcription factor *Neurog1*. We hypothesize the *Neurog1* gene is required for the normal development of GABAergic neurons in the mouse cerebellar cortex. To faithfully map the fate of all *Neurog1*-expressing progenitors in the adult cerebellum, we used genetic inducible fate-mapping (GIFM) with a transgenic *Neurog1-CreER* allele in mice. *Neurog1*-expressing progenitors in the VZ and pWM tracts are fate-mapped to become PCs and all GABAergic interneuron cell types of the cerebellum but not glia, with the spatiotemporal sequence of fate mapping unique to each neuronal cell type (Figure 22).

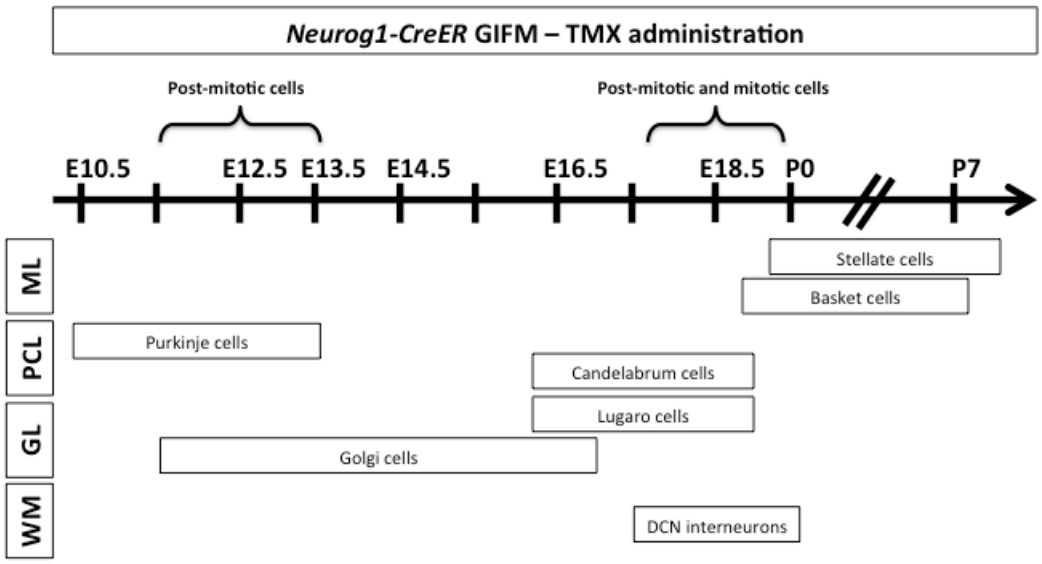

Figure 22. Summary Diagram: *Neurog1-CreER* GIFM in the developing mouse cerebellum

By combining BrdU pulse-labeling with *Neurog1-CreER* fate-mapping, we find the timing of *Neurog1* expression in cerebellar progenitors differs between early and later phases of GABAergic neurogenesis (Figure 22). *Neurog1* is expressed in PCs around the time they become post-mitotic but expressed in both mitotic and post-mitotic interneurons. A majority of cells fate-mapped by *Neurog1-CreER* GIFM are specified in the postnatal cerebellum. We developed a conditional gene deletion approach to overcome neonatal lethality of the conventional $Neurog1^{Neo/Neo}$ mutation (47) in order to permit a more longitudinal study of the effects of gene deletion. Our conditional *Neurog1* gene knockout mutant mice showed no significant differences in cerebellar morphology, the number of GABAergic neurons in the cerebellar cortex, rates of cell proliferation, cell cycle progression or re-entry. However, 4-5 day pulse-labeling of P5 and P6 progenitors suggest a requirement for *Neurog1* activity in inhibitory interneuron cell dispersal from pWM tracts in the developing cerebellum of postnatal mice (Figure 23). Taken together these data reveal *Neurog1* is expressed and functions in the differentiation of GABAergic neurons in the cerebellum but is not required for their survival and distribution in the adult cerebellar cortex.

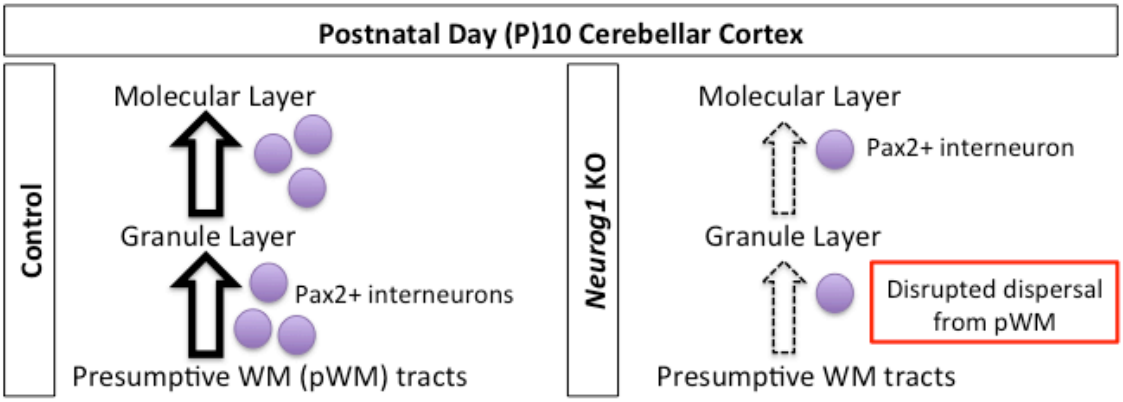

Figure 23. Summary Diagram: Conditional *Neurog1* deletion in postnatal mouse cerebellum

NEUROG1-CREER GIFM EXCLUSIVELY LABELS GABAERGIC NEURONS IN THE CEREBELLUM

Neurog1-CreER GIFM labels all GABAergic neuronal cell types of the cerebellar cortex. Temporal *Neurog1-CreER* GIFM initially labels PCs at E10.5-E12.5 and then transitions to interneuron cell fate early in cerebellar development. GABAergic interneurons of the cerebellar cortex were fate-mapped at E13.5-P7 in a temporal sequence that correlates with their final inside-to-outside resting position. These fate-mapped cells included Golgi cells of the innermost granule layer, Lugaro and candelabrum interneurons of the Purkinje cell layer, and basket and stellate cells in the outer molecular layer. Similar to our *Neurog1-CreER* fate map, GIFM using *Ascl1*^{CreER} mice labeled PCs during E10.5-E12.5, with inhibitory interneurons subsequently fate-mapped to granule layer, Purkinje cell and then molecular layers of the cerebellar cortex (74). GIFM of *Neurog2* with a knock-in *Neurog2*$^{CreER/+}$ allele did mark a vast majority of PCs (~75% of their total marked cells) with TMX delivery at E11.25 to E12.25, but cortical GABAergic interneurons were nearly absent (<1%) (19). These studies combined provide supporting evidence of overlapping but distinct lineage functions of these proneural bHLH transcription factor genes expressed in the cerebellar VZ.

Although TMX delivery at E10.5-E12.5 spans the time of DCN neurogenesis (10), *Neurog1-CreER* GIFM did not fate-map DCN cells at these time points, which is consistent with previous studies in our lab (45). Interestingly, *Neurog1-CreER* GIFM labeled DCN interneurons during late embryogenesis at E18.5. This result was unexpected, as DCN fates were not observed in short-term fate-mapping in *Neurog1-EGFP* mice (45) or long-term fate-mapping studies in *Neurog1-CreER* GIFM with a *Rosa26 β-glatactosidase* (*R26*$^{Lacz/+}$) reporter (35). Our *Neurog1-CreER* fate mapping of

DCN interneurons during late embryogenesis is unique among other proneural genes. *Ascl1*^{CreER} GIFM did reveal GABAergic DCN neurons as the first cells to be labeled at E10.5-E11.5 (74) and *Neurog2*$^{CreER/+}$ fate mapped DCN interneurons at E11.25 to E12.25 (19). The fate mapping of DCN cells during early and later periods of embryogenesis might indicate these bHLH factor genes specify different DCN neuronal subtypes.

Neurog1-CreER GIFM from E11.5 to P7 did not label cells in the white matter tracts of adult cerebellum and no reporter gene expressing cells displayed astrocyte morphology. IHC with antibodies to oligodendrocytes and glial cell makers confirmed *Neurog1-CreER* did not fate map any oligodendrocytes or glia at E13.5 or E18.5. *Ascl1*^{CreER} GIFM at E13.5-P7 marked Bergmann glia, astrocyte and oligodendrocyte lineages (74) and *Neurog2*$^{CreER/+}$ fate mapped a small percentage of Bergmann glia cells (19). Combined these data demonstrate the *Neurog1-CreER* allele fate maps GABAergic neurons but not glial cell types of the cerebellar cortex. *Neurog1* is distinct among other proneural bHLH transcription factors (91) in that progenitors expressing this gene exclusively give rise to neuronal fates.

There is supporting evidence that the cerebellar VZ gives rise to GABAergic interneuron and glia progenitors that translocate to the pWM during later embryonic development to generate interneurons. Lineage tracing from a *Ptf1a*^{Cre} knock-in allele marked PCs, DCN inhibitory interneurons, Golgi, basket and stellate cell inhibitory interneurons of the cerebellar cortex, and GFAP-positive astrocytes in the cerebellum (30). The mechanisms controlling interneuron or glial fate may require bHLH programs. Conditional *Ascl1* deletion in mice depletes GABAergic interneuron numbers in the cortex but increases the number of astrocytes (74). In addition to fate-mapping a vast

majority of PCs, GIFM in *Neurog2*$^{CreER/+}$ mice also marked a small percentage of Bergmann glial cells (19). These data provide supporting evidence glia cell types derive from VZ progenitors. A recent *in vivo* clonal analysis study reveals astroglial-like progenitors in the pWM that are bipotent and can produce GABAergic interneurons and astrocytes (64). The absence of marked glia cells in our *Neurog1-CreER* mice suggests *Neurog1* may function to commit bipotent progenitors to an exclusively neuronal cell fate in the pWM. Cell grafting studies that placed post-mitotic cells in developing cerebellum reveal donor cells acquired laminar position and phenotypes of host interneurons, suggesting cues within the pWM dictate cell fate (43). Therefore, we speculate *Neurog1*-expressing progenitors specify interneuron cell fates from cues within the pWM.

E12.5 GIFM-LABELED PCS THAT SETTLE IN DISTINCT PARASAGITTAL STRIPES

GIFM at E10.5, E11.5 and E12.5 fate-mapped PCs in the adult cerebellum with the highest number of PCs labeled from TMX delivery at E11.5. PCs were similarly labeled with E10.5-E12.5 GIFM in *Ascl1*^{CreER} mice with the maximum cell fating with TMX delivery at E11.5 (74). PCs have been fate-mapped using *Neurog1-CreER* GIFM with *R26*$^{Lacz/+}$reporter (35) with TMX administration at E10.5-E12.5 and E12.5 PCs settled preferentially in rostral cerebellar lobes. Interestingly, our GIFM study reveal PCs marked at E12.5 settled in a bilaterally symmetrical pattern of three parasagittal stripes along the medal-lateral axis in the adult cerebellar cortex, very similar to PCs marked with *Ascl1*^{CreER} GIFM with TMX delivery at E12.5 (74). E12.5 *Neurog1-CreER* GIFM patterns are also similar to parasagittal distribution of marked PCs in the vermis and paravermis following the labeling of E12.5 VZ progenitors with replication-defective adenoviral vectors (27).

Lobules of the cerebellum have a molecular code along the medial-lateral axis defined by these parasagittal domains of gene expression in PCs. Combination of afferents from different locations of the CNS project in to particular lobules of the cerebellum forming parasagittal zones (72). The proper connectivity of zones has been shown to be critical for motor coordination (22). The findings that *Neurog1*-expressing progenitors settle in organized parasagittal domains suggest distinct functional properties of these progenitors as they migrate from the VZ to their destined position along the medial-lateral axis of the adult cerebellum. However, the parasagittal stripes in the adult cerebellar cortex of *Neurog1-CreER* mice did not correlate with known PC subtype markers Zebrin II (Aldolase C), Hsp25, and PLCβ4.

While the electrical properties of *Neurog1*-expressing progenitors remain unknown, we speculate *Neurog1* may have a role in cerebellar compartmentation. A *Ptf1a-Neurog1/2-Early B-cell factor 2* (*Ebf2*) regulatory network is implicated in this PC subtype specification (41; 91). A subset of early-born PCs do not express *Neurog1/2* nor *Ebf2* and express ZebII+ phenotypes in the adult. Around E11, *Neurog1/2* is upregulated by *Ptf1a* in later-born PC progenitors that also express *Ebf2* and in turn, represses the ZebII+ phenotype (12; 41). Deletion of *Efb2* leads to transdifferentiated PCs that express markers characteristic of both ZebII+ and ZebII- subtypes (14). Therefore, *Neurog1/2* and *Ebf2* expressing progenitors are implicated in late-born PCs that adopt the ZebII- phenotype and suggest a role for *Neurog1* in PC phenotype specification in functional parasagittal stripes. PC subtype organization is hypothesized to play a role in instructing circuit wiring.

PCs fire two types of action potentials: simple spikes that are generated intrinsically, and complex spikes that are induced by climbing fiber afferents. PC complex spike rate increases abruptly at 3 weeks of age and simple spike firing rate increases gradually until it stabilizes at 4 weeks of age; this irregular pattern of PC firing during development shows PCs reach maturity by 4 weeks of age (3) and PC electrical activity is dynamically changing throughout postnatal development. Combined this data with *Neurog1*-exprssing progenitors settling in parasagittal domains in the adult cerebellum suggest *Neurog1* may have a role in acquiring such functional properties during development.

We found that E12.5 *Neurog1-CreER* fate-mapped PCs were uniformly distributed along the medial-lateral axis of the cerebellar anlage 24 hours post TMX injection at E13.5 and begin to aggregate into clusters 6 days post TMX injection at E18.5, arguing against any regionalization of *Neurog1*-expressing progenitors. These similarities in E12.5 fate maps suggest *Neurog1*- and *Ascl1*-expressing PCs function in the same cell lineages destined for the adult vermis and paravermis. It is probable these two proneural genes are co-expressed in newly born PCs and both fate-map to the same locations. These observations were supported with dual fluorescent ISH in our study, showing overlapping *Neurog1* and *Ascl1* expression in progenitor cells and the patterns suggest progenitor transition from *Ascl1* to *Neurog1* expression as they migrate dorsally from the VZ – *Neurog1* ISH territory overlaps but is shifted slightly dorsal to the *Ascl1* ISH territory that predominates at the VZ.

In *Neurog1-CreER* mice, the extensive overlap of PCs fate-mapped at E10.5, E11.5, and E12.5 supports the view that individual PCs were labeled with TMX delivery

on more than one date, showing *Neurog1* expression is sustained during PC specification. The relative distribution of marked PCs at E11.5 and E12.5 GIFM indicates that E12.5 marked cells are derived from a subset of PCs in which earlier *Neurog1* expression is maintained past E13. For example, one PC may no longer express *Neurog1* shortly after being fate-mapped at E11.5 but the neighboring PC may continue to express *Neurog1* on E12.5 onward. It is plausible subsets of PCs with sustained *Neurog1* expression acquire distinct functional properties. The transient expression of *Neurog1* in PCs with some PCs expressing *Neurog1* for an elongated time may suggest these cells have a distinct molecular identity with some function yet to be determined.

ANALYSIS OF *NEUROG1* FUNCTION DURING EARLY AND LATER PHASES OF GABAERGIC NEUROGENESIS

Our data indicates the timing of *Neurog1* expression in cerebellar progenitors differs between early and later phases of GABAergic neurogenesis. E11.5 to E13.5 GIFM primarily marked non-mitotic PC progenitors in the VZ and long-term BrdU retention indicated *Neurog1* is expressed in PCs around the time they become post-mitotic. In contrast, E18.5 GIFM primarily marked proliferating interneuron progenitors in the VZ and long-term BrdU retention indicated *Neurog1* is expressed in roughly equal ratios of mitotic and non-mitotic interneuron progenitors in pWM tracts. Differences in the timing of expression relative to mitotic status indicates distinct functions of *Neurog1* in VZ and pWM GABAergic progenitor cells. It is plausible *Neurog1* functions in neuronal differentiation in VZ PC progenitors and cell cycle regulatory functions in pWM inhibitory interneuron progenitors. We investigated the effects of *Neurog1* loss-of-function on pre- and postnatal cerebellar development in conditional knockout mice.

NEUROG1 LOSS-OF-FUNCTION IN VZ PROGENITORS

Our analysis of the proliferative status of PC progenitors and their long-term BrdU retention showed *Neurog1-CreER* was expressed in PCs immediately following or at terminal cell division, consistent with the notion *Neurog1* has a functional role in cell cycle progression and/or cell cycle exit. *Neurog2*^{CreER} is similarly expressed in PC progenitors exiting the cell cycle but conditional *Neurog2* loss-of-function delays G1 progression in E12.5 VZ progenitor cells rather than disrupt cell cycle exit (19). In our analysis, *Neurog1*$^{Neo/Neo}$ loss-of-function did not result in significant changes in the rate of progression from S-phase to G2/M-phase of the cell cycle nor did it disrupt the rate of cell cycle exit in E12.5 VZ progenitors. Possible explanations for our findings are that: like *Neurog2*, *Neurog1* functions during G1-phase of the cell cycle; that it functions redundantly with other bHLH genes such as *Neurog2* to control cell cycle dynamics; or that *Neurog1* functions post-mitotically to establish early cell polarity and migratory activity, as has been demonstrated for *Neurog2* in cortical pyramidal cells (25; 28).

Determining *Neurog1* function in postnatal progenitor cells in pWM tracts required our conditional *Neurog1* mutant. We began our analysis of *Neurog1* mutant mice at P21, the earliest postnatal development time point where cell genesis and cell positioning is complete. Stereological cell counts of GABAergic Purkinje cells, Golgi cells, basket and stellate cells did not reveal differences in cell number between conditional knockouts and littermate controls at P21. This is in contrast to data from similar conditional deletion studies of VZ co-expressed bHLH transcription factors *Ascl1* and *Neurog2*. Sudarov et al. (2011) have shown conditional deletion of *Ascl1* resulted in a smaller cerebellum and reduced Golgi, basket and stellate cell (as well as in

oligodendrocyte) numbers in adult mice. Interestingly these authors show reduced inhibitory interneuron cell numbers were associated with increased numbers of astrocytes in the cerebellar cortex of *Ascl1* mutants suggesting a mis-specification of pWM interneuron progenitors to glia. Preliminary data from cKO mice revealed no difference in GFAP expression intensity in white matter tracts of P21 cerebellum. Conditional deletion of *Neurog2* in mice resulted in a smaller cerebellar volume in addition to associated disruptions in VZ progenitor cell cycle progression, PC survival and dendritogenesis (Florio et al. 2012). It is possible either *Ascl1* or *Neurog2* or both genes function in concert with *Neurog1* and that their function compensates for *Neurog1* deletion in GABAergic cell specification. In support of this, RT-qPCR revealed significant upregulation of both *Ascl1* and *Neurog1* in *Neurog2* null cerebellar primordium at E12.5 (19). *Neurog1* may share overlapping functions with other proneural genes, requiring the generation and analysis of double (*Neurog1*/*Neurog2*) and triple (*Neurog1*/*Neurog2*/*Ascl1*) mutants to uncover *Neurog1* function(s) in cerebellar development.

Our dual fluorescence ISH data confirms co-expression of *Neurog1* and *Ascl1* in individual progenitor cells in the VZ of the cerebellar anlage at E12.5. Since *Ascl1* has been shown to be required for the generation of late-born GABAergic cerebellar interneurons (74), *Ascl1* may be responsible for genetic compensation of *Neurog1* in our conditional knockout mouse and the reason we do not see reductions in GABAergic cell populations at P21. If this is the case, the generation of double knockouts floxed for both *Ascl1* and *Neurog1* would be expected to result in greater losses of inhibitory interneurons than occurs with *Ascl1* cerebellar deletion alone. These experiments are now

possible with the development of our *Neurog1*^{loxP} line. Another possibility is that *Ptf1a* function compensates for *Neurog1* deletion to ensure normal GABAergic cell specification in our conditional mutants. *Neurog1*, *Neurog2* and *Ascl1* expression overlap with the *Ptf1a* expression domain in the VZ (91) and *Ptf1a* plus *Ascl1* double mutant mice have shown *Ptf1a* functions with *Ascl1* in generating interneurons in the ML (74). Mice lacking one copy of the *Ptf1a* gene in *Ascl1* conditional knockouts had a stronger phenotype of reduced stellate interneurons when compared to mice lacking only *Ascl1* in the cerebellum, suggesting overlap in the functions of *Ptf1a* and *Ascl1* in regulating generation of ML interneurons (74). Based off our data, we conclude *Neurog1* is not required for GABAergic neurogenesis in embryonic or postnatal mice and may have functions that overlap with other proneural genes like *Ascl1* and *Ptf1a*.

NEUROG1 LOSS-OF-FUNCTION EFFECTS PAX2+ INTERNEURON DISPERSAL FROM PWM

GIFM primarily marked proliferating interneuron progenitors in the VZ and long-term BrdU retention indicated *Neurog1* is expressed in mitotic and non-mitotic interneuron progenitors in pWM tracts. Therefore, we wanted to determine the effects of cerebellar *Neurog1* loss-of-function on the proliferation of inhibitory interneuron progenitor cells at early postnatal time points. The data indicate *Neurog1* loss-of-function did not significantly effect the number, proliferation or cell cycle re-entry rates of Pax2+ inhibitory interneuron progenitors in the cerebellum.

However, prolonged pulse-labeling of Pax2+ GABAergic interneuron progenitors in the postnatal cerebellum did reveal reduced cell dispersal from the pWM tracts to the granule and molecular layers of the cerebellar cortex with *Neurog1* deletion. This suggests a post-mitotic requirement for *Neurog1* in the differentiation and migration of

progenitors from the pWM. A functional requirement for pro-neural bHLH transcription factor genes (including *Neurog1*) in the migration of new neurons has been established in the developing neocortex. *Neurog2* has been shown to function in the migration of newly generated cortical neurons through the expression of a GTP binding protein, *Rnd2* (28). Moreover, cortical expression of *Rnd2* was severely reduced in *Neurog2* null-mutant embryos and completely eliminated in *Neurog1;Neurog2* double mutant embryos, suggesting *Neurog1* transcriptional activation is necessary for the expression of an essential regulator of neuronal migration. Similarly, *Ascl1* has been shown to promote neuronal migration in the embryonic cortex through regulation of *Rnd3* (62), where disruption of either *Ascl1* or *Rnd3* expression causes a defect in cortical neuron migration. The fact that disruptions in Pax2+ inhibitory interneuron cell dispersal did not lead to differences in GABAergic cell numbers in mutants suggests the requirement for *Neurog1* is transitory and that delayed maturation does not impair interneuron cell survival and integration into adult cerebellar circuits.

A technical limitation of this study was that we experienced relatively low BrdU compared to EdU incorporation rates in proliferating progenitors. This likely accounted for the lack of statistical differences in the distributions of Pax2+/BrdU+ and Pax2+/BrdU+/EdU+ populations between pKO and control mice (although Pax2+/BrdU+ and Pax2+/BrdU+/EdU+ counts in the GL were approaching significance). Nevertheless, based on the overall differences in distribution of pulse-labeled Pax2+ progenitors cells, we conclude cell distribution in the GL and ML between mutant and control mice are consistent with a significant impairment of inhibitory interneuron cell dispersal from the pWM with *Neurog1* loss-of-function.

CONDITIONAL *NEUROG1*$^{LOXP/LOXP}$ KNOCKOUT MICE ARE VIABLE AND CAN BE USED TO STUDY THE LONG-TERM EFFECTS OF *NEUROG1* LOSS-OF-FUNCTION IN MICE

We generated a viable mutant in which *Neurog1* is fully inactivated in the developing cerebellum. We show *Neurog1*^{loxP} mutants can be used for targeted gene deletion studies in mice when bred to constitutive Cre or inducible CreER recombinase mice - ISH labeling of *Neurog1* mRNA was entirely absent from the cerebellar primordium at E12.5 cKO mutants while *Neurog1* ISH signal remained robust in the adjacent pontine neuroepithelium. We experienced some TMX toxicity effects and parturition issues when crossing *Neurog1*^{loxP} mice with inducible *En2*$^{CreER/+}$ mice, and these issues could account for the differences in cell density and cerebellum volume between an inducible or constitutive Cre recombinase-mediated *Neurog1* deletion at P21. This highlights the sensitivity of using different transgenic mouse lines when inducing the same gene deletion. Nonetheless, we predict *Neurog1*$^{loxP/loxP}$ mice can be used with available Cre or CreER mice to study the long-term effects of *Neurog1* deletion in multiple regions of CNS expression such as the hippocampus, cortex or thalamus (Kim et al., 2011). Thus our *floxed Neurog1* mutant mouse can serve as an important tool to assess *Neurog1* function in CNS cell circuit specification and associated behaviors in postnatal mice.

FUTURE DIRECTIONS

While our conditional *Neurog1* loss-of-function approach did not reveal many significant differences when comparing *Neurog1*^{loxP} mice with control littermates, more future studies may supplement our understanding of *Neurog1* function in cerebellar development. One obvious approach would be to investigate gain-of-function effects in mice. In a gain-of-function approach, wild-type E12.5 embryos were injected with a

lentivirus encoding *Neurog2* and *GFP* or a control *GFP* vector and then pulsed with thymidine analogs. *Neurog2* overexpression accelerates cell-cycle withdrawal, as there was a decrease in the proliferating pool (19). Similarly, it would be interesting to overexpress *Neurog1* in P5 inhibitory interneurons followed by thymidine analog pulse-labeling. We predict an overexpression of *Neurog1* may increase the migration of cells away from the pWM into the GL and ML as well as increase the interneuron population in the ML of the postnatal cerebellum. *Neurog2* in the embryonic cerebral cortex directly induces the expression of a GTP-binding protein Rnd2, which is a key regulator of neuronal migration (28). Cortical expression of Rnd2 is downregulated in *Neurog2* mutants but completely eliminated in *Neurog1; Neurog2* double mutant embryos (28), suggesting a roll for *Neurog1* in Rnd2 expression. Therefore, by comparing the expression and localization of Rnd2 in the cerebellum of our conditional $Neurog1^{loxP}$ mice and their control littermates would provide supporting evidence of a function for *Neurog1* in cerebellar neuronal migration.

In addition to our understanding of *Neurog1* at the cellular level, it would be interesting to examine the physiological effects of altered gene function. The cerebellum has been associated with processing higher cognitive functions linking autism with cerebellar dysfunction (24). We observed no obvious defects in motor coordination of our conditional $Neurog1^{loxP}$ mutants, but we can examine other cognitive functions related to cerebellar dysfunction. The findings that *Neurog1*-expressing progenitors fate-map PCs in organized parasagittal domains in the adult cerebellar cortex suggest distinct functional properties of these progenitors that remain unknown. Thus, alternative strategies to assess *Neurog1* deletion on cerebellum neural circuitry may include water t-maze to asses

impaired motor learning, three-chambered assay with a novel object or mouse to assess social interaction, measuring the frequency of ultrasonic vocalizations, or observance of repetitive behaviors such as grooming, as abnormal PC function has been linked to these autism spectrum disorder-like behaviors deficits (78).

CONCLUSION

Our GIFM study created a detailed spatiotemporal fate map of *Neurog1* expression in the developing mouse cerebellum. We found that the timing of *Neurog1* expression is unique to each GABAergic neuronal cell type and determines the final resting position of neurons in the adult cerebellar cortex. Our spatiotemporal fate-map confirmed *Neurog1* is restricted to neuronal fates and also provided a framework for *Neurog1* loss-of-function analysis in our conditional mutant mice. GIFM in combination with BrdU pulse-labeling indicate *Neurog1* is expressed mainly in post-mitotic PC progenitors during early phases of GABAergic neurogenesis. From this finding, we expected *Neurog1* functions in cell cycle progression and/or cell cycle exit. To test this hypothesis we used conventional *Neurog1*$^{Neo/Neo}$ knockout mice to measure the effects of *Neurog1* loss-of-function on VZ cell cycle parameters in E12.5 mice. There was not a significant difference in the rate of cell cycle progression or the rate of cell cycle exit in E12.5-E13 VZ progenitors.

Using a conditional mouse knockout approach to target *Neurog1* deletion in the cerebellum, we were able to examine gene loss-of-function effects in postnatal mice. GIFM in combination with BrdU pulse-labeling indicate *Neurog1* is expressed in equal numbers of mitotic and post-mitotic interneuron progenitors during later phases of GABAergic neurogenesis. From this finding, we expected a requirement for *Neurog1* in

the normal development of GABAergic neurons in the adult cerebellum. Stereological quantification of GABAergic cell types in the cerebellum of P21 cKO or pKO mice revealed no differences from *Neurog1* deletion. Therefore, we shifted our analysis to an earlier postnatal period and assessed cell proliferation and migration of Pax2+ inhibitory interneurons. We reveal a significant impairment of Pax2+ inhibitory interneuron cell dispersal from the pWM with *Neurog1* loss-of-function.

This data suggests a post-mitotic requirement for *Neurog1* in the differentiation and migration of progenitors from the pWM. A functional requirement for proneural bHLH factors *Neurog2* and *Ascl1* have been established in the developing neocortex. Expression of these proneural genes are necessary for the expression of an essential regulator of neuronal migration. The fact that disruptions in Pax2+ inhibitory interneuron cell dispersal did not lead to differences in GABAergic cell numbers in mutants suggests the requirement for *Neurog1* is transitory and that delayed maturation does not impair interneuron cell survival and integration into adult cerebellar circuits. Our GIFM of *Neurog1-CreER* is very similar to fate-mapping of *Ascl1*. Our ISH experiments provide supporting evidence that *Neurog1* and *Ascl1* are temporally expressed in a subset of progenitors in early and later phases of GABAergic neurogenesis. Therefore, we speculate *Neurog1* deletion in our conditional mutant mice is overcome by genetic compensation from *Ascl1*. From our studies, we conclude *Neurog1* is not required for the generation of GABAergic neurogenesis in embryonic or postnatal mice but has probable functions in migration of newly born interneurons in pWM tracts of the developing cerebellum.

REFERENCES

1. Aldinger KA, Lehmann OJ, Hudgins L, Chizhikov VV, Bassuk AG, et al. 2009. FOXC1 is required for normal cerebellar development and is a major contributor to chromosome 6p25.3 Dandy-Walker malformation. *Nat Genet* 41:1037-42
2. Ali F, Hindley C, McDowell G, Deibler R, Jones A, et al. 2011. Cell cycle-regulated multi-site phosphorylation of Neurogenin 2 coordinates cell cycling with differentiation during neurogenesis. *Development* 138:4267-77
3. Arancillo M, White JJ, Lin T, Stay TL, Sillitoe RV. 2015. In vivo analysis of Purkinje cell firing properties during postnatal mouse development. *J Neurophysiol* 113:578-91
4. Ben-Arie N, Bellen HJ, Armstrong DL, McCall AE, Gordadze PR, et al. 1997. Math1 is essential for genesis of cerebellar granule neurons. *Nature* 390:169-72
5. Bolduc ME, Limperopoulos C. 2009. Neurodevelopmental outcomes in children with cerebellar malformations: a systematic review. *Dev Med Child Neurol* 51:256-67
6. Boyle CA, Boulet S, Schieve LA, Cohen RA, Blumberg SJ, et al. 2011. Trends in the prevalence of developmental disabilities in US children, 1997-2008. *Pediatrics* 127:1034-42
7. Britz O, Mattar P, Nguyen L, Langevin L-M, Zimmer C, et al. 2006. A Role for Proneural Genes in the Maturation of Cortical Progenitor Cells. *Cerebral Cortex* 16:i138-i51
8. Buffo A, Rossi F. 2013. Origin, lineage and function of cerebellar glia. *Progress in Neurobiology* 109:42-63
9. Canitano R, Pallagrosi M. 2017. Autism Spectrum Disorders and Schizophrenia Spectrum Disorders: Excitation/Inhibition Imbalance and Developmental Trajectories. *Front Psychiatry* 8:69
10. Carletti B, Rossi F. 2008. Neurogenesis in the cerebellum. *Neuroscientist* 14:91-100
11. Cerminara NL, Apps R. 2011. Behavioural significance of cerebellar modules. *Cerebellum* 10:484-94
12. Chung SH, Marzban H, Croci L, Consalez GG, Hawkes R. 2008. Purkinje cell subtype specification in the cerebellar cortex: early B-cell factor 2 acts to repress the zebrin II-positive Purkinje cell phenotype. *Neuroscience* 153:721-32
13. Crawley JN. 2008. Behavioral phenotyping strategies for mutant mice. *Neuron* 57:809-18
14. Croci L, Chung SH, Masserdotti G, Gianola S, Bizzoca A, et al. 2006. A key role for the HLH transcription factor EBF2COE2,O/E-3 in Purkinje neuron migration and cerebellar cortical topography. *Development* 133:2719-29
15. Crossley PH, Martin GR. 1995. The mouse Fgf8 gene encodes a family of polypeptides and is expressed in regions that direct outgrowth and patterning in the developing embryo. *Development* 121:439-51
16. Dalgard CL, Zhou Q, Lundell TG, Doughty ML. 2011. Altered gene expression in the emerging cerebellar primordium of Neurog1-/- mice. *Brain Res* 1388:12-21

17. Dixit R, Wilkinson G, Cancino GI, Shaker T, Adnani L, et al. 2014. Neurog1 and Neurog2 Control Two Waves of Neuronal Differentiation in the Piriform Cortex. *Journal of Neuroscience* 34:539-53
18. Englund C, Kowalczyk T, Daza RA, Dagan A, Lau C, et al. 2006. Unipolar brush cells of the cerebellum are produced in the rhombic lip and migrate through developing white matter. *J Neurosci* 26:9184-95
19. Florio M, Leto K, Muzio L, Tinterri A, Badaloni A, et al. 2012. Neurogenin 2 regulates progenitor cell-cycle progression and Purkinje cell dendritogenesis in cerebellar development. *Development* 139:2308-20
20. Franklin K, G P. 2008. *The mouse brain in stereotaxic coordinates*. Academic Press
21. Glickstein M, Doron K. 2008. Cerebellum: connections and functions. *Cerebellum* 7:589-94
22. Graham DJ, Wylie DR. 2012. Zebrin-immunopositive and -immunonegative stripe pairs represent functional units in the pigeon vestibulocerebellum. *J Neurosci* 32:12769-79
23. Grimaldi P, Parras C, Guillemot F, Rossi F, Wassef M. 2009. Origins and control of the differentiation of inhibitory interneurons and glia in the cerebellum. *Dev Biol* 328:422-33
24. Hampson DR, Blatt GJ. 2015. Autism spectrum disorders and neuropathology of the cerebellum. *Front Neurosci* 9:420
25. Hand R, Bortone D, Mattar P, Nguyen L, Heng JI, et al. 2005. Phosphorylation of Neurogenin2 specifies the migration properties and the dendritic morphology of pyramidal neurons in the neocortex. *Neuron* 48:45-62
26. Hashimoto M, Hibi M. 2012. Development and evolution of cerebellar neural circuits. *Dev Growth Differ* 54:373-89
27. Hashimoto M, Mikoshiba K. 2003. Mediolateral compartmentalization of the cerebellum is determined on the "birth date" of Purkinje cells. *J Neurosci* 23:11342-51
28. Heng JI, Nguyen L, Castro DS, Zimmer C, Wildner H, et al. 2008. Neurogenin 2 controls cortical neuron migration through regulation of Rnd2. *Nature* 455:114-8
29. Henke RM, Savage TK, Meredith DM, Glasgow SM, Hori K, et al. 2009. Neurog2 is a direct downstream target of the Ptf1a-Rbpj transcription complex in dorsal spinal cord. *Development* 136:2945-54
30. Hoshino M, Nakamura S, Mori K, Kawauchi T, Terao M, et al. 2005. Ptf1a, a bHLH transcriptional gene, defines GABAergic neuronal fates in cerebellum. *Neuron* 47:201-13
31. J A, SA B. 1997. Development of the cerebellar system. *CRC Press*
32. Jankowski J, Holst MI, Liebig C, Oberdick J, Baader SL. 2004. Engrailed-2 negatively regulates the onset of perinatal Purkinje cell differentiation. *J Comp Neurol* 472:87-99
33. Kawaguchi Y, Cooper B, Gannon M, Ray M, MacDonald RJ, Wright CV. 2002. The role of the transcriptional regulator Ptf1a in converting intestinal to pancreatic progenitors. *Nat Genet* 32:128-34

34. Kim EJ, Battiste J, Nakagawa Y, Johnson JE. 2008. Ascl1 (Mash1) lineage cells contribute to discrete cell populations in CNS architecture. *Mol Cell Neurosci* 38:595-606
35. Kim EJ, Hori K, Wyckoff A, Dickel LK, Koundakjian EJ, et al. 2011. Spatiotemporal fate map of neurogenin1 (Neurog1) lineages in the mouse central nervous system. *J Comp Neurol* 519:1355-70
36. Klockgether T, Paulson H. 2011. Milestones in ataxia. *Mov Disord* 26:1134-41
37. Koundakjian EJ, Appler JL, Goodrich LV. 2007. Auditory Neurons Make Stereotyped Wiring Decisions before Maturation of Their Targets. *Journal of Neuroscience* 27:14078-88
38. Lacomme M, Liaubet L, Pituello F, Bel-Vialar S. 2012. NEUROG2 Drives Cell Cycle Exit of Neuronal Precursors by Specifically Repressing a Subset of Cyclins Acting at the G1 and S Phases of the Cell Cycle. *Molecular and Cellular Biology* 32:2596-607
39. Laine J, Axelrad H. 1996. Morphology of the Golgi-impregnated Lugaro cell in the rat cerebellar cortex: a reappraisal with a description of its axon. *J Comp Neurol* 375:618-40
40. Lainé J, Axelrad H. 1994. The candelabrum cell: A new interneuron in the cerebellar cortex. *Journal of Comparative Neurology* 339:159-73
41. Leto K, Arancillo M, Becker EB, Buffo A, Chiang C, et al. 2016. Consensus Paper: Cerebellar Development. *Cerebellum* 15:789-828
42. Leto K, Bartolini A, Di Gregorio A, Imperiale D, De Luca A, et al. 2011. Modulation of cell-cycle dynamics is required to regulate the number of cerebellar GABAergic interneurons and their rhythm of maturation. *Development* 138:3463-72
43. Leto K, Bartolini A, Yanagawa Y, Obata K, Magrassi L, et al. 2009. Laminar fate and phenotype specification of cerebellar GABAergic interneurons. *J Neurosci* 29:7079-91
44. Leto K, Carletti B, Williams IM, Magrassi L, Rossi F. 2006. Different types of cerebellar GABAergic interneurons originate from a common pool of multipotent progenitor cells. *J Neurosci* 26:11682-94
45. Lundell TG, Zhou Q, Doughty ML. 2009. Neurogenin1 expression in cell lineages of the cerebellar cortex in embryonic and postnatal mice. *Dev Dyn* 238:3310-25
46. Ma Q, Chen Z, Barrantes IdB, Luis de la Pompa J, Anderson DJ. 1998. neurogenin1 Is Essential for the Determination of Neuronal Precursors for Proximal Cranial Sensory Ganglia. *Neuron* 20:469-82
47. Ma Q, Chen Z, del Barco Barrantes I, de la Pompa JL, Anderson DJ. 1998. neurogenin1 is essential for the determination of neuronal precursors for proximal cranial sensory ganglia. *Neuron* 20:469-82
48. Ma Q, Fode C, Guillemot F, Anderson DJ. 1999. NEUROGENIN1 and NEUROGENIN2 control two distinct waves of neurogenesis in developing dorsal root ganglia. *Genes & Development* 13:1717-28
49. Machold R, Fishell G. 2005. Math1 is expressed in temporally discrete pools of cerebellar rhombic-lip neural progenitors. *Neuron* 48:17-24

50. Madisen L, Zwingman TA, Sunkin SM, Oh SW, Zariwala HA, et al. 2010. A robust and high-throughput Cre reporting and characterization system for the whole mouse brain. *Nat Neurosci* 13:133-40
51. Maricich SM, Herrup K. 1999. Pax-2 expression defines a subset of GABAergic interneurons and their precursors in the developing murine cerebellum. *J Neurobiol* 41:281-94
52. Martinez S, Andreu A, Mecklenburg N, Echevarria D. 2013. Cellular and molecular basis of cerebellar development. *Front Neuroanat* 7:18
53. Matei V, Pauley S, Kaing S, Rowitch D, Beisel KW, et al. 2005. Smaller inner ear sensory epithelia in Neurog1 null mice are related to earlier hair cell cycle exit. *Developmental Dynamics* 234:633-50
54. Mathis L, Bonnerot C, Puelles L, Nicolas JF. 1997. Retrospective clonal analysis of the cerebellum using genetic laacZ/lacZ mouse mosaics. *Development* 124:4089-104
55. Mathis L, Nicolas J-F. 2003. Progressive restriction of cell fates in relation to neuroepithelial cell mingling in the mouse cerebellum. *Developmental Biology* 258:20-31
56. Mitsumura K, Hosoi N, Furuya N, Hirai H. 2011. Disruption of metabotropic glutamate receptor signalling is a major defect at cerebellar parallel fibre-Purkinje cell synapses in staggerer mutant mice. *J Physiol* 589:3191-209
57. Miyata T, Kawaguchi D, Kawaguchi A, Gotoh Y. 2010. Mechanisms that regulate the number of neurons during mouse neocortical development. *Current Opinion in Neurobiology* 20:22-8
58. Novak A, Guo C, Yang W, Nagy A, Lobe CG. 2000. Z/EG, a double reporter mouse line that expresses enhanced green fluorescent protein upon cre‐mediated excision. *genesis* 28:147-55
59. Obana EA, Lundell TG, Yi KJ, Radomski KL, Zhou Q, Doughty ML. 2015. Neurog1 Genetic Inducible Fate Mapping (GIFM) Reveals the Existence of Complex Spatiotemporal Cyto-Architectures in the Developing Cerebellum. *Cerebellum* 14:247-63
60. Orvis GD, Hartzell AL, Smith JB, Barraza LH, Wilson SL, et al. 2012. The engrailed homeobox genes are required in multiple cell lineages to coordinate sequential formation of fissures and growth of the cerebellum. *Dev Biol* 367:25-39
61. Ozol K, Hayden JM, Oberdick J, Hawkes R. 1999. Transverse zones in the vermis of the mouse cerebellum. *J Comp Neurol* 412:95-111
62. Pacary E, Heng J, Azzarelli R, Riou P, Castro D, et al. 2011. Proneural transcription factors regulate different steps of cortical neuron migration through Rnd-mediated inhibition of RhoA signaling. *Neuron* 69:1069-84
63. Palay SL, Chan-Palay V. 1974. Cerebellar Cortex. Springer Berlin Heidelberg
64. Parmigiani E, Leto K, Rolando C, Figueres-Onate M, Lopez-Mascaraque L, et al. 2015. Heterogeneity and Bipotency of Astroglial-Like Cerebellar Progenitors along the Interneuron and Glial Lineages. *J Neurosci* 35:7388-402
65. Pascual M, Abasolo I, Mingorance-Le Meur A, Martinez A, Del Rio JA, et al. 2007. Cerebellar GABAergic progenitors adopt an external granule cell-like

phenotype in the absence of Ptf1a transcription factor expression. *Proc Natl Acad Sci U S A* 104:5193-8
66. Radomski KL, Zhou Q, Yi KJ, Doughty ML. 2013. Cortical contusion injury disrupts olfactory bulb neurogenesis in adult mice. *BMC Neuroscience* 14:142
67. Sellick GS, Barker KT, Stolte-Dijkstra I, Fleischmann C, Coleman RJ, et al. 2004. Mutations in PTF1A cause pancreatic and cerebellar agenesis. *Nat Genet* 36:1301-5
68. Seto Y, Nakatani T, Masuyama N, Taya S, Kumai M, et al. 2014. Temporal identity transition from Purkinje cell progenitors to GABAergic interneuron progenitors in the cerebellum. *Nat Commun* 5:3337
69. Sgaier S, Millet S, Villanueva M, Berenshteyn F, Song C, Joyner A. 2005. Morphogenetic and Cellular Movements that Shape the Mouse CerebellumInsights from Genetic Fate Mapping. *Neuron* 45:27-40
70. Sgaier SK, Millet S, Villanueva MP, Berenshteyn F, Song C, Joyner AL. 2005. Morphogenetic and cellular movements that shape the mouse cerebellum; insights from genetic fate mapping. *Neuron* 45:27-40
71. Shaker T, Dennis D, Kurrasch DM, Schuurmans C. 2012. Neurog1 and Neurog2 coordinately regulate development of the olfactory system. *Neural Development* 7:28
72. Sillitoe RV, Joyner AL. 2007. Morphology, molecular codes, and circuitry produce the three-dimensional complexity of the cerebellum. *Annu Rev Cell Dev Biol* 23:549-77
73. Sotelo C. 2008. Viewing the cerebellum through the eyes of Ramon Y Cajal. *Cerebellum* 7:517-22
74. Sudarov A, Turnbull RK, Kim EJ, Lebel-Potter M, Guillemot F, Joyner AL. 2011. Ascl1 genetics reveals insights into cerebellum local circuit assembly. *J Neurosci* 31:11055-69
75. Sun Y, Nadal-Vicens M, Misono S, Lin MZ, Zubiaga A, et al. 2001. Neurogenin Promotes Neurogenesis and Inhibits Glial Differentiation by Independent Mechanisms. *Cell* 104:365-76
76. Taylor MD, Northcott PA, Korshunov A, Remke M, Cho YJ, et al. 2012. Molecular subgroups of medulloblastoma: the current consensus. *Acta Neuropathol* 123:465-72
77. Timmann D, Dimitrova A, Hein-Kropp C, Wilhelm H, Dörfler A. 2003. Cerebellar Agenesis: Clinical, Neuropsychological and MR Findings. *Neurocase* 9:402-13
78. Tsai PT, Hull C, Chu Y, Greene-Colozzi E, Sadowski AR, et al. 2012. Autistic-like behaviour and cerebellar dysfunction in Purkinje cell Tsc1 mutant mice. *Nature* 488:647-51
79. Wang J, Wechsler-Reya RJ. 2014. The role of stem cells and progenitors in the genesis of medulloblastoma. *Exp Neurol* 260:69-73
80. Wang VY, Rose MF, Zoghbi HY. 2005. Math1 expression redefines the rhombic lip derivatives and reveals novel lineages within the brainstem and cerebellum. *Neuron* 48:31-43
81. Wang VY, Zoghbi HY. 2001. Genetic regulation of cerebellar development. *Nat Rev Neurosci* 2:484-91

82. Wassarman KM, Lewandoski M, Campbell K, Joyner AL, Rubenstein JL, et al. 1997. Specification of the anterior hindbrain and establishment of a normal mid/hindbrain organizer is dependent on Gbx2 gene function. *Development* 124:2923-34
83. Wechsler-Reya RJ, Scott MP. 1999. Control of neuronal precursor proliferation in the cerebellum by Sonic Hedgehog. *Neuron* 22:103-14
84. Weisheit G, Gliem M, Endl E, Pfeffer PL, Busslinger M, Schilling K. 2006. Postnatal development of the murine cerebellar cortex: formation and early dispersal of basket, stellate and Golgi neurons. *Eur J Neurosci* 24:466-78
85. White JJ, Sillitoe RV. 2013. Development of the cerebellum: from gene expression patterns to circuit maps. *Wiley Interdiscip Rev Dev Biol* 2:149-64
86. Yacubova E, Komuro H. 2003. Cellular and molecular mechanisms of cerebellar granule cell migration. *Cell Biochem Biophys* 37:213-34
87. Yamada K, Watanabe M. 2002. Cytodifferentiation of Bergmann glia and its relationship with Purkinje cells. *Anat Sci Int* 77:94-108
88. Yamada M, Seto Y, Taya S, Owa T, Inoue YU, et al. 2014. Specification of spatial identities of cerebellar neuron progenitors by ptf1a and atoh1 for proper production of GABAergic and glutamatergic neurons. *J Neurosci* 34:4786-800
89. Yang ZJ, Ellis T, Markant SL, Read TA, Kessler JD, et al. 2008. Medulloblastoma can be initiated by deletion of Patched in lineage-restricted progenitors or stem cells. *Cancer Cell* 14:135-45
90. Zhang L, Goldman JE. 1996. Developmental fates and migratory pathways of dividing progenitors in the postnatal rat cerebellum. *The Journal of Comparative Neurology* 370:536-50
91. Zordan P, Croci L, Hawkes R, Consalez GG. 2008. Comparative analysis of proneural gene expression in the embryonic cerebellum. *Dev Dyn* 237:1726-35